

WOOD, PATEL & ASSOCIATES, INC.

Civil Engineers, Hydrologists, Land Surveyors
 4105 North 20th Street Suite 130
 PHOENIX, ARIZONA 85016

LETTER OF TRANSMITTAL

(602) 957-3149 234-1344
 FAX 955-3765

DATE	5/24/93	JOB NO.	91755.02
ATTENTION	R. W. SHOBE, P.E.		
RE:	NEW RIVER DROP STRUCTURE		
Tech. Data on Stepped Spillway			

FLOOD CONTROL DISTRICT
OF MARICOPA COUNTY

Property of
 Flood Control District of MC Library
 Please Return to
 2001 W. Durango
 Phoenix, AZ 85009

WE ARE SENDING YOU Attached Under separate cover via _____ the following items:

- | | | | | |
|---|---------------------------------------|--------------------------------|----------------------------------|---|
| <input type="checkbox"/> Shop drawings | <input type="checkbox"/> Prints | <input type="checkbox"/> Plans | <input type="checkbox"/> Samples | <input type="checkbox"/> Specifications |
| <input type="checkbox"/> Copy of letter | <input type="checkbox"/> Change order | <input type="checkbox"/> | <input type="checkbox"/> | <input type="checkbox"/> |

COPIES	DATE	NO.	DESCRIPTION
1 ea			DROP STRUCTURE HYDRAULIC CALCULATIONS - 100 YR, SPF
1			ARTICLE BY CHRISTODOULOU, Jour. of Hyd. Enj.
1			SKIMMING FLOW ARTICLE BY RAJARATNAM
1			ARTICLE BY SORENSEN
1			ARTICLE BY PEYRAS, ET AL.
1			JET FLOW ARTICLE BY CHAMANI ET AL.
1			ARTICLE BY ESSERY ET AL.

FLOOD CONTROL DISTRICT RECEIVED
 MAY 24 1993

CHENG	P & PM
DEP	HYDRO
ADMIN	CMST
FILE	FILE
G&D	RWS
ICC	KA

THESE ARE TRANSMITTED as checked below:

- | | | |
|--|---|---|
| <input type="checkbox"/> For approval | <input type="checkbox"/> Approved as submitted | <input type="checkbox"/> Resubmit _____ copies for approval |
| <input checked="" type="checkbox"/> For your use | <input type="checkbox"/> Approved as noted | <input type="checkbox"/> Submit _____ copies for distribution |
| <input checked="" type="checkbox"/> As requested | <input type="checkbox"/> Returned for corrections | <input type="checkbox"/> Return _____ corrected prints |
| <input checked="" type="checkbox"/> For review and comment | <input type="checkbox"/> | |
- FOR BIDS DUE _____ 19 _____ PRINTS RETURNED AFTER LOAN TO US

REMARKS _____

(preliminary)
 per request from Kofi, we are submitting the technical backup data on the stepped drop structure. We have selected the S-stepped drop based on best performance (other steps tried 3-7-1)
 please note that our calcs are based upon the best available data. Adjustments to the drop size will be needed per more current geotechnical data by Thomas-Hanfig.
 please call if you need any other info.

COPY TO KOFI AWUMAH, FCDMC

SIGNED: Anthony J. Regis

STEPPED SPILLWAY DROP STRUCTURE - CONCRETE

12-May-93

HYDRAULIC ANALYSIS

File: drop100.wq1

REFERENCES:

Chamani, M. R. and N. Rajaratnam, "Jet Flow on Stepped Spillways,"
Department of Civil Engineering, University of Alberta, Edmonton, Alberta, Canada,
1993.

Rajaratnam, N., "Skimming flow in Stepped Spillways,"
Journal of Hydraulic Engineering,
Vol. 166 No. 4, April 1990.

GIVEN DATA:

DESIGN FLOW	41000 CFS	need	(100-72)
SPILLWAY WIDTH	250 FT	need	
TAILWATER DEPTH	18 FT	need	
SPILLWAY CREST ELEVATION	1152 MSL	need	
STILLING BASIN BOTTOM ELEV	1135.5 MSL	need	
DOWNSTREAM FLOWLINE ELEV	1137.5 MSL	need	
alpha (if jet flow)	0.15	need	
NUMBER OF STEPS	5	need	
STEP HEIGHT/LENGTH RATIO	1	need	

SOLUTION:

HYDRAULIC PARAMETERS:

DISCHARGE INTENSITY $q = Q/W$	164 cfs/ft
DROP HEIGHT	16.5 ft
STEP HEIGHT (h)	3.3 ft
STEP LENGTH (L)	3.3 ft
$Y_c = .315 * q^{.667}$	9.45 ft
Y_c/h	2.86 SKIMMING FLOW
$V_c = q/Y_c$	17.35 fps

RELATIVE ENERGY LOSS ACROSS DROP 0.52 ft/ft

$E_0 = H + 1.5 * Y_c$ 30.68 ft

$E_1 = y_1 + (V_1^2)/(2g)$ 30.68 ft

$q = V_1 * y_1$ 164 cfs/ft

ENERGY LOSS ACROSS DROP 15.83 ft

USING assumed trial values of $y_1 =$ 3.950 need
then $V_1 =$ 41.52
and $E_1 =$ 30.72

THEREFORE, $V_1 =$ 41.52 fps

AND $y_1 =$ 3.95 ft

Froude $Fr = V_1 / (g * y_1)^{.5}$ 3.68

STILLING BASIN:

Length of stilling basin 39.1 ft
 $= 4.5 * y_1^2 / (Fr^{0.76}) + 2 * y_1$

Height of baffle blocks = y_1 3.95 ft

Length of baffle blocks = $2 * y_1$ 7.9 ft

Width, spacing of baffle blocks = y_1 3.95 ft

Location of baffle blocks from last step 13.0 ft
 $= \text{basin length} / 3$

CHECK TAILWATER REQUIREMENTS:

	1137.50	downstream flowline elevation
	+ 18.00	ft (tailwater depth)
tailwater per channel hydraulics	1155.50	
	1135.50	basin bottom elevation
$y_2 = y_1 * 0.5 * ((1 + FR^2)^{0.5} - 1)$	18.68	ft
tailwater required for hyd jump	1154.18	

ADJUSTMENT REQUIRED TO BASIN BOTTOM ELEVATION: 0.00 ft

RECOMMENDED ELEVATIONS:

BASIN BOTTOM ELEVATION	1135.50
TOP OF BANK ELEVATION AT CREST	1166.18
TOP OF BANK ELEVATION AT STILLING BASIN	1157.00
TOP OF BANK ELEVATION AT TAILWATER	1157.00

DESIGN DATA FOR QUANTITY ESTIMATION:

UPSTREAM RIPRAP PROTECTION LENGTH (L0)	50 ft	need
UPSTREAM RIPRAP PROTECTION THICKNESS (T6)	4 ft	need
UPSTREAM CUTOFF WALL HEIGHT (H1)	10 ft	need
UPSTREAM CUTOFF WALL THICKNESS (T1)	0.8 ft	need
CONCRETE LENGTH AT CREST (L1)	15 ft	need
CONCRETE THICKNESS AT CREST (T2)	1.5 ft	need
SPILLWAY CONCRETE THICKNESS (T3)	3.5 ft	need
BASIN CONCRETE THICKNESS (T4)	3 ft	need
DOWNSTREAM CUTOFF WALL HEIGHT (H2)	15 ft	need
DOWNSTREAM CUTOFF WALL THICKNESS (T5)	0.8 ft	need
DOWNSTREAM RIPRAP PROTECTION LENGTH (L2)	50 ft	need
DOWNSTREAM RIPRAP PROTECTION THICKNESS (T6)	4 ft	need
SIDESLOPES	1 : 1	need

STEPPED SPILLWAY DROP STRUCTURE - CONCRETE

12-May-93

HYDRAULIC ANALYSIS File DROPSPF.WQ1

REFERENCES:

Chamani, M. R. and N. Rajaratnam, "Jet Flow on Stepped Spillways,"
Department of Civil Engineering, University of Alberta, Edmonton, Alberta, Canada,
1993.

Rajaratnam, N., "Skimming flow in Stepped Spillways,"
Journal of Hydraulic Engineering,
Vol. 166 No. 4, April 1990.

GIVEN DATA:

DESIGN FLOW	68000 CFS	need	(JPF)
SPILLWAY WIDTH	250 FT	need	
TAILWATER DEPTH	27 FT	need	
SPILLWAY CREST ELEVATION	1152 MSL	need	
STILLING BASIN BOTTOM ELEV	1135.5 MSL	need	
DOWNSTREAM FLOWLINE ELEV	1137.5 MSL	need	
alpha (if jet flow)	0.15	need	
NUMBER OF STEPS	5	need	
STEP HEIGHT/LENGTH RATIO	1	need	

SOLUTION:

HYDRAULIC PARAMETERS:

DISCHARGE INTENSITY $q = Q/W$	272 cfs/ft
DROP HEIGHT	16.5 ft
STEP HEIGHT (h)	3.3 ft
STEP LENGTH (L)	3.3 ft
$Y_c = .315 * q^{.667}$	13.25 ft
Y_c/h	4.01 SKIMMING FLOW
$V_c = q/Y_c$	20.53 fps

RELATIVE ENERGY LOSS ACROSS DROP 0.40 ft/ft

$E_0 = H + 1.5 * Y_c$ 36.37 ft

$E_1 = y_1 + (V_1^2)/(2g)$ 36.37 ft

$q = V_1 * y_1$ 272 cfs/ft

ENERGY LOSS ACROSS DROP 14.55 ft

USING assumed trial values of $y_1 =$ 6.150 need
then $V_1 =$ 44.23
and $E_1 =$ 36.52

THEREFORE, $V_1 =$ 44.23 fps

AND $y_1 =$ 6.15 ft

Froude $Fr = V_1/(g * y_1)^{.5}$ 3.14

STILLING BASIN:

Length of stilling basin 58.3 ft
 $= 4.5 * y_1^2 / (Fr^{0.76}) + 2 * y_1$

Height of baffle blocks = y_1 6.15 ft

Length of baffle blocks = $2 * y_1$ 12.3 ft

Width, spacing of baffle blocks = y_1 6.15 ft

Location of baffle blocks from last step 19.4 ft
 $= \text{basin length} / 3$

CHECK TAILWATER REQUIREMENTS:

	1137.50	downstream flowline elevation
	+ 27.00	ft (tailwater depth)
tailwater per channel hydraulics	1164.50	
	1135.50	basin bottom elevation
$y_2 = y_1 * 0.5 * ((1 + FR^2)^{0.5} - 1)$	24.43	ft
tailwater required for hyd jump	1159.93	

ADJUSTMENT REQUIRED TO BASIN BOTTOM ELEVATION: 0.00 ft

RECOMMENDED ELEVATIONS:

BASIN BOTTOM ELEVATION	1135.50
TOP OF BANK ELEVATION AT CREST	1171.87
TOP OF BANK ELEVATION AT STILLING BASIN	1166.00
TOP OF BANK ELEVATION AT TAILWATER	1166.00

DESIGN DATA FOR QUANTITY ESTIMATION:

UPSTREAM RIPRAP PROTECTION LENGTH (L0)	50 ft	need
UPSTREAM RIPRAP PROTECTION THICKNESS (T6)	4 ft	need
UPSTREAM CUTOFF WALL HEIGHT (H1)	10 ft	need
UPSTREAM CUTOFF WALL THICKNESS (T1)	0.8 ft	need
CONCRETE LENGTH AT CREST (L1)	15 ft	need
CONCRETE THICKNESS AT CREST (T2)	1.5 ft	need
SPILLWAY CONCRETE THICKNESS (T3)	3.5 ft	need
BASIN CONCRETE THICKNESS (T4)	3 ft	need
DOWNSTREAM CUTOFF WALL HEIGHT (H2)	15 ft	need
DOWNSTREAM CUTOFF WALL THICKNESS (T5)	0.8 ft	need
DOWNSTREAM RIPRAP PROTECTION LENGTH (L2)	100 ft	need
DOWNSTREAM RIPRAP PROTECTION THICKNESS (T6)	4 ft	need
SIDESLOPES	1 : 1	need

Abstract: Potentially high energy dissipation on stepped overflow spillways would imply a significant reduction of the size of downstream stilling basins. The amount of energy loss on such spillways under skimming-flow conditions is examined experimentally for structures with a moderate number of steps and a width-to-height ratio equal to 0.7. The experimental results, supported by dimensional considerations, indicate that the most important parameters governing energy dissipation are the ratio of the critical depth of flow passing over the spillway to the step height y_c/h , and the number of steps N . Dissipation is highest for the small values of y_c/h tested, near unity, and decreases with increasing y_c/h ; for a certain y_c/h the dissipation increases with N . The results are compared to those of earlier investigations referring to a large number of steps. For commonly used ranges of the step dimensions, a general relation is established between the energy loss and the parameter y_c/h , which may be useful in practical applications.

INTRODUCTION

Usually, the crest of overflow spillways follows the standard shapes that were determined after extensive experiments at the U.S. Waterways Experiment Station (Chow 1959). The flow accelerates along the downstream face and high velocities are attained at the spillway toe, so that stilling basins or other types of energy dissipators need to be provided. Some concrete gravity dams and the associated spillways are being constructed with a stepwise profile by application of rollcrete technology [e.g., Hollingworth and Druys (1986); Bouyge et al. (1988)]. However, the performance of stepped spillways is not well known. Limited experimental research in the past (Young 1982; Sorensen 1985) has suggested that considerable energy dissipation may take place on the stepped surface of the spillway, and, consequently, the stilling basin might be severely reduced in size or even eliminated. Rajaratnam (1990) proposed a theoretical estimate for the energy loss due to the steps, assuming the establishment of uniform skimming flow. This assumption would imply a high spillway with many steps—a requirement that may not be typical of stepped structure. Peyras et al. (1992) presented experimental results for small gabion weirs with a flat crest and up to seven steps. According to these results, the relative energy dissipation decreases with increasing flowrate and also depends on the slope of the downstream face. The objective of the present paper is to further assess the energy loss characteristics of stepped spillways by means of laboratory experiments.

EXPERIMENTS

The experiments were conducted at the Applied Hydraulics Laboratory of the National Technical University of Athens. The spillway tested had the form shown in Fig. 1, in which all dimensions are given in centimeters. The

¹Assoc. Prof., Dept. Civ. Engrg., Nat. Tech. Univ. of Athens, Athens 15773, Greece.

Note. Discussion open until October 1, 1993. To extend the closing date one month, a written request must be filed with the ASCE Manager of Journals. The manuscript for this paper was submitted for review and possible publication on May 22, 1992. This paper is part of the *Journal of Hydraulic Engineering*, Vol. 119, No. 5, May, 1993. ©ASCE, ISSN 0733-9429/93/0005-0644/\$1.00 + \$.15 per page. Paper No. 4137.

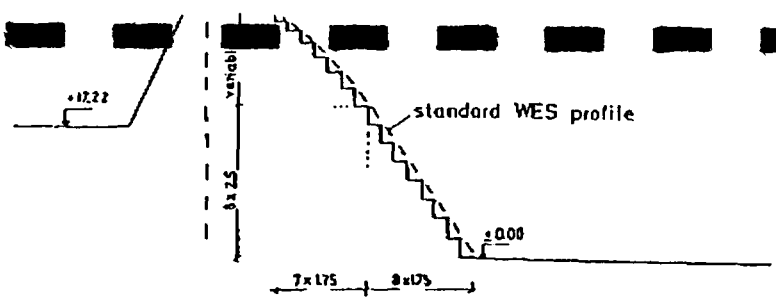


FIG. 1. Side View of Spillway Tested (Dimensions in cm)

steps are designed so that the envelope of their tips, indicated by the broken line, follows the standard Waterways Experiment Station (WES) profile up to a constant slope of 1:0.7 (55° angle to the horizontal). There are seven steps on the curved part of the spillway face with variable height-to-width ratios, and eight steps on the straight part with constant width $l = 1.75$ cm and height $h = 2.50$ cm ($lh = 0.7$). The spillway was made of wood, and epoxy coated to avoid warping. It was placed in a laboratory flume 10 m long and 0.5 m wide, which was connected upstream to a 2.0 m × 1.5 m supply reservoir through an elliptical transition. Beyond the toe of the spillway, the flume had a bottom slope of 0.04, and there was no downstream control, so that supercritical flow was maintained without formation of a hydraulic jump.

Eight experimental runs were carried out, with discharges ranging between 10 L/s and 45 L/s. The measurement of discharge Q was performed by means of a carbon-tetrachloride differential manometer installed on the main supply line of the laboratory. In each run, the vertical water depth was measured at the brink of the 10th and the 13th step by means of a point gage mounted on an aluminum frame so that it could be moved longitudinally and transversely over any point on the spillway. The gage was equipped with a vernier, readable to within 0.1 mm. However, minor irregularities of the water surface, due primarily to the influence of the side walls, render an overall accuracy on the order of 0.1 cm. The depth was recorded at three points across each step (at $B/4, B/2, 3B/4$, where B is the flume width), and the arithmetic mean of the three values was considered as the vertical depth d over the respective step. The water level was measured on the flume axis 1 m upstream of the crest. Based on the preceding measurements, the head loss was calculated as discussed in the following section.

ANALYSIS OF RESULTS

Referring to the notation shown in Fig. 2, the total head loss up to a certain step is expressed by

$$\Delta H = H_0 - H \dots \dots \dots (1)$$

where $H = y \cos \theta + (V^2/2g) =$ head on the step under consideration; $H_0 = \Delta z + Y + (V_0^2/2g) =$ head upstream of the spillway relative to the same datum; $V = Q/(yB) =$ local mean velocity; and $V_0 = Q/(YB) =$ approach velocity.

MAY 10 1993 05:29PM CRSS CIVIL ENGINEERS

P. 2/5

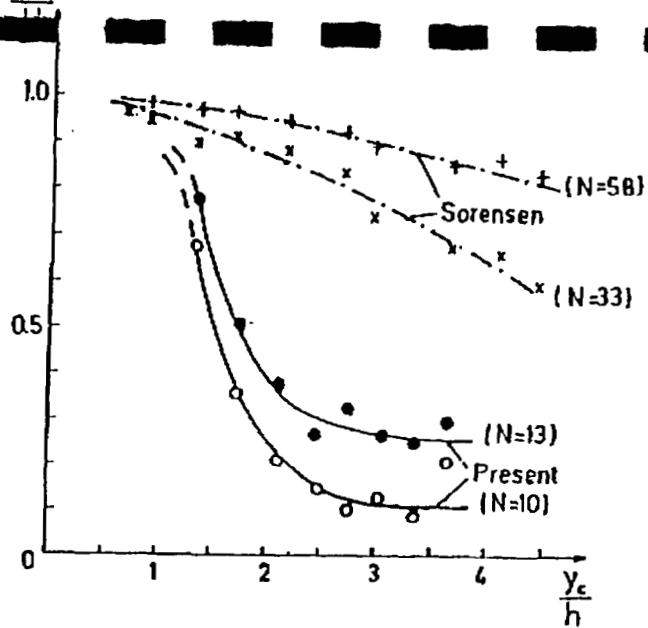


FIG. 3. Variation of Relative Head Loss $\Delta H/H_0$ with y_c/h and N

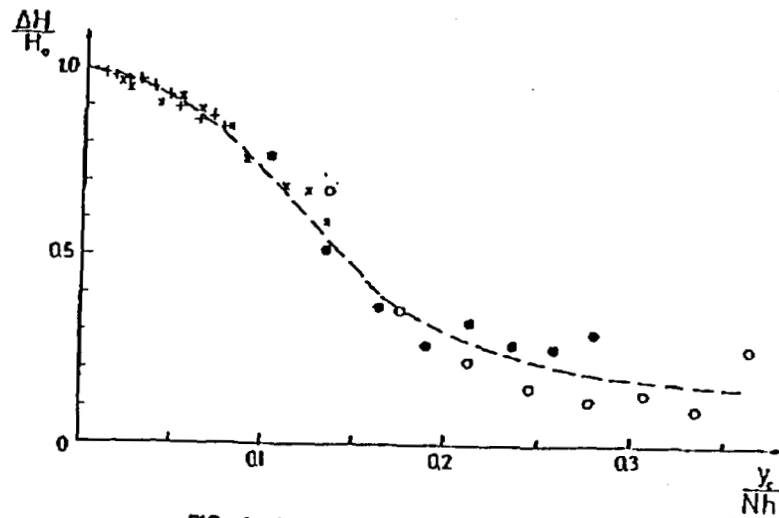


FIG. 4. Dependence of $\Delta H/H_0$ on y_c/Nh

With the stated limitations, the experimental curve of Fig. 4 may be used to design practical straight downward minimum time spillways by loss.

CONCLUSIONS

Experiments on a moderately sized stepped spillway indicate that the energy dissipation may be significantly less than suggested by earlier studies based on the establishment of uniform flow on high spillways. It is found that the energy loss due to the steps depends primarily on the ratio y_c/h , where y_c is the critical depth of flow passing over the spillway, and h is the step height, as well as on the number of steps N . For small values of y_c/h near unity, i.e., near the limit of skimming flow, the stepped surface is very effective in dissipating energy. For higher values of y_c/h , the effect of N becomes appreciable: at a certain y_c/h , the relative energy loss increases with N . The present and previous experimental results can be combined in a single experimental curve expressing the relative energy loss in terms of the parameter y_c/Nh for the commonly used values of h/h close to 0.7 and y_c/h in the range of 1-4.

ACKNOWLEDGMENTS

Partial financial support for this study was provided by the Public Power Corporation of Greece. Experimental measurements were taken by the students H. Tsiotra and G. Halari.

APPENDIX I. REFERENCES

- Bouyge, B., Garnier, G., Jensen, A., Martin, J. P., and Sterenberg, J. (1988). "Construction et controle d'un barrage en beton compacte au rouleau (BCR): Un travail d'equipe." *Proc., 16^{me} Congres des Grands Barrages*, Commission International des Grands Barrages, 588-612 (in French).
- Chow, V. T. (1959). "Open-channel hydraulics." McGraw-Hill, New York, N.Y.
- Hollingworth, F., and Druyts, F. H. W. M. (1986). "Rollcrete: Some applications to dams in South Africa." *Water Power and Dam Constr.*, 38(1), 13-16.
- Peyras, L., Royet, P., and Degoutte, G. (1992). "Flow and energy dissipation over stepped gabion weirs." *J. Hydr. Engrg.*, ASCE, 118(5), 707-717.
- Rajaratnam, N. (1990). "Skimming flow in stepped spillways." *J. Hydr. Engrg.*, ASCE, 116(4), 587-591.
- Sorensen, R. M. (1985). "Stepped spillway hydraulic model investigation." *J. Hydr. Engrg.*, ASCE, 111(12), 1461-1472.
- Young, M. F. (1982). "Feasibility study of a stepped spillway." *Proc. Hydr. Div. Spec. Conf.*, ASCE, New York, N.Y., 96-106.

APPENDIX II. NOTATION

The following symbols are used in this paper:

- B = flume width;
- c_f = effective roughness coefficient;
- d = vertical depth of flow over brink of step;
- f = function;

- h = step height;
- b = step width;
- n = number of steps from crest to chosen level;
- Q = discharge;
- V = local mean velocity;
- V_0 = approach velocity;
- Y = upstream depth;
- y = depth of flow normal to spillway slope;
- y_c = critical depth;
- y_0 = uniform depth;
- $\Delta H = H_0 - H$;
- Δz = elevation difference between chosen step and bottom of flume in front of spillway; and
- θ = angle of downstream face of spillway to horizontal [Fig. 2(a)].

ABSTRACT: The inner layer of a turbulent boundary layer consists of a linear layer in which the velocity distribution is linear, the log-law region having a logarithmic velocity distribution and a buffer layer lying in between them. Separate equations are available for the linear layer and the log-law region. The available inner region equations pertain to flow over smooth boundary and they are explicit (containing involved expressions) or implicit. No equation is available that includes the effect of roughness. Presented herein is a generalized equation for velocity distribution in the inner law region of a turbulent boundary layer. The equation includes linear and logarithmic velocity distributions and it is valid for hydraulically smooth and rough boundaries and the transition range in between.

INTRODUCTION

The flow over a smooth flat plate is composed of two regions: The inner region, in which the velocity distribution is influenced by viscous shear; and the outer region, in which the velocity profiles are dominated by turbulent shear. The inner region is further subdivided into two parts: the viscous sublayer, in which the viscous stresses are significant; and the log-law region, in which the velocity distribution is logarithmic. Again the viscous sublayer consists of two parts: the linear sublayer, in which the velocity distribution is linear; and the buffer layer, which provides a smooth transition between the linear and the logarithmic velocity distributions.

The aforementioned classification is characterized by the nondimensional variable y^+ , defined as

$$y^+ = \frac{u_* y}{\nu} \dots\dots\dots (1)$$

in which y = the distance from the surface; ν = kinematic viscosity of the fluid; and u_* = the wall shear velocity, given by

$$u_* = \left(\frac{\tau_0}{\rho} \right)^{0.5} \dots\dots\dots (2)$$

in which τ_0 = the wall shear stress; and ρ = mass density of fluid. The velocity u at y is nondimensionalized by u_* , i.e.,

$$u^+ = \frac{u}{u_*} \dots\dots\dots (3)$$

For $y^+ \leq 5$, the velocity distribution in the linear layer is given by

$$u^+ = y^+ \dots\dots\dots (4)$$

¹Prof., Dept. of Civ. Engrg., Univ. of Roorkee, Roorkee 247 667, India.
 Note. Discussion open until October 1, 1993. To extend the closing date one month, a written request must be filed with the ASCE Manager of Journals. The manuscript for this paper was submitted for review and possible publication on April 29, 1991. This paper is part of the *Journal of Hydraulic Engineering*, Vol. 119, No. 5, May, 1993. ©ASCE, ISSN 0733-9429/93/0005-0651/\$1.00 + \$.15 per page. Paper No. 1782.

MAY 10 1993 05:31PM CRSS CIVIL ENGINEERS

P. 15/15

APPENDIX. REF

Gill, M. (1977).
 Hecgen, R. (1984
Bull., 20(1), 11
 O'Donnell, T. (1
 ing lateral inflc

Nordic Hydr., 8, 163-170.
 flood routing." *Water Res.*

1gum procedure incorporat-

SKIMMING FLOW IN STEPPED SPILLWAYS

By N. Rajaratnam,¹ Member, ASCE

INTRODUCTION

In a stepped spillway, the spillway face is provided with a series of steps, from near the crest to the toe. The energy dissipation caused by the steps reduces the size of the energy dissipator, generally provided at the toe of the spillway. Stepped spillways have been built in the past but there appears to be renewed interest in them because of significant cost savings. A recent example is the Monksville dam (Sorensen 1985).

Based on the experimental observations of Essery and Horner (1971) and Sorensen (1985), the flow over stepped spillways can be divided into nappe flow and skimming flow regimes [Figs. 1(a) and (b)]. In the nappe flow regime, the flow from each step hits the step below as a falling jet, with the energy dissipation occurring by jet breakup in air, jet mixing on the step, with or without the formation of a partial hydraulic jump on the step. In the skimming flow regime, the water flows down the stepped face as a coherent stream, skimming over the steps and cushioned by the recirculating fluid trapped between them. The energy dissipation in the flow appears to be enhanced by the momentum transfer to the recirculating fluid. In this note, a method for predicting the shear stress, thus frictional energy loss of the skimming flow is presented.

ANALYSIS OF SKIMMING FLOW

For a stepped spillway of constant slope, $S_0 = \sin \alpha$, with a large number of identical steps of height, h , and (horizontal) length, l (note that $\sin \alpha = h/\sqrt{l^2 + h^2}$), the flow is assumed to become fully developed after the first few steps. For such a fully developed flow, with a constant mean velocity of V_0 and normal depth of y_0 , considering unit width of the spillway, we write

$$y_0 \gamma \sin \alpha = \tau \dots\dots\dots (1)$$

where γ = the weight per unit volume of the fluid (water); and τ = the average Reynolds shear stress that exists between the skimming stream and the recirculating fluid underneath. Let us assume

$$\tau = c_f \frac{\rho V_0^2}{2} \dots\dots\dots (2)$$

where c_f = the coefficient of fluid friction and would be equal to $f/4$, where f = the Darcy-Weisbach friction factor; and ρ = the mass density of the

¹Prof., Dept. of Civ. Engrg., Univ. of Alberta, Edmonton, Alberta, Canada, T6G 2G7.

Note. Discussion open until September 1, 1990. To extend the closing date one month, a written request must be filed with the ASCE Manager of Journals. The manuscript for this paper was submitted for review and possible publication on July 11, 1988. This paper is part of the *Journal of Hydraulic Engineering*, Vol. 116, No. 4, April, 1990. ©ASCE, ISSN 0733-9429/90/0004-0587/\$1.00 + \$.15 per page. Paper No. 24515.

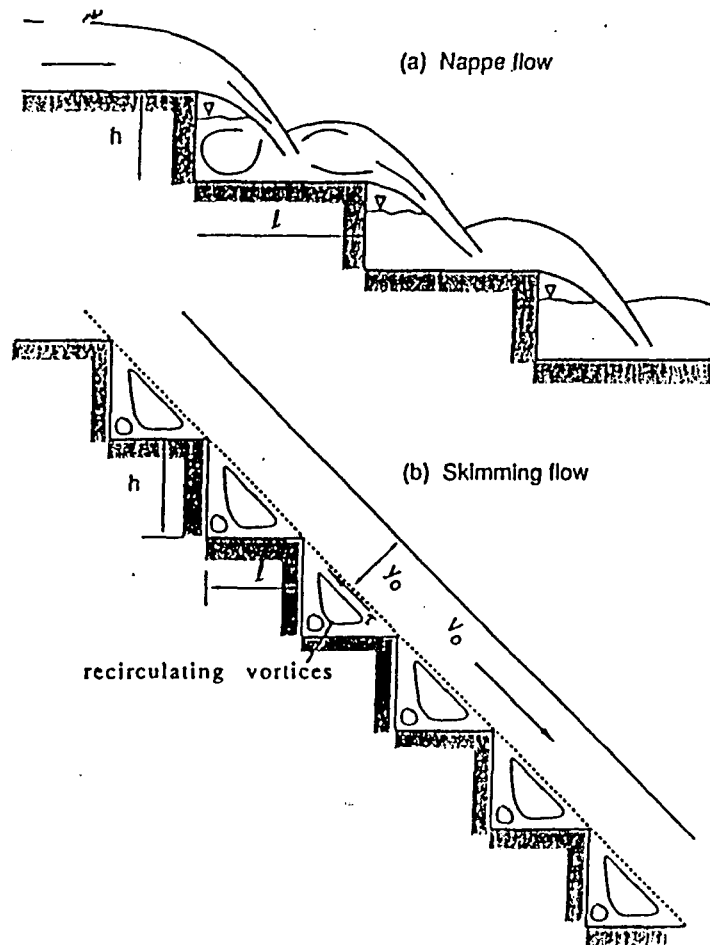


FIG. 1. Definition Sketches for Flow Over Stepped Spillways

fluid. Combining Eqs. 1 and 2, we obtain

$$c_f = \frac{2y_0^3 g \sin \alpha}{q^2} \dots \dots \dots (3)$$

where g = the acceleration due to gravity; and q = discharge per unit width of the spillway.

The idea of Eq. 2 is to represent the turbulent shear stress between the main stream and the recirculating fluid, trapped between the steps of the spillway. For example, this method has been used in developing flow equations for Denil, Vertical Slot, and other fishways (Rajaratnam and Katopodis 1984; Rajaratnam et al. 1986; Rajaratnam et al. 1988). For a Denil fishway, with the depth of flow much larger than its width, so that the shear comes mainly from the sides and for subcritical flows, c_f has been found to be equal to about 0.09 and for relatively smaller depths, values of c_f have been found

to be as large as 0.6. The Reynolds number $R = V_0 y_0 / \nu$, with ν being the kinematic viscosity of the fluid, was in the range of 10^3 – 10^6 for the prototype and equal to about 10^3 for the 1/3 scale model of the Denil fishway. For pool and weir fishways, c_f has been found to be about 0.09. Ervine and Baird (1982) used the same idea to express the apparent shear between the main channel and flood-plain channel flows and found a value of 0.05 for c_f . The slopes for Denil fishways had a maximum value of about 0.3 whereas for the compound channel of Ervine and Baird, they were very small. The point is that the idea of Eq. 2 appears to be generally valid for the range of slopes studied so far and is used for stepped spillway only to attempt to estimate its flow characteristics. It should be pointed out that for smooth boundaries, the coefficient of skin friction decreases from about 0.0035 to 0.0025 as R increases from 10^3 to 10^6 .

To evaluate c_f for skimming flow in a stepped spillway, the experimental observations of Sorensen on a 1:25 scale model of the new Monksville dam spillway of approximate height of 32 m are used. Steps at the crest were fitted to the standard Waterways Experiment Station (WES) spillway profile. But for the small number of steps near the crest, the height h of the remaining steps was 0.6 m with a spillway slope of 1 (vertical) on 0.78 (horizontal). The horizontal length, l , of the steps was 0.47 m, thus giving a value of 1.28 for h/l .

For experiments (C1–C8), c_f was found to vary from 0.11 to 0.2 with an average value of 0.18. For experiments C9 and C10, with very small flow rates, c_f was found to be 0.25 and 0.28, respectively, and it is possible that in these experiments the flow was in a transition state between nappe and skimming regimes. It is realized that for the C-series, Sorensen measured the flow depths downstream of the toe and on the stepped spillway the flow would have been aerated. Sorensen also admits to 10–15% error in depth measurements between continuity calculations and stagnation tube measurements. Aeration aspects are also important. Hence, calculations of c_f and energy loss on the spillway (presented later) would have to be considered very approximate. The average value of 0.18 for the skimming flow in the stepped spillway studied by Sorensen, is about twice as large as the value for a Denil fishway with a relatively large depth of flow. For a vertical slot fishway, c_f was found to be equal to about 0.14 for a 1/16 scale model with R equal to about 5,000. For a pool and weir fishway, $c_f = 0.09$ in the streaming flow regime (Rajaratnam et al. 1988). Considering all these values including 0.05 (Ervine and Baird 1982), c_f is the range of 0.05–0.18 with the Reynolds number in the approximate range of 5,000– 10^6 . It would be interesting and useful to find c_f for skimming flow stepped spillways for a range of slopes or h/l .

For convenience of use, rewrite Eq. 3 as

$$V_0 = \sqrt{\frac{2}{c_f}} \sqrt{g y_0 S_0} \dots \dots \dots (4)$$

For the discharge per unit width q , write

$$q = \sqrt{\frac{2}{c_f}} y_0^{3/2} \sqrt{g S_0} \dots \dots \dots (5)$$

ENERGY LOSS IN A STEPPED SPILLWAY

An estimate of the energy loss for skimming flow in a stepped spillway is presented using the analysis presented in the previous sections. If E is the energy in the flow at the toe of the stepped spillway

$$E = y_0 + \frac{V_0^2}{2g} \dots \dots \dots (6)$$

$$E = \left(\frac{c_f q^2}{2g \sin \alpha} \right)^{1/3} + \left(\frac{q \sin \alpha}{c_f \sqrt{2g}} \right)^{2/3} \dots \dots \dots (7)$$

If y'_0 and V'_0 = the corresponding depth and velocity at the toe of a smooth spillway without steps

$$E' = y'_0 + \frac{V'^2_0}{2g} \dots \dots \dots (8)$$

and one can write an equation similar to Eq. 7 with c'_f replacing c_f , where c'_f = the coefficient of skin friction for the smooth spillway. Sorensen's tests (B series) on a smooth spillway give a value of 0.0065 for c'_f . If ΔE is defined as

$$\Delta E = E' - E \dots \dots \dots (9)$$

ΔE gives the energy loss caused by the steps over that caused by the smooth spillway face. If the relative energy loss is defined as $\Delta E/E'$, it can be shown that

$$\frac{\Delta E}{E'} = \frac{(1 - A) + \frac{F_0'^2 (A^2 - 1)}{2 A^2}}{1 + \frac{F_0'^2}{2}} \dots \dots \dots (10)$$

where $A = (c_f/c'_f)^{1/2}$, and F_0' = the Froude number at the toe of the smooth spillway. Taking $c_f \approx 0.18$ and $c'_f \approx 0.0065$, $A \approx 3$ and for a relatively large value of F_0' , $\Delta E/E'$ is approximately equal to $(A^2 - 1)/A^2$, which further reduces to 8/9. This indicates the considerable amount of energy loss that can be produced by steps, as was found by Sorensen.

ONSET OF SKIMMING FLOW

Based on their experimental observations, Essery and Horner (1971) found that for horizontal steps, for the onset of skimming flow, the ratio y_c/l , wherein y_c is the critical depth, increased with h/l from about 0.32 for $h/l = 0.4$ to about 0.69 for $h/l = 0.9$. By a reanalysis of their data, it was found that for the whole range of h/l from 0.4 to 0.9, at the onset of skimming flow, y_c/h was approximately equal to 0.8. This means that for y_c/h greater than 0.8, skimming flow occurs. The observations of Sorensen for $h/l = 1.28$ support this criteria. For y_c/h less than 0.8, one would expect to get nappe flow and in Sorensen's experiments, nappe flow occurred for $y_c/h = 0.16$.

CONCLUSIONS

This technical note presents a method of predicting the characteristics of skimming flow on stepped spillways. For a stepped spillway with a slope of 1 vertical on 0.78 horizontal, the fluid friction coefficient c_f was evaluated using the experimental results of Sorensen and found to be about 0.18. An estimate has been made of the energy loss on stepped spillways for skimming flow.

APPENDIX. REFERENCES

- Ervine, D. A., and Baird, J. I. (1982). "Rating Curves for Rivers with Overbank Flow," *Proc. Instn. of Civ. Engrs., Part 2*, Institute of Civil Engineers, 465-472.
- Essery, I. T. S., and Horner, M. W. (1971). "The hydraulic design of stepped spillways." *Report 33*, Constr. Industry Res. and Information Assoc., London, England.
- Rajaratnam, N., and Katopodis, C. (1984). "Hydraulics of Denil fishways." *Proc., ASCE*, 110(9), 1219-1233.
- Rajaratnam, N., Katopodis, C., and Mainali, A. (1988). "Plunging and streaming flows in pool and weir fishways." *Proc., ASCE*, 114(8), 939-944.
- Rajaratnam, N., Van der Vinne, G., and Katopodis, C. (1986). "Hydraulics of Vertical Slot fishways." *Proc., ASCE*, 112(10), 909-927.
- Sorensen, R. M. (1985). "Stepped spillway hydraulic model investigation." *Proc., ASCE*, 111(12), 1461-1472.

$$\begin{aligned} \frac{y_0^2}{2g} &= \frac{2g y_0 \sin \alpha}{c_f 2g} & \frac{y_0^3}{(2g)^{3/2}} &= \frac{q \sin \alpha}{c_f \sqrt{2g}} \\ &= \frac{y_0 \sin \alpha}{c_f} & \left(\frac{y_0^2}{2g} \right)^{3/2} &= \\ &= \frac{q \sin \alpha}{c_f y_0} & \frac{y_0^2}{2g} &= \left(\frac{q \sin \alpha}{c_f \sqrt{2g}} \right)^{2/3} \\ \frac{y_0^3}{2g} &= \frac{q \sin \alpha}{c_f} & & \\ \frac{y_0^3}{2g \sqrt{2g}} &= \frac{q \sin \alpha}{c_f \sqrt{2g}} & & \end{aligned}$$

VOL. 116 NO. 4 APR. 1990

ISSN 0733-9429
CODEN: JHEND8

Journal of
**Hydraulic
Engineering**

AMERICAN SOCIETY OF CIVIL ENGINEERS

HYDRAULICS DIVISION

Gill, M. (1977).
 Heggen, R. (1984
 Bull., 20(1), 11
 O'Donnell, T. (1
 ing lateral inflc

Vordic Hydr., 8, 163-170.
 flood routing." *Water Res.*
 igum procedure incorporat-

SKIMMING FLOW IN STEPPED SPILLWAYS

By N. Rajaratnam,¹ Member, ASCE

INTRODUCTION

In a stepped spillway, the spillway face is provided with a series of steps, from near the crest to the toe. The energy dissipation caused by the steps reduces the size of the energy dissipator, generally provided at the toe of the spillway. Stepped spillways have been built in the past but there appears to be renewed interest in them because of significant cost savings. A recent example is the Monksville dam (Sorensen 1985).

Based on the experimental observations of Essery and Horner (1971) and Sorensen (1985), the flow over stepped spillways can be divided into nappe flow and skimming flow regimes [Figs. 1(a) and (b)]. In the nappe flow regime, the flow from each step hits the step below as a falling jet, with the energy dissipation occurring by jet breakup in air, jet mixing on the step, with or without the formation of a partial hydraulic jump on the step. In the skimming flow regime, the water flows down the stepped face as a coherent stream, skimming over the steps and cushioned by the recirculating fluid trapped between them. The energy dissipation in the flow appears to be enhanced by the momentum transfer to the recirculating fluid. In this note, a method for predicting the shear stress, thus frictional energy loss of the skimming flow is presented.

ANALYSIS OF SKIMMING FLOW

For a stepped spillway of constant slope, $S_0 = \sin \alpha$, with a large number of identical steps of height, h , and (horizontal) length, l (note that $\sin \alpha = h/\sqrt{l^2 + h^2}$), the flow is assumed to become fully developed after the first few steps. For such a fully developed flow, with a constant mean velocity of V_0 and normal depth of y_0 , considering unit width of the spillway, we write

$$y_0 \gamma \sin \alpha = \tau \dots \dots \dots (1)$$

where γ = the weight per unit volume of the fluid (water); and τ = the average Reynolds shear stress that exists between the skimming stream and the recirculating fluid underneath. Let us assume

$$\tau = c_f \frac{\rho V_0^2}{2} \dots \dots \dots (2)$$

where c_f = the coefficient of fluid friction and would be equal to $f/4$, where f = the Darcy-Weisbach friction factor; and ρ = the mass density of the

¹Prof., Dept. of Civ. Engrg., Univ. of Alberta, Edmonton, Alberta, Canada, T6G 2G7.

Note. Discussion open until September 1, 1990. To extend the closing date one month, a written request must be filed with the ASCE Manager of Journals. The manuscript for this paper was submitted for review and possible publication on July 11, 1988. This paper is part of the *Journal of Hydraulic Engineering*, Vol. 116, No. 4, April, 1990. ©ASCE, ISSN 0733-9429/90/0004-0587/\$1.00 + \$.15 per page. Paper No. 24515.

403-492-3903
 fix: 403-492-0249 (fix)

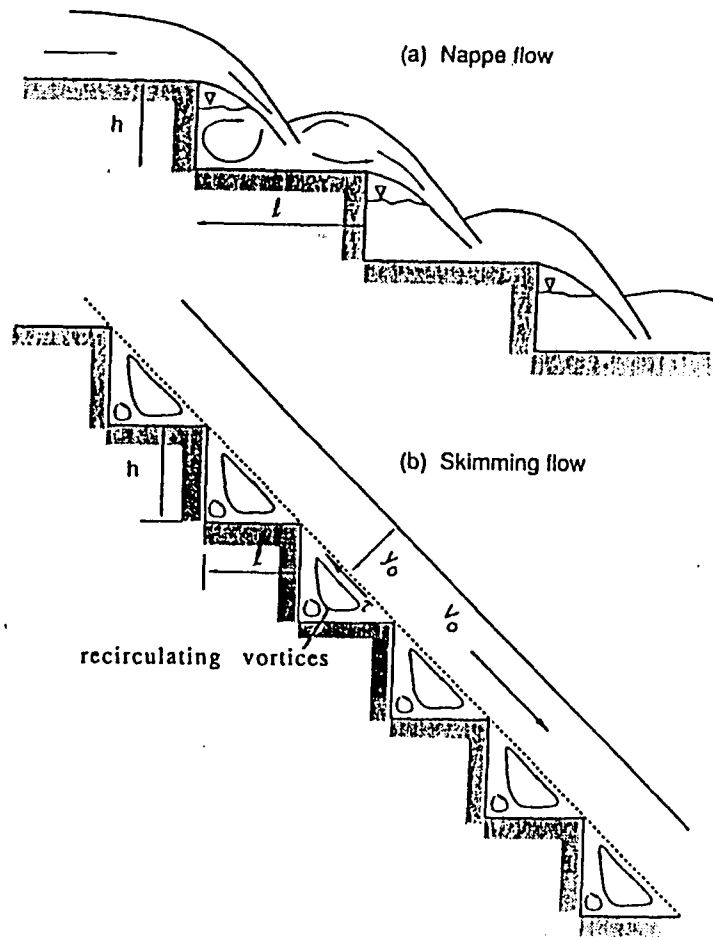


FIG. 1. Definition Sketches for Flow Over Stepped Spillways

fluid. Combining Eqs. 1 and 2, we obtain

$$c_f = \frac{2y_0^3 g \sin \alpha}{q^2} \dots \dots \dots (3)$$

where g = the acceleration due to gravity; and q = discharge per unit width of the spillway.

The idea of Eq. 2 is to represent the turbulent shear stress between the main stream and the recirculating fluid, trapped between the steps of the spillway. For example, this method has been used in developing flow equations for Denil, Vertical Slot, and other fishways (Rajaratnam and Katopodis 1984; Rajaratnam et al. 1986; Rajaratnam et al. 1988). For a Denil fishway, with the depth of flow much larger than its width, so that the shear comes mainly from the sides and for subcritical flows, c_f has been found to be equal to about 0.09 and for relatively smaller depths, values of c_f have been found

to be as large as 0.6. The Reynolds number $R = V_0 y_0 / \nu$, with ν being the kinematic viscosity of the fluid, was in the range of 10^3 – 10^6 for the prototype and equal to about 10^5 for the 1/3 scale model of the Denil fishway. For pool and weir fishways, c_f has been found to be about 0.09. Ervine and Baird (1982) used the same idea to express the apparent shear between the main channel and flood-plain channel flows and found a value of 0.05 for c_f . The slopes for Denil fishways had a maximum value of about 0.3 whereas for the compound channel of Ervine and Baird, they were very small. The point is that the idea of Eq. 2 appears to be generally valid for the range of slopes studied so far and is used for stepped spillway only to attempt to estimate its flow characteristics. It should be pointed out that for smooth boundaries, the coefficient of skin friction decreases from about 0.0035 to 0.0025 as R increases from 10^3 to 10^6 .

To evaluate c_f for skimming flow in a stepped spillway, the experimental observations of Sorensen on a 1:25 scale model of the new Monksville dam spillway of approximate height of 32 m are used. Steps at the crest were fitted to the standard Waterways Experiment Station (WES) spillway profile. But for the small number of steps near the crest, the height h of the remaining steps was 0.6 m with a spillway slope of 1 (vertical) on 0.78 (horizontal). The horizontal length, l , of the steps was 0.47 m, thus giving a value of 1.28 for h/l .

For experiments (C1–C8), c_f was found to vary from 0.11 to 0.2 with an average value of 0.18. For experiments C9 and C10, with very small flow rates, c_f was found to be 0.25 and 0.28, respectively, and it is possible that in these experiments the flow was in a transition state between nappe and skimming regimes. It is realized that for the C-series, Sorensen measured the flow depths downstream of the toe and on the stepped spillway the flow would have been aerated. Sorensen also admits to 10–15% error in depth measurements between continuity calculations and stagnation tube measurements. Aeration aspects are also important. Hence, calculations of c_f and energy loss on the spillway (presented later) would have to be considered very approximate. The average value of 0.18 for the skimming flow in the stepped spillway studied by Sorensen, is about twice as large as the value for a Denil fishway with a relatively large depth of flow. For a vertical slot fishway, c_f was found to be equal to about 0.14 for a 1/16 scale model with R equal to about 5,000. For a pool and weir fishway, $c_f \approx 0.09$ in the streaming flow regime (Rajaratnam et al. 1988). Considering all these values including 0.05 (Ervin and Baird 1982), c_f is the range of 0.05–0.18 with the Reynolds number in the approximate range of 5,000– 10^6 . It would be interesting and useful to find c_f for skimming flow stepped spillways for a range of slopes or h/l .

For convenience of use, rewrite Eq. 3 as

$$V_0 = \sqrt{\frac{2}{c_f}} \sqrt{g y_0 S_0} \dots \dots \dots (4)$$

For the discharge per unit width q , write

$$q = \sqrt{\frac{2}{c_f}} y_0^{3/2} \sqrt{g S_0} \dots \dots \dots (5)$$

ENERGY LOSS IN A STEPPED SPILLWAY

An estimate of the energy loss for skimming flow in a stepped spillway is presented using the analysis presented in the previous sections. If E is the energy in the flow at the toe of the stepped spillway

$$E = y_0 + \frac{V_0^2}{2g} \dots \dots \dots (6)$$

$$E = \left(\frac{c_f q^2}{2g \sin \alpha} \right)^{1/3} + \left(\frac{q \sin \alpha}{c_f \sqrt{2g}} \right)^{2/3} \dots \dots \dots (7)$$

If y'_0 and V'_0 = the corresponding depth and velocity at the toe of a smooth spillway without steps

$$E' = y'_0 + \frac{V_0'^2}{2g} \dots \dots \dots (8)$$

and one can write an equation similar to Eq. 7 with c'_f replacing c_f , where c'_f = the coefficient of skin friction for the smooth spillway. Sorensen's tests (B series) on a smooth spillway give a value of 0.0065 for c'_f . If ΔE is defined as

$$\Delta E = E' - E \dots \dots \dots (9)$$

ΔE gives the energy loss caused by the steps over that caused by the smooth spillway face. If the relative energy loss is defined as $\Delta E/E'$, it can be shown that

$$\frac{\Delta E}{E'} = \frac{(1 - A) + \frac{F_0'^2 (A^2 - 1)}{2 A^2}}{1 + \frac{F_0'^2}{2}} \dots \dots \dots (10)$$

where $A = (c_f/c'_f)^{1/2}$; and F_0' = the Froude number at the toe of the smooth spillway. Taking $c_f = 0.18$ and $c'_f = 0.0065$, $A \approx 3$ and for a relatively large value of F_0' , $\Delta E/E'$ is approximately equal to $(A^2 - 1)/A^2$, which further reduces to 8/9. This indicates the considerable amount of energy loss that can be produced by steps, as was found by Sorensen.

ONSET OF SKIMMING FLOW

Based on their experimental observations, Essery and Horner (1971) found that for horizontal steps, for the onset of skimming flow, the ratio y_c/l , wherein y_c is the critical depth, increased with h/l from about 0.32 for $h/l = 0.4$ to about 0.69 for $h/l = 0.9$. By a reanalysis of their data, it was found that for the whole range of h/l from 0.4 to 0.9, at the onset of skimming flow, y_c/h was approximately equal to 0.8. This means that for y_c/h greater than 0.8, skimming flow occurs. The observations of Sorensen for $h/l = 1.28$ support this criteria. For y_c/h less than 0.8, one would expect to get nappe flow and in Sorensen's experiments, nappe flow occurred for $y_c/h = 0.16$.

CONCLUSIONS

This technical note presents a method of predicting the characteristics of skimming flow on stepped spillways. For a stepped spillway with a slope of 1 vertical on 0.78 horizontal, the fluid friction coefficient c_f was evaluated using the experimental results of Sorensen and found to be about 0.18. An estimate has been made of the energy loss on stepped spillways for skimming flow.

APPENDIX. REFERENCES

Ervine, D. A., and Baird, J. I. (1982). "Rating Curves for Rivers with Overbank Flow," *Proc. Instn. of Civ. Engrs., Part 2*, Institute of Civil Engineers, 465-472.
 Essery, I. T. S., and Horner, M. W. (1971). "The hydraulic design of stepped spillways." *Report 33*, Constr. Industry Res. and Information Assoc., London, England.
 Rajaratnam, N., and Katopodis, C. (1984). "Hydraulics of Denil fishways." *Proc., ASCE*, 110(9), 1219-1233.
 Rajaratnam, N., Katopodis, C., and Mainali, A. (1988). "Plunging and streaming flows in pool and weir fishways." *Proc., ASCE*, 114(8), 939-944.
 Rajaratnam, N., Van der Vinne, G., and Katopodis, C. (1986). "Hydraulics of Vertical Slot fishways." *Proc., ASCE*, 112(10), 909-927.
 Sorensen, R. M. (1985). "Stepped spillway hydraulic model investigation." *Proc., ASCE*, 111(12), 1461-1472.

$$\begin{aligned} \frac{V_0^2}{2g} &= \frac{Zg y_0 \sin \alpha}{C_f Zg} & \frac{V_0^3}{(2g)^{3/2}} &= \frac{q \sin \alpha}{C_f \sqrt{2g}} \\ &= \frac{y_0 \sin \alpha}{C_f} & \left(\frac{V_0^2}{2g} \right)^{3/2} &= \\ &= \frac{q \sin \alpha}{C_f V_0} & \frac{V_0^2}{2g} &= \left(\frac{q \sin \alpha}{C_f \sqrt{2g}} \right)^{2/3} \\ \frac{V_0^3}{2g} &= \frac{q \sin \alpha}{C_f} & & \\ \frac{V_0^2}{2g \sqrt{2g}} &= \frac{q \sin \alpha}{C_f \sqrt{2g}} & & \end{aligned}$$

- F¹ Routing," *Journal of the Environmental Engineering Division, ASCE*, Vol. 1, No. 331, Feb., 1978.
21. Muzik, I., "State Variable Model of Overland Flow," *Journal of Hydrology*, Vol. 22, No. 3/4, 1974.
 22. Napiorkowski, J. J., Strupczewski, W. G., and Dooge, J. C. I., "Lumped Non-Linear Flood Routing Model and Its Simplification to the Muskingum Model," Rainfall-Runoff Relationship, V. P. Singh, Ed., *Proceedings of International Symposium on Rainfall-Runoff Modeling*, at Mississippi State Univ., May 18-21, 1981.
 23. Nash, J. E., and Farell, J. P., "A Graphical Solution of the Flood Routing Equation for Linear Storage Discharge Relations," *Transactions, American Geophysical Union*, Vol. 36, 1955, pp. 319-320.
 24. Nash, J. E., "A Note on the Muskingum Method of Flood Routing," *Journal of Geophysical Research*, Vol. 64, 1959, pp. 1053-1056.
 25. Overton, D. E., "Muskingum Flood Routing of Upland Streamflow," *Journal of Hydrology*, Vol. 4, 1966, pp. 185-200.
 26. Ponce, V. M., and Yevjevich, V., "Muskingum-Cunge Method with Variable Parameters," *Journal of the Hydraulic Division, ASCE*, Vol. 104, No. HY12, Dec., 1978, pp. 1663-1667.
 27. Ponce, V. M., "Simplified Muskingum Routing Equation," *Journal of Hydraulic Division, ASCE*, Vol. 105, No. HY1, Jan., 1979, pp. 85-91.
 28. Prasad, R., "A Nonlinear Hydrologic Systems Response Model," *Journal of Hydraulic Division, ASCE*, Vol. 93, No. HY4, 1967, pp. 201-221.
 29. Singh, V. P., and McCann, R. C., "Some Notes on Muskingum Method of Flood Routing," *Journal of Hydrology*, Vol. 48, 1980, pp. 343-361.
 30. Stephenson, D., "Direct Optimization of Muskingum Routing Coefficients," *Journal of Hydrology*, Vol. 41, 1979.
 31. Strupczewski, W., and Kundzewicz, Z., "Muskingum Method Revisited," *Journal of Hydrology*, Vol. 48, 1980, pp. 327-342.
 32. Strupczewski, W., and Kundzewicz, Z., "Translatory Characteristics of the Muskingum Method of Flood Routing—A Comment," *Journal of Hydrology*, Vol. 48, 1980, pp. 363-368.
 33. Tung, Y. K., and Mays, L. W., "State Variable Model of Urban Rainfall-Runoff Process," *Water Resources Bulletin, AWRA*, Vol. 17, Apr., 1981.
 34. Venetia, C., "The IUH of Muskingum Channel Reach," *Journal of Hydrology*, Vol. 4, 1969, pp. 185-200.
 35. Wilson, E. M., *Engineering Hydrology*, MacMillan, London, England, 1974.
 36. Young, P., and Beck, B., "The Modeling and Control of Water Quality in River System," *Automatica*, Vol. 10, No. 5, 1974.

RECEIVED

STEPPED SPILLWAY HYDRAULIC MODEL INVESTIGATION

By Robert M. Sorensen,¹ F. ASCE

WOGD, PATEL &
ASSOCIATES

ABSTRACT: A physical hydraulic model investigation was conducted to evaluate the performance of a stepped overflow spillway. The spillway has a standard ogee profile with continuous steps cut into the spillway face from just below the crest, to the toe. The steps significantly increase the rate of energy dissipation on the spillway face, thus eliminating or greatly reducing the need for a large energy dissipation basin at the spillway toe. Primary objectives of the investigation were to evaluate the effectiveness of the flow transition from the smooth crest profile to the steps, to quantify the energy dissipation on the spillway face, and to define the flow characteristics on the steps. The investigation demonstrated that this stepped spillway is quite effective at dissipating energy and that smooth flow transition from the spillway crest to the stepped face is easily achieved.

INTRODUCTION

A stepped spillway has been designed for the new Monksville Dam, which is to be part of the Wanaque South Project being developed by the North Jersey District Water Supply Commission and the Hackensack Water Company. This spillway will be a modification of the Waterways Experiment Station (WES) standard profile for an uncontrolled ogee spillway. At a point just downstream of the spillway crest, steps are designed into the profile so that the envelope of their tips follows the standard profile down to the toe of the spillway. The steps significantly increase the rate of energy dissipation taking place on the spillway face and eliminate or greatly reduce the need for a large energy dissipation basin at the toe of the spillway. The performance of this type of spillway has not been extensively investigated so the designers, O'Brien and Gere Engineers, Inc., contracted with the Hydraulics Division, Fritz Engineering Laboratory, Lehigh University, to conduct hydraulic model investigations of the proposed design.

The stepped spillway concept is not new; a stepped spillway was used on the New Croton Dam built in 1892-1906 (8). However, the writer is not aware of any model or prototypical hydraulic investigations done on this type of spillway prior to 1982. In 1982, results of a Bureau of Reclamation model study of a stepped spillway for the Upper Stillwater Dam (to be constructed in Utah) were published (9). The design cross section for the Upper Stillwater Dam spillway is significantly different from that proposed for the Monksville Dam spillway. Results from the Bureau of Reclamation model study are generally useful for the design of stepped spillways and provided incentive for the use of this concept at Monksville Dam.

¹Prof. of Civ. Engrg., Lehigh Univ., Bethlehem, PA 18015.

Note.—Discussion open until May 1, 1986. To extend the closing date one month, a written request must be filed with the ASCE Manager of Journals. The manuscript for this paper was submitted for review and possible publication on May 16, 1984. This paper is part of the *Journal of Hydraulic Engineering*, Vol. 111, No. 12, December, 1985. ©ASCE, ISSN 0733-9429/85/0012-1461/\$01.00. Paper No. 20220.

The McCallie Dam spillway will have a crest elevation of 400 ft (121.9 m) and a toe elevation that will vary irregularly between 280 ft (85.3 m) and 310 ft (94.5 m). Its crest width will be 200 ft (61 m). The design discharge per foot of spillway crest for energy dissipation considerations is 65 sq ft/sec (6 m²/s) and the probable maximum flood discharge, used to determine the spillway profile, is 100 sq ft/sec (9.3 m²/s). For these two flow rates, the reservoir heads above the spillway crests are 6.3 ft (1.9 m) and 8.6 ft (2.6 m), respectively.

During the preliminary design phase, alternate means of providing energy dissipation for these spillway flows were considered. They include:

1. A standard hydraulic jump stilling basin, which would dissipate a sufficient percentage of the flow energy. However, since the water surface elevation at the spillway toe commonly will fluctuate by 20 ft (6.1 m) or more, extensive rock excavation would be required to set the basin floor at the proper elevation or a large basin end sill would have to be constructed.

2. A 50 ft (15.2 m) wide flip bucket at the toe to deflect the flow sufficiently far from the toe. A resulting jet velocity of about 75 ft/sec (22.9 m/s) would develop a significant scour hole. Design of a successful spillway chute that converges from 200 ft (61 m) to 50 ft (15.2 m) in width and conveys highly super-critical flow would be difficult.

3. A properly designed and constructed stepped ogee spillway should dissipate sufficient energy to not require a stilling basin. It would allow full aeration of spillway flows and should be aesthetically pleasing for typical flow rates over the spillway. The estimated construction cost for this third alternative offers substantial savings over the first two alternatives.

The objective of this study was to investigate the specific stepped spillway design proposed by the design engineers. Primary concerns included:

1. The effectiveness of flow transition from the smooth surface profile at and below the spillway crest, to the first few steps on the spillway face.
2. The amount of energy dissipation in the flow over the stepped spillway and resulting flow velocities at the spillway toe.
3. Training wall heights required to contain the flow along the stepped spillway face.

The specific spillway design being investigated is basic in that it is a straightforward modification of a standard ogee spillway profile. Results of this investigation, which address the aforementioned concerns and indicate that this stepped spillway design is effective, are thus of general value to spillway designers.

SPILLWAY DESIGN PROFILE

The WES standard spillway profile (see Ref. 2, p. 364) was determined for the design flow conditions (probable maximum flood) and then steps

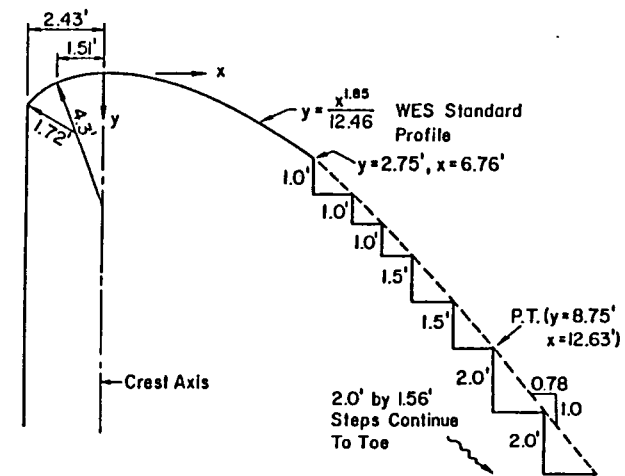


FIG. 1.—WES Standard Profile and Stepped Profile, Upper Portion of Spillway (Prototypical Dimensions)

were fitted to this profile. The standard profile from the upstream face to the point of tangency on the spillway face, which depends on both the design head and the upstream face slope, is shown in Fig. 1. Below the point of tangency the spillway profile has a 0.78 H:1V slope.

Owing to construction techniques for the concrete dam and spillway, the designers decided to use 2 ft (0.61 m) vertical steps below the initial few transition steps. Fig. 1 also shows the resulting step geometry on the face of the upper portion of the spillway. Below the point of tangency, 2 ft by 1.56 ft (0.61 m by 0.48 m) steps continue down to the toe. Above the point of tangency, step sizes decrease in transition to the standard nonstepped ogee profile.

EXPERIMENTAL SETUP

The experimental phase of this study consisted of tests on three two-dimensional sectional models of the proposed spillway. Model scales of 1:10 and 1:25 were used.

Similitude Requirements.—Flow over a spillway involves significant horizontal and vertical components of velocity and acceleration. Thus, a spillway model should be built to undistorted scale. Since gravity forces dominate, Froude similarity criteria define model/prototype scale relationships.

Bureau of Reclamation (3) spillway models for large dams have typically been constructed to scale ratios between 1:30 and 1:100. The Bureau recommends that medium-size spillway models not be smaller than a 1:60 scale. Sharp (7) concurs with this recommendation. Thus, the 1:10 and 1:25 scale models used in this study quite well satisfy these recommended minimum scale requirements. The surface roughness of a concrete spillway is relatively small so the models were built of plexiglas.

The Bureau of Reclamation recommends that the flow depth over the crest of a spillway model be at least 75 mm (0.246 ft) at the design normal operating range to reduce effects of viscosity and surface tension. They also recommend, for two-dimensional spillway models, that the model crest width be at least 150 mm (0.492 ft). These recommendations have been satisfied in this study.

For Froude similarity, the following scale relationships must hold:

$$q_r = L_r^{3/2} \dots\dots\dots (1)$$

$$v_r = L_r^{1/2} \dots\dots\dots (2)$$

where L_r is the model/prototype length ratio; q_r is the discharge per unit width of spillway ratio; and v_r is the velocity ratio. For the 1:10 and 1:25 scale ratios used in this study, this yields discharge ratios of 1:31.6 and 1:125, respectively, and velocity ratios of 1:3.16 and 1:5, respectively.

Flume.—Fig. 2 shows schematic plan and profile sections of the test flume. An 8-in. (20.3-cm) pipe with a butterfly valve for adjusting the flow rate provided flow to the head box. Flow from the tailbox dropped into a 5-ft (1.52-m) diam, 6-ft (1.83-m) high steel cylindrical volumetric tank on the floor below. A flexible pipe from the tailbox allowed direction of the flow into the tank for a flow rate measurement or directly into the sump for recirculation by the pump. The maximum discharge through the flume was limited by the capacity of the tailbox to just under 3 cfs (0.085 m³/s). Flow in the head box passed two baffles before entering the narrower (1-ft wide) test section. The first head box baffle, made of plywood drilled with 1-1/2-in. (38.1-cm) diam holes, smoothed the flow. The second and shorter baffle consisting of a thin aluminum plate with fine holes was installed primarily to dampen surface waves.

There were two model test bays, each having a plywood back wall painted white and a clear plexiglas front wall. The clear viewing sections of each were 45 in. by 70 in. (114 cm by 178 cm) and 42 in. by 52

in. (107 cm by 132 cm), respectively. The first and smaller model was installed in model bay 2; the larger second and third models were placed primarily in bay 1 and extended into bay 2.

Spillway Models.—Three cross-sectional plexiglas spillway models were tested. Specifically, they were:

1. Model A—A 1:10 scale model of the upper 22.75 ft (6.9 m) of the spillway. The model extended down to seven steps below the point of tangency. Model A was used to evaluate the flow transition from the spillway crest to the first several steps and the nature of flow over the steps, for the range of spillway discharges of interest.
2. Model B—A 1:25 scale model of the standard WES ogee spillway profile used as the basis for the stepped spillway. It was a model of the entire 120 ft (36.6 m) spillway profile. This model was briefly tested to provide comparison data for the full stepped spillway profile model (model C).
3. Model C—A 1:25 scale model of the entire stepped spillway profile. Tests with model C were primarily to evaluate energy dissipation in the flow over the stepped spillway and anticipated flow depths along the spillway, to establish training wall dimensions.

Measurements.—The water surface elevation upstream of the spillway crest was measured by a point gage that could be read to the nearest thousandth of a foot. The gage was located 1 ft (0.30 m) upstream of the crest for model A and 0.4 ft (0.12 m) upstream of the crest for models B and C.

The volumetric tank used to measure the flow rate in the system had a capacity of over 115 cu ft (3.26 m³) and could be read to the nearest half cubic foot. Flow rate measurements were probably accurate to within ±2%. A few repeat flow rate measurements made during the testing program were within these limits.

During each test run with models A and C, color photographs of flow conditions were taken. Also, for models A and C, flow conditions between zero flow and the peak flow at which the model was run, were recorded on video tape.

A scale was used to measure the vertical water depth on the spillway in model C, at the spillway crest and at the tips of steps 6, 15, 24, 33, 42, 51 and 59 (toe). When air-entrained flow was encountered, a conservative flow depth that included the bulk of the flow was recorded.

During the tests with models B and C, at least six depth measurements were made at equally spaced intervals across the toe of the structure. In model B, these measurements were made right at the toe while in model C they were made on the horizontal slope downstream of the toe where air entrainment had significantly diminished. With the measured flow rate and the depth measurements, average flow velocities could be calculated from continuity. As a check on this method of determining flow velocities, some velocity measurements were made with a stagnation tube. These measurements yielded results within 10–15% of the values calculated from continuity.

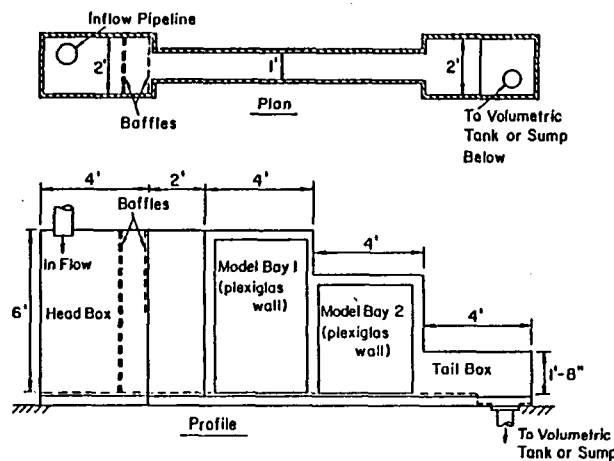


FIG. 2.—Schematic Plan and Profile of Model Test Flume

Test Conditions

Table 1 lists the discharge and related upstream head (upstream surface elevation minus spillway crest elevation) for each test run for the three spillway section models. The head-discharge data are plotted in Fig. 3. The rating curve for the line fit by eye to model A (the larger scale model) data is

TABLE 1.—Model Test Data—Discharge, Upstream Head and Toe Velocity

Model A			Model B				Model C			
Run number (1)	Discharge (cfs/ft) (2)	Head (ft) (3)	Run number (4)	Discharge (cfs/ft) (5)	Head (ft) (6)	Toe velocity (fps) (7)	Run number (8)	Discharge (cfs/ft) (9)	Head (ft) (10)	Toe velocity (fps) (11)
A-1	2.53	0.710	B-1	1.56	0.432	21.3	C-1	1.20	0.413	7.5
A-2	2.27	0.658	B-2	1.14	0.398	17.6	C-2	1.06	0.377	6.6
A-3	1.96	0.626	B-3	0.78	0.321	16.7	C-3	0.89	0.333	7.4
A-4	1.90	0.621	B-4	0.77	0.315	16.9	C-4	0.65	0.283	6.7
A-5	1.83	0.586	B-5	0.70	0.300	16.5	C-5	0.55	0.255	5.9
A-6	1.30	0.476	B-6	0.57	0.267	15.7	C-6	0.40	0.213	4.7
A-7	0.96	0.399	B-7	0.47	0.240	17.9	C-7	0.28	0.168	4.4
A-8	0.55	0.275	B-8	0.33	0.195	15.5	C-8	0.20	0.137	3.8
A-9	0.38	0.217	B-9	0.16	0.115	15.2	C-9	0.097	0.080	2.7
A-10	0.056	0.063	B-10	0.071	0.071	10.3	C-10	0.067	0.068	2.5

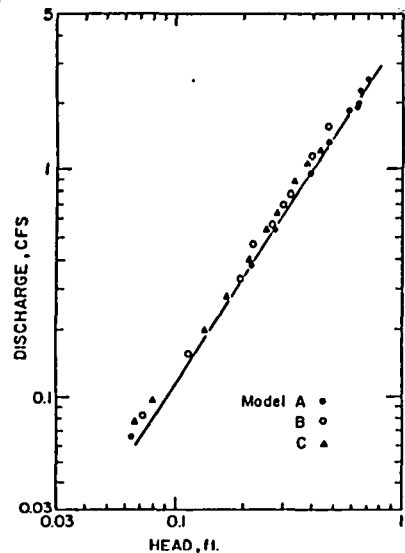


FIG. 3.—Head versus Discharge for each Model

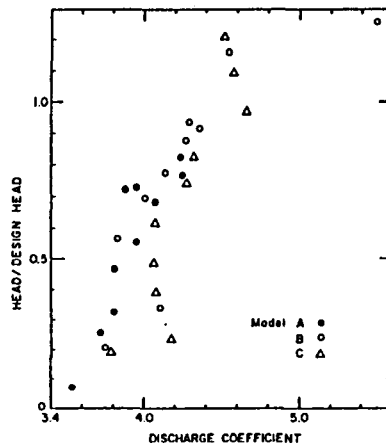


FIG. 4.—Dimensionless Head versus Discharge Coefficient for each Model

$$Q = 4.1 LH^{1.54} \dots \dots \dots (3)$$

where Q is the discharge in cubic feet per second, for a crest width L and upstream head H in feet. The smaller scale models (B and C) have a head-discharge relationship that yields a slightly higher discharge for a given head.

Fig. 4 is a plot of the discharge coefficient, C (from $Q = CLH^{1.5}$), evaluated for each test run, versus the dimensionless head (head/spillway design discharge head). The data very approximately fit a straight-line relationship with a discharge coefficient that varies from 3.5 to over 5. At the design head the discharge coefficient is approximately 4.4. This range of discharge coefficient values is typical (see Ref. 2, Fig. 14-4), but commonly the discharge coefficient increases at a decreasing rate rather than increasing linearly with increasing head. This suggests that the head measuring station might not have been located far enough from the spillway crest.

Results

Test results are presented in three sections as they address, in order, the three study objectives listed in the introduction.

Flow Transition from Crest to Initial Steps.—The 10 test runs with model A were conducted specifically to determine whether any undesirable disturbance of flow developed in the flow transition from the crest to the stepped portion of the spillway profile. For the range of discharges from the highest model discharge of 2.53 cfs/ft (0.233 m³/s/m) down to Run A-9 with a discharge of 0.38 cfs/ft (0.035 m³/s/m), there was a smooth transition of flow onto the steps. The free surface was smooth down to the point of initiation of air entrainment. This point of air entrainment was located past the end of the spillway section for Runs A-1 to A-6 and moved progressively up from step 10 in Run A-7 to step 4 in Run A-9. For flow rates less than the flow rate in A-9,

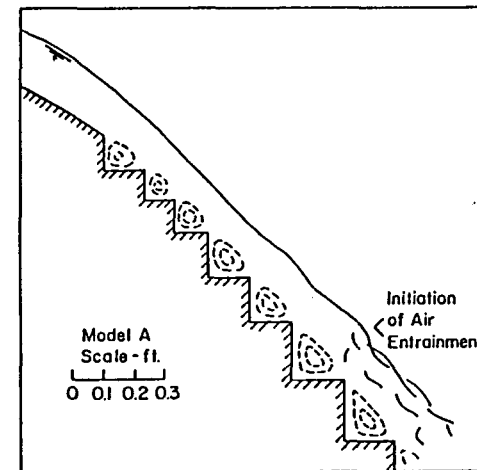


FIG. 5.—Flow Conditions, Run A-8

the air entrainment worked its way up to step 1.

For test runs A-1 to A-9, the typical flow conditions over the steps were as demonstrated in Fig. 5 for Run A-8. At each step, whether air entrainment was occurring or not, a stable rolling vortex developed in the step. The overlying flow moved down the spillway supported by the vortices and tips of the steps. Injection of dye indicated that flow enters a vortex, rotates in the vortex for a brief period and then returns to the main flow to proceed on down the spillway face. At the steps where air entrainment occurs, air bubbles penetrated the vortices and could be seen rotating with the vortex flow.

For Run A-10, which had a very low flow rate of 0.056 cfs/ft (0.0052 m³/s/m), a thin film of water approximately 0.01-ft (0.3-cm) thick flowed off the spillway crest, hit the top of the first step, and deflected outward/downward hitting the spillway face again several steps further down the spillway. The model flow rate in Run A-10 represents a prototypical flow rate of 1.8 cfs/ft (0.16 m³/s/m), which is typical of normal daily summertime flows at the site.

The spillway designers wanted to eliminate this deflecting jet of water so that modifications in the model A profile were made and tested for low model rates of 0.2 cfs/ft (0.019 m³/s/m) and less. These tests indicated that the best way to eliminate the deflecting jet of water was to add a few smaller steps on up the face of the spillway. Fig. 6 shows the

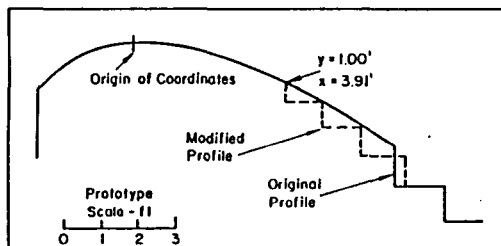


FIG. 6.—Original and Modified Spillway Crest Profiles

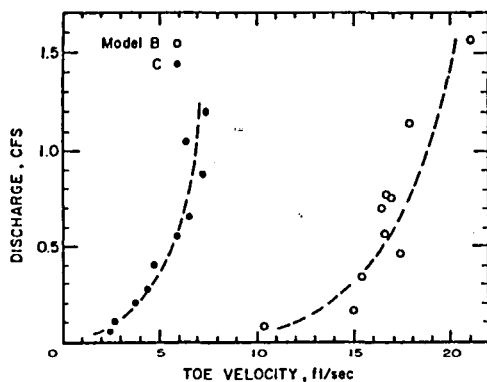


FIG. 7.—Toe Velocities for Models B and C

original and final modified spillway profiles near the crest. Three steps, each having a vertical rise of 0.75 ft (0.23 m) and one step with a rise of 0.5 ft (0.15 m) were added. The worst jet from the new first step only deflected to the new third step, a vertical distance of 1.5 ft (0.46 m) in the prototype.

With extremely low flows in the model of the order of 0.03 cfs/ft (0.0028 m³/s/m), the flow cascades over the steps, falling from step to step in a thin choppy layer that clings to the face of each step.

Thus, with the modified profile, for flow rates from zero up to the probable maximum flood, there is effectively a smooth flow transition from the crest to the spillway steps.

Energy Dissipation.—Table 1 also lists the flow velocities at the spillway toe for models B and C. Fig. 7 is a plot of toe velocity versus discharge for both models. Data scatter is somewhat greater for model B, owing to the smaller depths being measured at the toe. However, the expected trend of increasing toe velocity with increasing discharge is clear and the general amount of velocity reduction caused by the addition of steps is well defined.

For the model probable maximum flood discharge of 0.80 cfs/ft (0.074 m³/s/m), the toe velocity was reduced from approximately 18 fps (5.5 m/s) for the standard spillway to 6.5 fps (2.0 m/s) for the stepped spillway. At the model energy dissipation design discharge of 0.52 cfs/ft (0.048 m³/s/m), the toe velocity was reduced from approximately 16.5 fps (5.0 m/s) to 5.5 fps (1.7 m/s). The model B to model C toe velocity ratios thus were 2.8 and 3.0, respectively, and increased to just over 4 for a low model discharge of 0.1 cfs/ft (0.009 m³/s/m). Consequently, the kinetic energy in the flow at the stepped spillway toe varies from about 12 to 6% of the energy at the standard spillway toe for this range of model discharges.

Training Wall Heights.—Vertical water depth measurements made at the crest and at the tips of selected steps along the spillway for model

TABLE 2.—Depth Measurements and Step at which Air Entrainment Commences—Model C

Run (1)	Crest (2)	Step 6 (3)	Step 15 (4)	Step 24 (5)	Step 33 (6)	Step 42 (7)	Step 51 (8)	Step 59 (9)	Air entrainment step (10)
C-1	0.318	0.308	0.230	0.213	0.230	0.279	0.279	0.295	36
C-2	0.289	0.256	0.187	0.197	0.230	0.262	0.279	0.295	31
C-3	0.249	0.213	0.148	0.171	0.197	0.213	0.213	0.230	25-26
C-4	0.213	0.164	0.131	0.164	0.164	0.180	0.180	0.196	22-23
C-5	0.190	0.144	0.131	0.164	0.180	0.197	0.197	0.213	19
C-6	0.157	0.112	0.131	0.164	0.164	0.180	0.197	0.197	15
C-7	0.119	0.079	0.131	0.148	0.148	0.164	0.164	0.180	11
C-8	0.097	0.052	0.082	0.082	0.082	0.092	0.098	0.115	8-9
C-9	0.056	0.046	0.059	0.059	0.059	0.066	0.066	0.069	6
C-10	0.038	0.046	0.049	0.049	0.049	0.049	0.049	0.049	4

Note: Depths measured vertically, in feet, from tip of step to water surface. Step at which air entrainment starts is listed in last column.

C are listed in Table 2. Also listed for each run is the step at which air entrainment commenced. Typically, the depth decreased as flow descends from the crest to the point at which air entrainment commences. Beyond this point, owing to bulking of the flow by the air entrainment, the depth continually increased toward the spillway toe.

DISCUSSION

The toe velocity and discharge data for the stepped and unstepped spillway models (C and B, respectively) was scaled up to prototypical conditions using the scale ratios given in a previous section. These data are plotted in Fig. 8.

Bradley and Peterka (1) present a chart based on "experience, computation, and a limited amount of experimental information obtained from prototype tests on Shasta and Grand Coulee Dams," that yields a preliminary design estimate of toe velocities for ogee spillways with slopes between $0.6H:1V$ and $0.8H:1V$. Toe velocities calculated using this chart are also plotted in Fig. 8. Velocities scaled from model B test results for the unstepped spillway typically exceed velocities calculated from Ref. 1 by 15–20%. Even at discharges exceeding the probable maximum flood in model B, there was no air entrainment on the spillway face. In the prototype, air entrainment would be expected. This scale effect is likely to be the primary cause for the unstepped spillway velocity differences in Fig. 8. In other words, the model surface roughness and resulting turbulent boundary layer growth and air entrainment were not sufficient to exactly simulate the prototypical conditions.

For the stepped spillway, the scaled steps form the dominant "surface roughness." So with typical model spillway face depth Reynolds numbers in the order of 10^5 , scale effects should be less and predicted prototypical toe velocities should be closer (but still probably a bit higher) to true prototypical values.

Thus (see Fig. 7), the prototype stepped spillway designed for Monksville Dam will typically have toe velocities of 30 fps (9.2 m/s) at the probable maximum flood discharge, compared to toe velocities of 75 fps

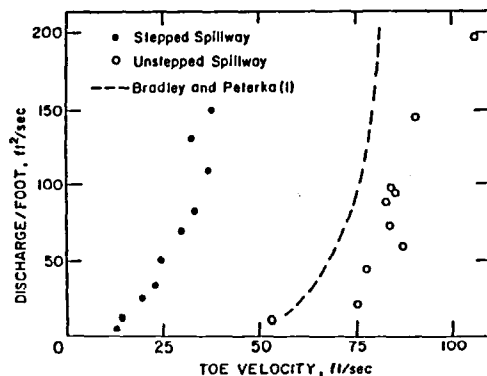


FIG. 8.—Prototypical Toe Velocities for Stepped and Unstepped Spillways

(22.9 m/s) for a prototypical unstepped spillway. This represents a kinetic energy dissipation of 84%, which is as good as or superior to the energy dissipation achieved in a typical well-developed hydraulic jump (see Ref. 2, p. 396).

Morris (5,6) investigated flow past surfaces with large uniformly spaced surface roughness elements and defined three regimes: (1) isolated roughness flow in which each element generates a wake that diffuses into the main flow before reaching the next element; (2) wake interference flow where the elements are sufficiently close together that the wake extends to the following element; and (3) skimming or quasi-smooth flow in which surface elements are spaced so close as to form a "pseudo-wall" that flow skims over and between which stable depression vortices form. In skimming flow, the vortices are maintained through transmission of shear stress from the fluid flowing past the tips of the elements. In addition, small-scale vorticity will be generated continuously at the tips of the elements. Energy is expended to generate the tip vorticities and to maintain the stable depression vortices. Quasi-smooth flow well defines the conditions observed on the stepped spillway.

Knight and MacDonald (4) investigated subcritical open channel flow resistance caused by roughness elements with square cross sections at 10 uniform spacings including one that caused quasi-smooth flow. Their results, and their evaluation of data from other authors, shed further insight into the rectangular cross section depression dimensions for which quasi-smooth flow will develop, and they recommend an improved form of bed resistance equation for quasi-smooth flow. They also demonstrate that the maximum bed resistance for square resistance elements will occur for the wake interference flow regime.

Much fruitful research can still be done to develop useful information to guide the design of steps for spillway faces, designs that will optimize response to construction and energy dissipation requirements. Specifically, the optimum depression shapes, sizes and spacings for supercritical flow need to be determined.

CONCLUSION

An ogee spillway with a stepped face can be designed to perform satisfactorily for the full range of discharges encountered by the spillway. A stepped spillway's energy dissipation characteristics are comparable to those of an unstepped spillway with a hydraulic jump stilling basin at the toe.

Research should be conducted to provide additional information necessary to optimize the step geometry for a given spillway discharge, face slope, and crest elevation.

ACKNOWLEDGMENT

This study was funded through a contract with O'Brien and Gere Engineers, Inc., Blue Bell, PA.

G. P. Lennon and R. N. Weisman from the Hydraulics Division assisted with planning of the test setup and procedure and conduct of the tests. Cathy Miller, Nate Beil, Gary Wisniewski, Tim Kyper, Pete Sit-

kowski, Jo.ifford, Jeff Bell and Jon Sorensen, all from the Hydraulics Division, provided support in numerous ways.

APPENDIX.—REFERENCES

1. Bradley, J. N., and Peterka, A. J., "The Hydraulic Design of Stilling Basins: Short Stilling Basin for Canal Structures, Small Outlet Works and Small Spillways (Basin III)," *Journal of the Hydraulics Division*, Vol. 83, No. HY5, Paper 1403, Oct., 1957, 22 pp.
2. Chow, V. T., *Open-Channel Hydraulics*, McGraw-Hill Book Co., Inc., New York, NY, 1959, 680 pp.
3. *Hydraulic Laboratory Techniques*, Water and Power Resource Service, Department of the Interior, Denver, CO, 1980, 208 pp.
4. Knight, D. W., and MacDonald, J. A., "Hydraulic Resistance of Artificial Strip Roughness," *Journal of the Hydraulics Division*, ASCE, Vol. 105, No. HY6, June, 1979, pp. 675-690.
5. Morris, H. M., "A New Concept of Flow in Rough Conduits," *Transactions*, ASCE, Vol. 120, 1955, pp. 373-410.
6. Morris, H. M., "Design Methods for Flow in Rough Conduits," *Transactions*, ASCE, Vol. 126, Part 1, 1961, pp. 454-490.
7. Sharp, J. J., *Hydraulic Modeling*, Butterworth and Co., London, U.K., 1981, 242 pp.
8. Wegman, E., "The Design of the New Croton Dam," *Transactions*, ASCE, Paper 1047, June, 1907, pp. 398-457.
9. Young, M. F., "Feasibility Study of a Stepped Spillway," Hydraulics Division Specialty Conference, Jackson, MS, Aug., 1982, pp. 96-105.

TURBIDITY CURRENT WITH EROSION AND DEPOSITION

By J. Akiyama¹ and H. Stefan²

ABSTRACT: The equations which govern the movement of two-dimensional gradually varied turbidity currents in reservoirs and over beaches are derived and solved numerically. Turbidity currents are sediment-laden gravity currents that exchange sediment with the bed by erosion or deposition as the flow travels over the downslope. Turbidity currents derive this driving force from the sediment in suspension. They experience a resisting shear force on the bed and entrain water from above. Turbidity currents can be eroding or depositive, accelerating or decelerating, dependent on the combination of initial conditions, bed slope, and size of sediment particles. They can be controlled from upstream (supercritical) or downstream (subcritical). Gravity currents with and without erosion and deposition are examined in order to understand the effects of sediment exchange on the flow.

INTRODUCTION

Turbidity currents are gravity currents consisting of a sediment-water mixture flowing over a sloping bottom (Fig. 1). Similar gravity currents can be produced by salinity or temperature differences and have then been referred to as inclined plumes or underflows (8,17,18,19,26). In turbidity currents, suspended sediment makes the density of the mixture greater than the density of the ambient water and provides the driving force; the sediment laden flow must generate enough turbulence to hold the sediment in suspension. Uniform or gradually varied turbidity currents with very fine sediment and therefore without erosion or deposition of sediment have been studied by Ashida and Egashira (3), Bonnefille and Goddet (5), and Stefan (25) among others.

Turbidity currents have been observed where inflows carrying a relatively high concentration of suspended material enter lakes (20), reservoirs (11), or the ocean (16). Two types of turbidity currents can be distinguished: (1) Low velocity, low density (5); and (2) high velocity, high density (16). High velocity, high density turbidity currents often carry suspended materials introduced near the shore to the deep sea, and even have enough erosive power to produce submarine canyons (13).

Turbidity currents can be originated by various processes. Discharges of large amounts of sediments, e.g., mine tailings (Silver Bay in Lake Superior), underwater landslides caused by earthquakes (the Grand Banks), and resuspension of suspended materials by waves during storms are three possibilities. Turbidity currents can be erosive or depositional.

¹Grad. Student, St. Anthony Falls Hydraulic Lab., Dept. of Civ. & Mineral Engrg., Univ. of Minnesota, Minneapolis, MN 55414.

²Prof. and Assoc. Dir., St. Anthony Falls Hydraulic Lab., Dept. of Civ. & Mineral Engrg., Univ. of Minnesota, Minneapolis, MN 55414.

Note.—Discussion open until May 1, 1986. To extend the closing date one month, a written request must be filed with the ASCE Manager of Journals. The manuscript for this paper was submitted for review and possible publication on August 20, 1984. This paper is part of the *Journal of Hydraulic Engineering*, Vol. 111, No. 12, December, 1985. ©ASCE, ISSN 0733-9429/85/0012-1473/\$01.00. Paper No. 20216.

Flow and energy dissipation in gabion stepped weirs

L. Peyras, P. Royet, G. Degoutte

ABSTRACT. Gabions are commonly used for building small dams in the Sahel region of Africa; gabion weir technology is widespread in flood spillways. In addition to good mechanical stability and a high level of resistance to flood flows, a gabion weir dissipates large amounts of energy above the stilling basin. Nevertheless, the optimum dimensions for this type of structure are not yet well defined. In order to quantify the energy dissipated on the steps of such structures, a systematic study of standard spillways 3 to 5 m high, with flowrates up to $3 \text{ m}^3 \cdot \text{s}^{-1} \cdot \text{m}^{-1}$, has been carried out on a 1:5 scale model.

The energy dissipation has been quantified and the dimensioning parameters of the stilling basin have been determined. The test results led to a 10 to 30 % reduction of the stilling basin length compared to the methods previously used. The study also attempted to characterize flow over steps and define the phenomena observed during the different hydraulic regimes.

Introduction

Gabions remain the preferred material for buiding hydraulic structures. Especially in the Sahel region of Africa, the social, economic and technical contexts are such that gabions are commonly used for building small earth dams. The design of these dams is relatively standard; in particular, gabions are commonly used in flood spillways. As a matter of fact, gabion spillways offer a solution which is often selected. These weirs are characterized by good mechanical stability, high resistance to flood flows and relative ease of construction.

Nevertheless, the rules for dimensioning this type of weir are not well established, especially the length of the stilling basin. The existing literature on gabion structures at best proposes methods similar to those applied to smooth inclined weirs [3] or to straight drop weirs [1]. The analytic methods provided do not take into account the energy dissipation due to the stepped profile, and lead to oversized stilling basins. Only STEPHENSON has run tests on gabion stepped sills at the 1:10 scale [9]. However, the scale models were less than 4 m in height and involved infiltration through the upstream facing, thus restricting the application of the test results to permeable sills in streams.

Because of the complexity of flow over stepped surfaces and within the gabions themselves, analytic methods such as numerical modelling are hard to apply and scale models remain the preferred method of investigation. Many stepped weirs have been tested,

mainly in connection with large concrete dams for which infiltration phenomena are excluded and transient hydraulic regimes, basic to our study, are negligible [4], [8].

For these reasons, we carried out scale model testing in order to observe flow over small weirs with steps of uniform height, in order to quantify the energy dissipation over "standard" gabion stepped weirs and to establish the dimensioning parameters for the stilling basin. Finally, we attempted to analyse gabion deformation and some problems related to the durability of structures during floods.

Scale model testing

Scale models

The 1:5 scale used was sufficiently large to approximate closely the actual hydraulic phenomena and minimize similitude and measurement errors. The gabions used in the model were exactly at the 1:5 scale, i.e. geometric dimensions of 20 cm x 20 cm x 60 cm (actual gabions of 1 m x 1m x 3m), hexagonal wire mesh of 20 mm x 30 mm (actual 100 x 120 mesh type) and 0.7 mm wire diameter (3.5 mm actual diameter), and filling aggregate (30 to 40 mm ballast). The terminology and units used in this paper are described in the appendix.

Testing was carried out in the 80 cm wide glass-enclosed canal of the Société du Canal de Provence. The simulated flowrates (10 per test) ranged from 0.5 to 3 m³.s⁻¹.ml⁻¹. Only the downstream dam facing was reproduced; the upstream facing was replaced with a waterproof membrane.

We tested energy dissipation on weirs having the following characteristics (*fig.1*):

- downstream facing slopes of 1:1, 1:2 and 1:3;
- weir heights of 3, 4 and 5 m, i.e. 3, 4 and 5 steps respectively (standard step height of 1 m).

Different stepped profiles were reproduced (*fig. 2*):

- gabion steps or "bare" gabions;
- steps with a tread protected by a horizontal concrete slab; the "concrete slab" technique is recommended when floodwaters are loaded with sediments;
- steps with a tread protected by a "counter-sloped" concrete slab;
- steps with a nose having a "counter-sill" made of a flat gabions.

The flow of water over surface weirs is characterized by high velocities. The gravitational force dominates all other external forces, allowing Froude's similitude to be used. All results correspond to the 1:1 scale.

Instruments

The specific loads at the weir toe were measured with a Pitot ramp, i.e. a series of Pitot tubes placed along a cross-section and connected to the same reading tube. This ramp, a copper tube with small openings facing the flow lines, integrates the specific load (H_s) over a weir section. As opposed to a Pitot tube which would record all flow variations at a specific point of the section, the Pitot ramp gives stable readings of (H_s). An accurate calibration of the ramp gave a default error between 6 and 10 % depending on the flowrate; the test results were correspondingly increased.

The flowrate of the water entering the glass-enclosed canal was measured with a standard thin-walled triangular weir. Volume measurements have shown the flowrate error to be less than 3 %.

Testing methodology

The total initial head of the flow over the sill (E_0) is calculated in the critical section, from the flowrate :

[Formula]

H : weir height

Y_c : critical depth; $Y_c = (q^2/2g)^{1/3}$, with q the flow rate per unit of sill length (in $m^3 \cdot s^{-1} \cdot m^{-1}$).

The residual head (E_1) at the weir toe (at the stilling basin entrance, upstream of the jump) is measured with the Pitot ramp. The head loss $E_0 - E_1$ can then be calculated.

Flow over steps

Testing has shown two flow types: *nappe flow* and *skimming flow*.

Nappe flow

Nappe flow is observed for low to medium flowrates. The overflowing sheet of water strikes the tread of the next lower step, totally first (*free nappe*) and then partially (*partial nappe*).

Free nappe flow

Two hydraulic regimes are possible, one characterized by the alternation of fluvial and torrential regimes, and the other

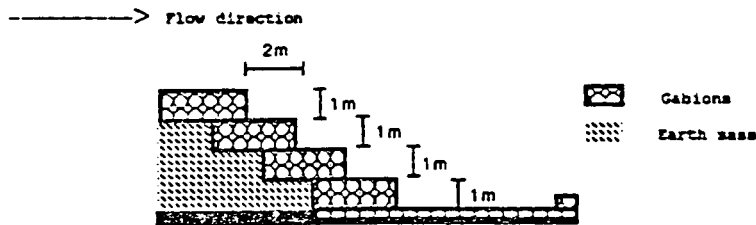
exclusively torrential.

a. *Alternation of fluvial and torrential regimes*: an hydraulic jump begins just downstream of the striking point of the overflowing sheet of water. This type of flow has been observed only for counter-sloped or counter-silled profiles and for low flowrates (lower than $1 \text{ m}^3 \cdot \text{s}^{-1} \cdot \text{ml}^{-1}$).

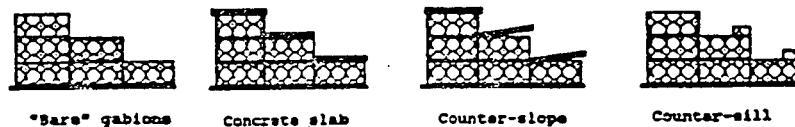
A simple model can be proposed for this particular case, which correlates well with our test results (fig. 3):

- at the striking point of the overflowing sheet of water, the flow has a minimal depth Y_1 . Under the sheet of water, at the foot of the step, a water cushion forms, with a depth Y_2 ;
- the jump starts in section 1;
- just downstream of the jump in section 2, the flow becomes fluvial, with the depth Y_2 ;
- between section 2 and section 3, the flow speeds up because of the drop, becomes torrential again and takes the critical depth Y_c in section 3.

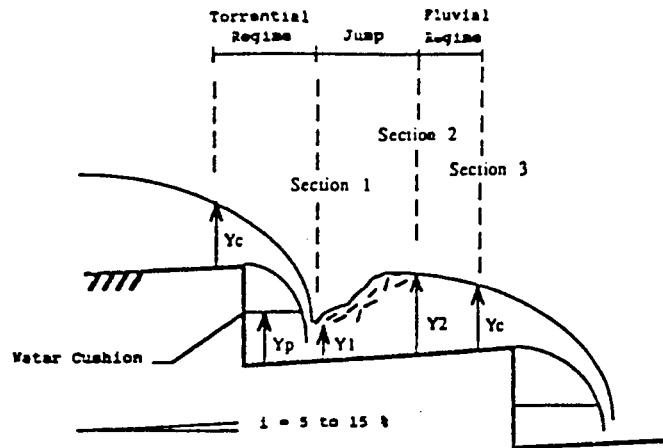
The hydraulic conditions are identical from one step to the next; for each step, the flow dissipates an amount of energy equivalent to its height. We can then propose an energy dissipation formula for stepped weirs and free nappe flow:



1. Example of a downstream stepped facing made of gabions (height 4 m and slope 1:2), with the gabion-lined stilling basin at the weir toe.



2. Stepped profiles included in the tests



3. Free nappe flow with alternation of fluvial and torrential regimes.

- weir crest energy:

$$E_0 = n \cdot h + 3/2 Y_c, \text{ for a weir with } n \text{ steps, each } h \text{ meters high (} nh = H \text{).}$$

- weir toe energy:

$$E_1 = Y_1 + V_1^2/2g$$

$$\Rightarrow E_0 - E_1 = n \cdot h + 3/2 Y_c - Y_1 - q^2/(2g \cdot Y_1^3) \quad (1)$$

RAND has investigated the hydraulic behavior of water falling onto a concrete step h meters high; he proposes a set of empirical equations defining the parameters: [7]

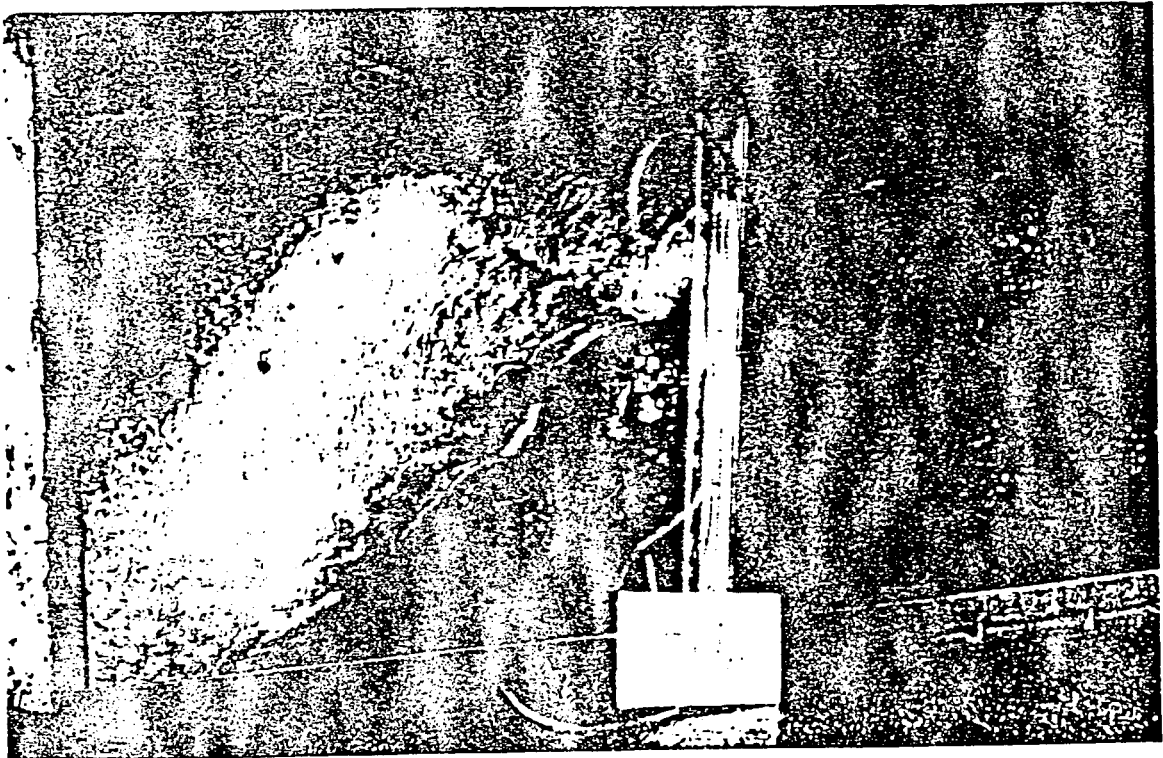
$$\begin{aligned} Y_1/h &= 0.54 \cdot (q^2/(g \cdot h^3))^{0.425} \\ Y_2/h &= 1.66 \cdot (q^2/(g \cdot h^3))^{0.27} \\ Y_p/h &= (q^2/(g \cdot h^3))^{0.22} \end{aligned} \quad (2)$$

with q the flowrate ($m^3 \cdot s^{-1} \cdot m^{-1}$) of the sheet of water and (Y_1, Y_2, Y_p) the depths defined above.

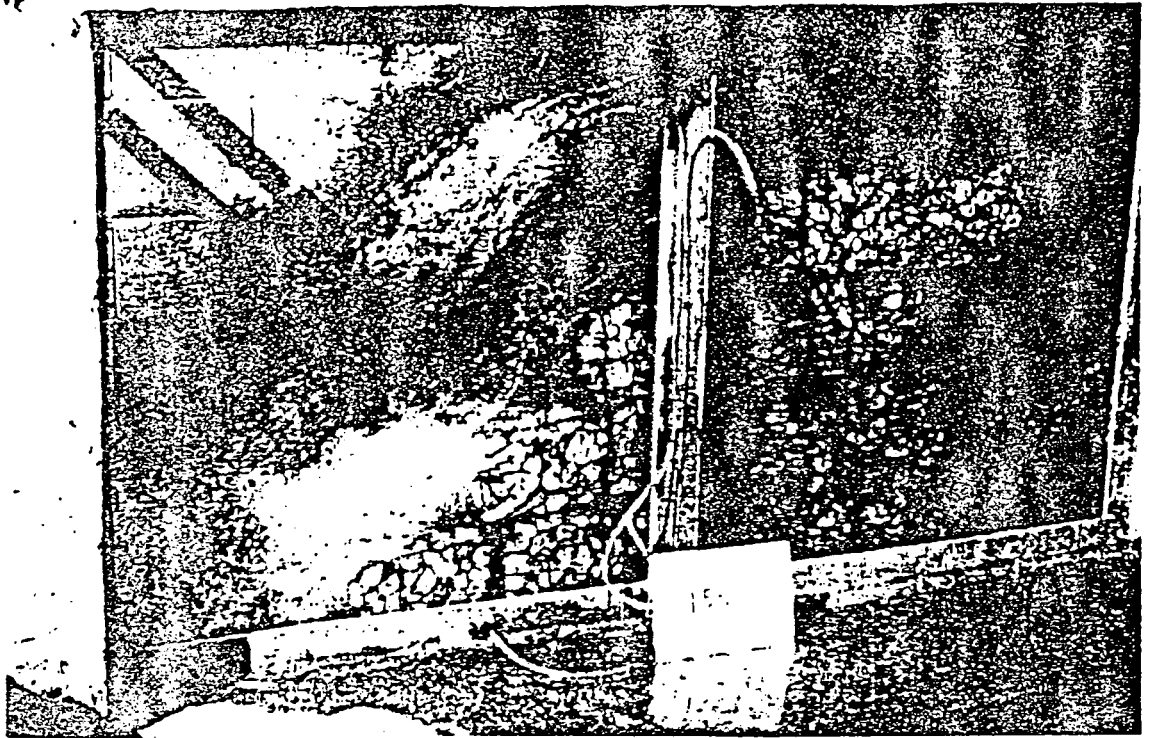
By combining equations (1) and (2), we can calculate the head loss over stepped weirs, and check the validity of these formulas for gabion structures by using $h = 1$ m. The test results for free nappe flow, but also for all types of nappe flow, are close to those from modelling: the actual energy dissipation is at most 10 % greater than that calculated from the model. This difference between testing and modelling can be attributed to the fact that some parameters such as infiltration into the gabions, roughness difference between gabions and concrete and weir slope, are not taken into account in the analytical model.



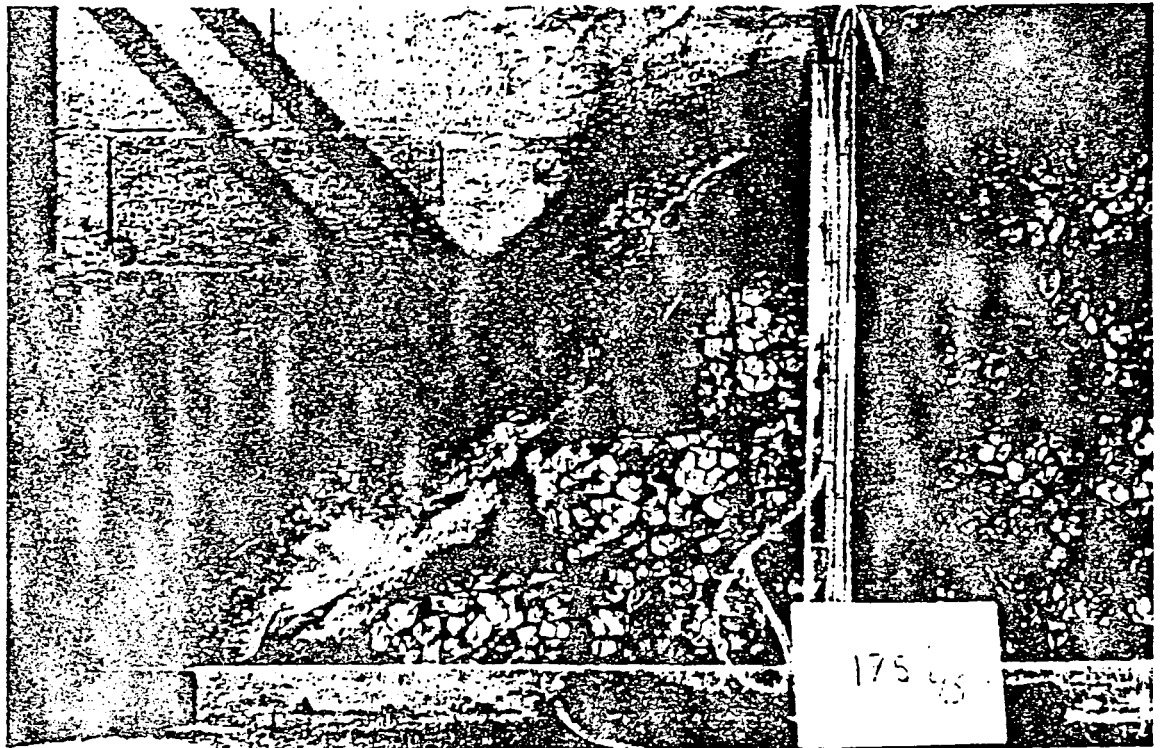
(A)



(B)



(c)



(d)

A. Free nappe flow over a weir of slope 1:3 and height 4 m; counter-sloped steps; alternation of fluvial and torrential regimes; flowrate of $0.60 \text{ m}^3 \cdot \text{s}^{-1} \cdot \text{ml}^{-1}$.

B. Free nappe flow over a weir of slope 1:1 and height 5 m; steps with concrete slab protection; torrential regime; flowrate of $1.03 \text{ m}^3 \cdot \text{s}^{-1} \cdot \text{ml}^{-1}$.

C. Skimming flow over a weir of slope 1:1 and height 5 m; steps of "bare" gabions; torrential regime; flowrate of $2.17 \text{ m}^3 \cdot \text{s}^{-1} \cdot \text{ml}^{-1}$.

D. Skimming flow over a weir of slope 1:1 and height 5 m; steps of "bare" gabions; torrential regime; flowrate of $2.45 \text{ m}^3 \cdot \text{s}^{-1} \cdot \text{ml}^{-1}$.

b. *Torrential regime:* Without a counter-sill or a counter-slope, water velocity remains high and the hydraulic jump is forced downstream of the step. Intense bubbling can be observed downstream of the striking zone of the overflowing sheet of water, but the flow remains torrential over the entire weir (fig. 4).

The nappe flow regime over horizontal steps ("bare gabion" or "concrete slab" profiles) is always torrential. For "counter-sloped" or "counter-silled" weirs, the regime becomes torrential above a certain flowrate.

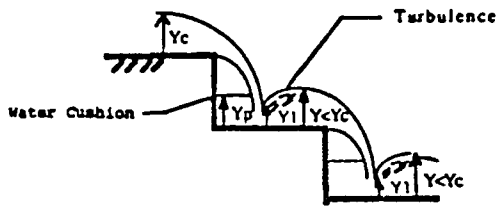
Partial nappe flow

The overflowing sheet of water partially strikes the tread of the next lower step and the jet bursting at each step generates intense bubbling. The regime remains torrential over all the steps (fig. 5).

Nappe flow energy dissipation

Nappe flow energy dissipation occurs in two phases: when the sheet of water strikes the step, then in the zone of intense bubbling after the jet has burst, with or without formation of an hydraulic jump.

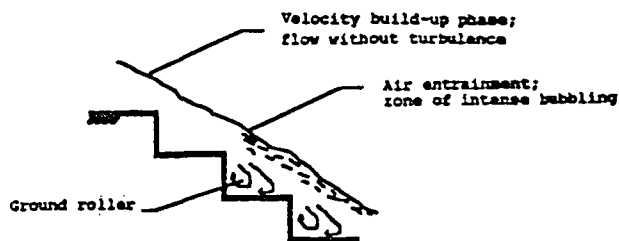
As a first approximation, we can evaluate the energy dissipation over gabion weirs by extrapolating the modelling of free nappe flow to all types of nappe flow. Our results show that this extrapolation of formulas (1) and (2) is valid within 10 %.



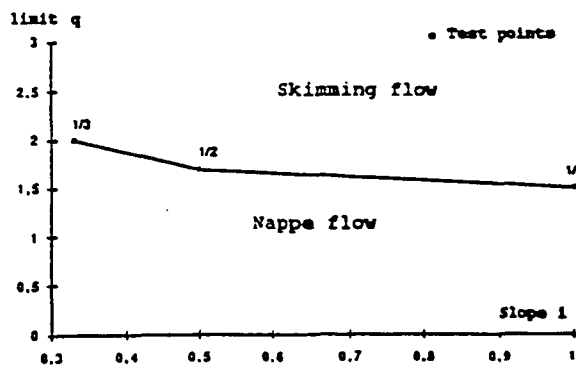
4. Free nappe flow with constant torrential regime



5. Partial nappe flow



6. Skimming flow



7. Limit unit flowrate q ($m^3/s/ml$) between nappe and skimming flows, as a function of slope i (m/m) for stepped weirs made of "bare" gabions.

g flow was observed for average to high flowrates; the weir is not visible and the weir is totally submerged in relatively smooth current.

stream to downstream, two zones can be identified (fig.

transient zone over the first two steps; the flow until it reaches the maximum limit velocity V_{max} for entrainment begins; there is no bubbling during this build-up phase and the upper surface of the flow is undisturbed over the weir.

reaches the limit velocity V_{max} for which air entrainment particles mix with the stream of water and intense turbulence develops down to the weir toe. The water cushion at the first step is replaced by a ground roller showing the entrained air bubbles; the stream of water moving along is supported by the ground rollers and the noses of steps.

limit velocity of air entrainment depends only on the weir characteristics, especially step height ($h = 1$ m in this case) and whatever the flowrate of the simulated flood (up to 3 m/s) the measured values of V_{max} ranged from 5.5 to 6 m/s on a weir slope. When V_{max} was attained, the water velocity decreased slightly; in addition to losing h meters of potential energy at each step, the flow also dissipated some of its kinetic energy.

SORENSEN proposes a *skimming flow* model based on tests by SORENSEN [6], [8].

Transition between nappe and skimming flows

Flow develops for flowrates higher than those of nappe flow. Geometrical characteristics of the steps are definitely modified at the onset of air entrainment: a steep slope and the steps are conducive to *skimming flow*. Figure 7 shows the transition between the two flow regimes.

Flow over gabion weirs

Experimental presentation of the results

Parameters controlling flow over gabion steps are the

parameters of the flow (from h to H steps);

counter-slope; on steps with

with the slope i ,

other external

parameters necessary to determine the head loss h_f/H

dimensionless

weir;

proportional to the square

h_f/H (weir toe

and 9) in the form $Y_2 = Y_1/H$; $Y_1 = h_f/H$

proportional to X when X is of the form:

giving the least

The best-fit coefficients are provided in tables I and II.

Table I

Relationship between $Y_1 = (E_0 - E_1)/H$ and $X = q^2/(g.H^3)$ in the form $1/(1 - Y_1) = a_1 \cdot X^{b_1}$; best-fit coefficients a_1 and b_1 ; coefficient of determination r^2 .

	Ln (a_1)	b_1	r^2 (Coef. of determination)
Slope 1:3 (16 pairs)	-1.568	-0.647	0.904
Slope 1:2 (25 pairs)	-1.778	-0.654	0.964
Slope 1:1 (28 pairs)	-1.434	-0.526	0.874

Table II

Relationship between $Y_2 = Y_1/H$ and $X = q^2/(g.H^3)$ in the form $Y_2 = a_2 \cdot X^{b_2}$; best-fit coefficients a_2 and b_2 ; coefficient of determination r^2 .

	Ln (a_2)	b_2	r^2 (Coef. of determination)
Slope 1:3 (15 pairs)	-1.074	0.248	0.974
Slope 1:2 (25 pairs)	-1.157	0.247	0.941
Slope 1:1 (28 pairs)	-1.163	0.263	0.888

Domain of validity of the graphs

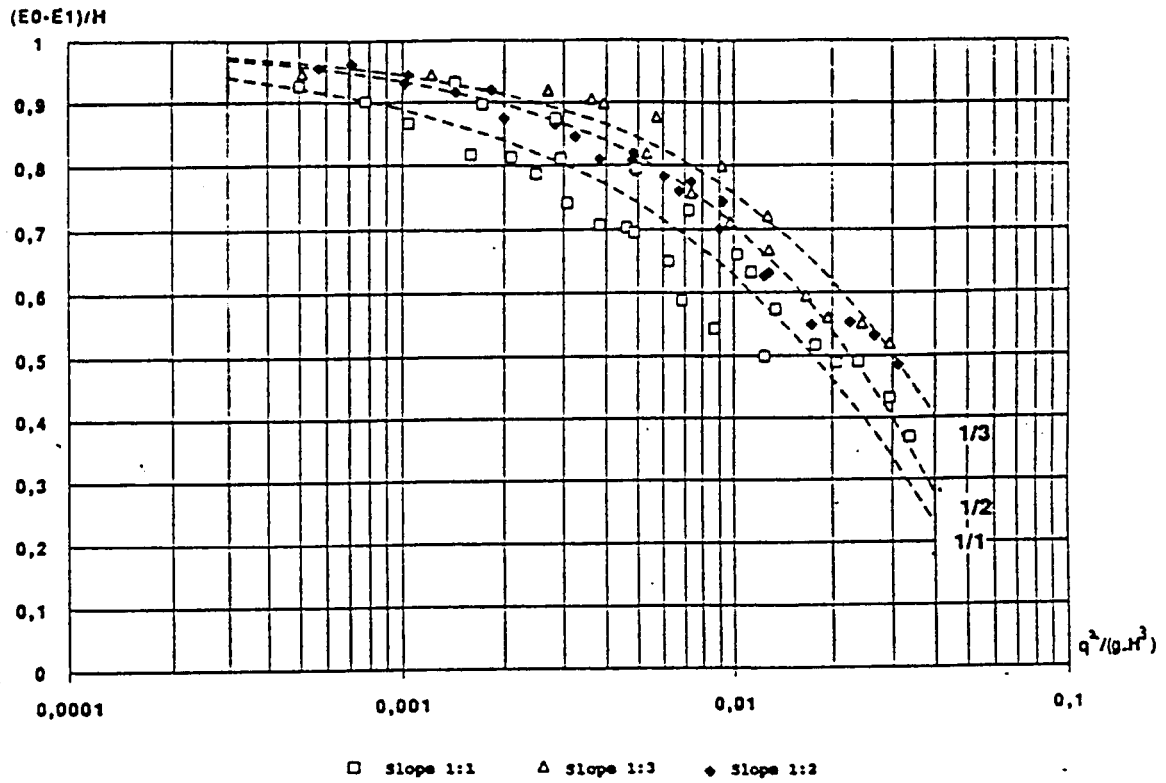
Only flowrates of less than $3 \text{ m}^3 \cdot \text{s}^{-1} \cdot \text{ml}^{-1}$ are considered, since the weir could be damaged by higher flowrates (see the "gabion deformation" section).

The graphs (figs. 8 and 9) represent tests carried out on weirs 3, 4 and 5 m high. The dimensionless representation allows us to extrapolate these results. We nevertheless recommend restricting extrapolation to heights between 2 and 7 m, in order not to deviate too much from our test range.

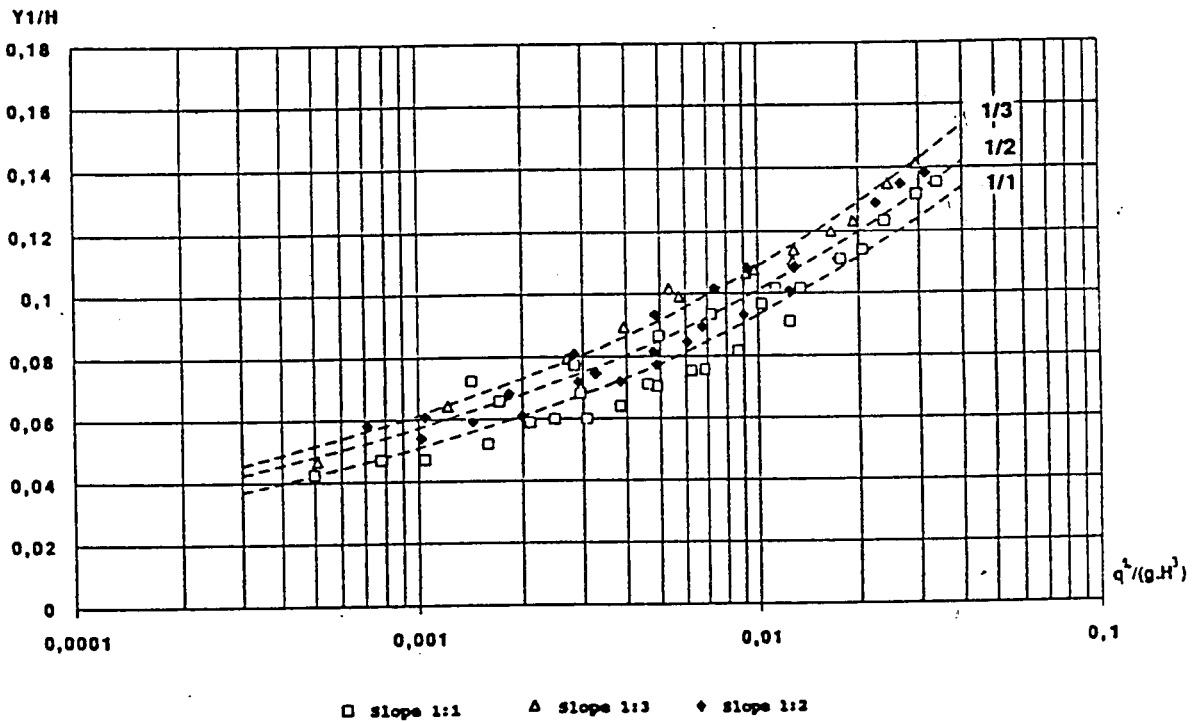
The results can nevertheless be interpolated for weirs with slopes between those we experimented with, 1:1.5 or 1:2.5 for example.

Methodology for dimensioning the stilling basin

Knowing the weir geometry (slope, height and spilling length) and the flood parameters of the project, this study allows us to determine the depth Y_1 corresponding to "bare" gabion steps (graph of fig. 9)



8. Unit head loss over a stepped weir made of "bare" gabions

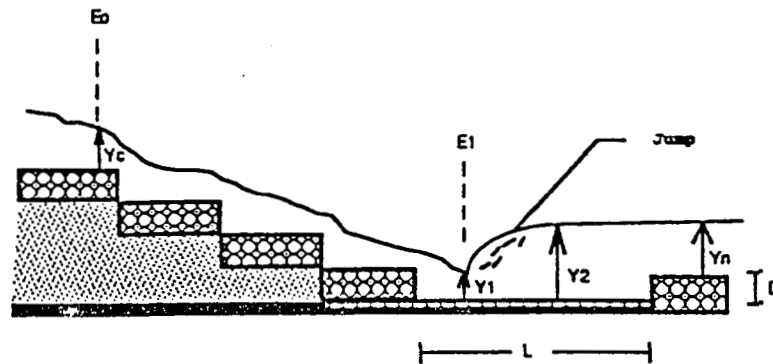


9. Depth Y_1 at the toe of a weir made of "bare" gabions

In order to dimension the stilling basin, we need to calculate (fig. 10):

- the Froude's number at the weir toe:

$$F_1 = q(g \cdot Y_1^3)^{1/2}$$



10. Dimensioning of the stilling basin

- the conjugate depth Y_2 at the jump end:

$$Y_2 = 0,5 \cdot Y_1 \cdot [(1 + 8 \cdot F_1^2)^{1/2} - 1]$$

- the length L of the stilling basin, using the empirical formula [11]: $L = 6 Y_2$

- the depth D of the stilling basin in order to reach the normal depth Y_n of the stream; Y_n depends only on downstream conditions:

$$D = Y_n - Y_1.$$

The type of step determines the energy dissipation:

- the concrete slabs on the step treads partially seal the weir and energy dissipation is reduced; to accurately dimension the stilling basin, testing has shown that the length L calculated by using the above method for "bare" gabion steps should be increased by 15 %, 8 % and 0 % respectively for the slopes 1:3, 1:2 and 1:1.

- counter-slopes and counter-sills create water pockets which cushion the overflowing sheets of water and lead to the formation of hydraulic jumps, thus improving energy dissipation. Depending on the slope of the weir, the length of the stilling basin can be reduced by up to 10 % [5].

Discussion

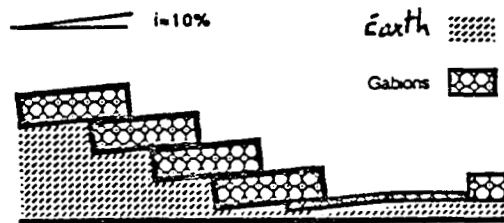
The head loss per unit of height $(E_0 - E_1)/H$ decreases sharply when $q^2/(g.H^3)$ increases and thus, for H constant, when the flowrate increases. This phenomenon is explained by the change of regime (from *nappe flow* to *skimming flow*) which occurs when $q^2/(g.H^3)$ increases. The energy dissipated by *skimming flow* is much lower than that of *nappe flow*.

We also see that the graphs of variables $(E_0 - E_1)/H$ and Y_1/H for various slopes tend to merge when $q^2/(g.H^3)$ (and thus q) decreases. As was shown for the modelling of *free nappe flow*, the same hydraulic conditions exist for each step, independently of the weir slope.

Gabion deformation

Scale model testing has shown some deformation of the gabions used for building the weirs. Gabions are subject to shifting of their filling material, and thus should be constructed with great care, as described in [2]:

- quality and placement of the stones in the upper portion of the gabions ;
- strict conformity with granulometric rules (size of material more than 1.5 times the mesh size).



11. Counter-sloped weir

If the gabions are exposed to high floods (above $1.5 \text{ m}^3 \cdot \text{s}^{-1} \cdot \text{ml}^{-1}$), the wire mesh and the ties must be reinforced. It is also recommended to increase the rigidity of the wire cage with a third row of additional tie-rods and to increase the number of diaphragms in the gabions.

The solid particles transported by the stream may abrade or even break the wire mesh of the gabions. When such a risk is present, each step tread can be protected by pouring a concrete slab, 5 to 10 cm thick.

The gabions can be counter-sloped simply by tilting the entire weir in the upstream direction (fig. 11). In that case, the step treads can also be protected by concrete slabs.

In addition to increasing energy dissipation, this type of facing increases the overall stability of the structure. It nevertheless requires more sophisticated technical means to place the tilted gabions.

Conclusion

Provided the construction rules are respected, weirs with a stepped downstream facing made of gabions can withstand floods up to $3 \text{ m}^3 \cdot \text{s}^{-1} \cdot \text{ml}^{-1}$ without noticeable damage. This is without any doubt the only gabion spilling structure capable of withstanding such floods; on the other hand, sloped downstream facings made of gabions cannot withstand floods in excess of $1 \text{ m}^3 \cdot \text{s}^{-1} \cdot \text{ml}^{-1}$ [2], [5].

Moreover, stepped weirs induce a high level of energy dissipation above the stilling basin. This study has shown how to quantify this dissipation over the steps and to establish the parameters of the basin.

The final results lead to a 10 to 30 % reduction of the stilling basin length in comparison with traditional methods. Knowing the cost of the flood spillway on this type of dam, the savings amount to 5 to 10 % of the project cost.

Acknowledgments

We wish to thank the Société du Canal de Provence for the valuable help which was provided during the experimental work.

APPENDIX

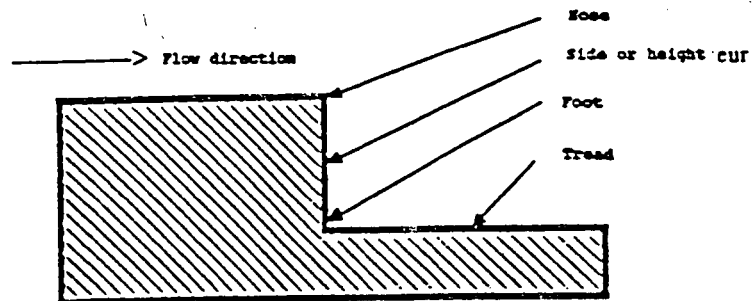
1. Units

ml	linear meter
$m^3 \cdot s^{-1} \cdot ml^{-1}$	flowrate per unit length of sill
m/m	weir slope

2. Notation

Y_c	Critical depth
Y_1	Weir toe depth
Y_2	Conjugate depth of Y_1 , downstream of the jump
Y_p	Water cushion depth under the overflowing sheet of water
E_0	Total load of the flow on the weir sill
E_1	Total load of the flow on the weir toe
q	Flowrate per unit length of sill
g	Gravitational acceleration
H	Weir height
h	Step height
n	Number of steps of the weir
i	Weir slope
V_m	Flow velocity in section m
H_s	Specific load: $H_s = Y + V^2/2g$

3. Terminology for steps



References

- [1] AGOSTINI R., BIZARRI A., MASETTI M.: *Ouvrages flexibles pour tronçons torrentiels et fluviaux (1^{re} partie : Ouvrages transversaux)*. [Flexible structures for torrential and fluvial sections (First part: Transverse structures).] Ed. France Gabions s.a., Le Pouzin, 1987.
- [2] CEMAGREF: *Les ouvrages en gabions*. [Gabion structures.] In the course of publication by the French department of cooperation and development. Previous publication : *Collection Techniques Rurales en Afrique*. [Series on Rural Techniques in Africa.] Ed. Eyrolles, Paris. 1974.
- [3] DURAND J.-M.: *Etude de variantes techniques dans la conception des petits barrages en terre au Burkina Faso*. [Study of technical alternatives for small earth dams in Burkina Faso.] Ed. CEMAGREF, Aix-en-Provence Group, Le Tholonet, May 1989.
- [4] ESSERY S.. HORNER W.: *The hydraulic design of stepped spillways (CIRIA Report 33)*. Ed. CIRIA (Construction Industry Research and Information Association), London, January 1978.
- [5] PEYRAS L.: *Etude de la dissipation de l'énergie sur les déversoirs en gradins de gabions*. [Study of energy dissipation on stepped weirs made of gabions.] Ed. CEMAGREF, Aix-en-Provence Group, Le Tholonet, May 1990.
- [6] RAJARATNAM N.: *Skimming flow in stepped spillways*. J. hydraul. eng. ASCE, vol. 116. no. 4, April 1990, pp. 587-591.
- [7] RAND W.: *Flow geometry at straight drop spillways*. Proc. ASCE, 81 E, Paper 791, September 1955, pp. 1-13.
- [8] SORENSEN R.M.: *Stepped spillway hydraulic mode investigation*. J. hydraul. eng., ASCE, vol. 111. No. 12, December 1985, pp. 1461-1472.
- [9] STEPHENSON D.: *Gabion energy dissipators*. Thirteenth Congress on Large Dams. New-Delhi, 1979. Ed. International Commisiion on Large Dams, Q. 50, R. 3, pp. 33-43, 1979.
- [10] STEPHENSON D.: *Rockfill in hydraulic engineering*. Ed: Elsevier Scientific Publishing Company, *Developments in Geotechnical Engineering Series*, vol. 27, Amsterdam, Oxford, New York, 1979.
- [11] UNITED STATES DEPARTMENT OF THE INTERIOR (Bureau of Reclamation). *Design of small dams*. Ed. Water Resources Technical Publication (United States Government Printing Office), Denver, 1987.

DRAFT

RECEIVED

APR 3 1993

WOOD, PATEL &
ASSOCIATES

Jet Flow on Stepped Spillways

by M.R.Chamani¹ and N.Rajaratnam,² M. ASCE

ABSTRACT: This paper presents an estimate of the energy loss on stepped spillways for the jet flow regime, which occurs when the ratio of the critical depth y_c to the height of the step h is approximately less than 0.8. Using the extensive experimental results of Horner, the proportion of the energy loss per step α was evaluated and found to be a function of y_c / h and h / l , where l is the length of the step. It was also found that the energy loss on a stepped spillway with a large number of steps can be very significant in the jet flow regime.

INTRODUCTION

In a stepped spillway, the provision of steps can produce significant energy dissipation. Based on the experimental observations of Essery and Horner (1971) and Sorensen (1985), the flow on stepped spillways can be in either the skimming or jet (or nappe) flow regimes. It also appears that for a wide range of slopes, that the transition from the (lower) jet flow to the (higher) skimming flow occurs when y_c / h is approximately equal to 0.8, where y_c is the critical depth and h is the height of the steps (Rajaratnam,1990). Rajaratnam (1990) presented a method of analyzing skimming flow by introducing a Reynolds stress at the bottom of the skimming flow. This note presents a method of estimating the energy loss for the jet flow regime.

1.Grad. student, Dept. of Civil Engrg., Univ. of Alberta, Edmonton, Alberta, Canada, T6G 2G7

2.Prof., Dept. of Civil Engrg., Univ. of Alberta, Edmonton, Alberta, Canada, T6G 2G7.

ANALYSIS OF JET FLOW

On the basis of the experimental observations of Essery and Horner (1971) on stepped spillways and Moore (1943) on a single step, it appears that the energy loss in the jet flow regime (Fig. 1(a)) is mostly due to jet mixing with the recirculating backwater and perhaps additional dissipation due the formation of a partial hydraulic jump on the deflected jet. With reference to Fig.1(b), let h and l be the height and (horizontal) length of a step and let N be the total number of steps so that the total height H of the spillway is equal to Nh . Let α be the proportion of head lost on each step. The energy loss on the first step is then equal to $\alpha(h+1.5y_c)$ and the remaining energy is $(1-\alpha)(h+1.5y_c)$. The remaining energy at the base of the second step will be equal to $(1-\alpha)[(1-\alpha)(h+1.5y_c)+h]$. Following this argument further, at the bottom of the spillway with N steps, the remaining energy E can be shown to be

$$E = (1-\alpha)^N (h+1.5y_c) + h \sum_{i=1}^{N-1} (1-\alpha)^i \quad (1)$$

If ΔE is the energy loss over the spillway and E_0 is the total energy at the base without any loss, it can be shown that

$$\frac{\Delta E}{E_0} = 1 - \frac{\left[(1-\alpha)^N (1+1.5(y_c/h)) + \sum_{i=1}^{N-1} (1-\alpha)^i \right]}{N+1.5(y_c/h)} \quad (2)$$

In his doctoral thesis, Horner (1969) has presented experimental results, from which the value of α can be calculated for stepped spillways, with $h/l=0.421$ (8, 10, 20 & 30 steps), 0.526 (10 & 30 steps), 0.736(10 & 30 steps), and 0.842(10 &30 steps). The results of these calculations are shown in Fig. 2(a-d). The results for all the four values of h/l are collected together in Fig. 3. A study of Figures 2 and 3 shows that α varies mainly with y_c/h and decreases continuously with y_c/h , with the maximum values of y_c/h being about 0.8. At this stage, the flow regime might change to skimming flow. For any given value of y_c/h , α decreases as h/l increases, thereby indicating that the formation of a partial jump might be responsible for a portion of the energy loss. This point is further supported by Fig. 4, wherein the results of Horner are shown along with those of Moore for a single step, with a supercritical downstream flow. Fig. 5(a-d) show the variation of α with y_c/h for four values of h/l , for several values of θ , where θ is the reverse angle of the originally horizontal step. Fig. 5(a-d) shows that for smaller values of h/l , α increases with the increment of θ for a given value of y_c/h . For larger values of h/l , the increase in α is relatively small, which supports the argument of additional energy loss from a partial jump on the step.

Returning to the relative energy loss equation (Eq. 2), let us develop an asymptotic value for small values of y_c/h . For relatively smaller values of y_c/h , α is large and $(1-\alpha)^N$ becomes negligible when the number of steps N is large. Under such conditions, Eq. 2 can be further reduced to show that the relative energy loss $\Delta E/E_0$ approaches unity. This approximation is supported by Fig. 6 for $h/l=0.421$ from the observations of Horner, where for the case with 30 steps and y_c/h approximately equal to 0.3, the relative energy loss is about 0.97.

Going back to the horizontal steps, it was found that the variation of α with h/l was described well by the equation

$$\alpha = a - b \log(y_c / h) \quad (3)$$

wherein the coefficients a and b are described by the following equations

$$a = 0.30 - 0.35(h/l) \quad (4)$$

$$b = 0.54 + 0.27(h/l) \quad (5)$$

It appears that for skimming flow, which occurs for y_c/h larger than about 0.8, an analysis of the observations of Sorensen indicate that the average energy loss per step would be less than that for jet flow.

CONCLUSIONS

This paper presents a method of estimating the energy loss in a stepped spillway, for the jet flow regime, which occurs for y_c/h less than about 0.8, wherein y_c is the critical depth and h is the height of the step. Using the extensive experimental observations of Horner, the proportion α of the average energy loss per step was found to vary with y_c/h and h/l and equations have been developed to describe this variation. It was also possible to develop an asymptotic expression to show that the energy loss in the jet flow regime could be significant, especially with a large number of steps. The energy loss in the jet flow regime appears to be due to jet mixing aided by the formation of a partial jump on the step.

APPENDIX 1. REFERENCES

Essery, I.T.S., and Horner, M.W. (1971). "The hydraulic design of stepped spillways." Report 33, Constr. Industry Res. and Information Assoc., London, England, 42 p.

Horner, M.W. (1969). "An analysis of flow on cascades of steps." Doctoral thesis, Univ. of Birmingham, UK, 316 p.

Moore, W.L. (1943). "Energy loss at the base of a free overfall." Trans. ASCE, 108, 1343- 1392.

Rajaratnam, N. (1990). "Skimming flow in stepped spillways." ASCE, Journal of Hydraulic Engrg., 116(4), 587- 591.

Sorensen, R.M. (1985). "Stepped spillway hydraulic model investigation." ASCE, Journal of Hydraulic Engrg., Vol. 111 (12), 1461-1472.

APPENDIX 2. NOTATION

The following symbols are used in this paper:

a = coefficient

b = coefficient

E = specific energy

E_0 = specific energy at the bottom of the spillway

H = total height of spillway

- h = height of step
 l = length of step
 N = number of steps
 y_c = critical depth
 α = proportion of energy lost per step
 ΔE = energy lost on the spillway
 θ = reverse angle of the steps.

LIST OF FIGURE TITLES

- Fig.1(a-b) Definition sketches of jet flow on stepped spillways
- Fig. 2(a-d) Variation of α with y_c / h for $h / l = 0.421, 0.526, 0.736$ and 0.842
- Fig. 3 Consolidated results on the variation of α with y_c / h
- Fig. 4 Variation of α with y_c / h for multiple steps (Horner) and single step (Moore)
- Fig. 5(a-d) Variation of α with y_c / h and several values of h / l for steps with reverse slopes
- Fig. 6 Variation of relative energy loss over several steps for $h / l = 0.421$

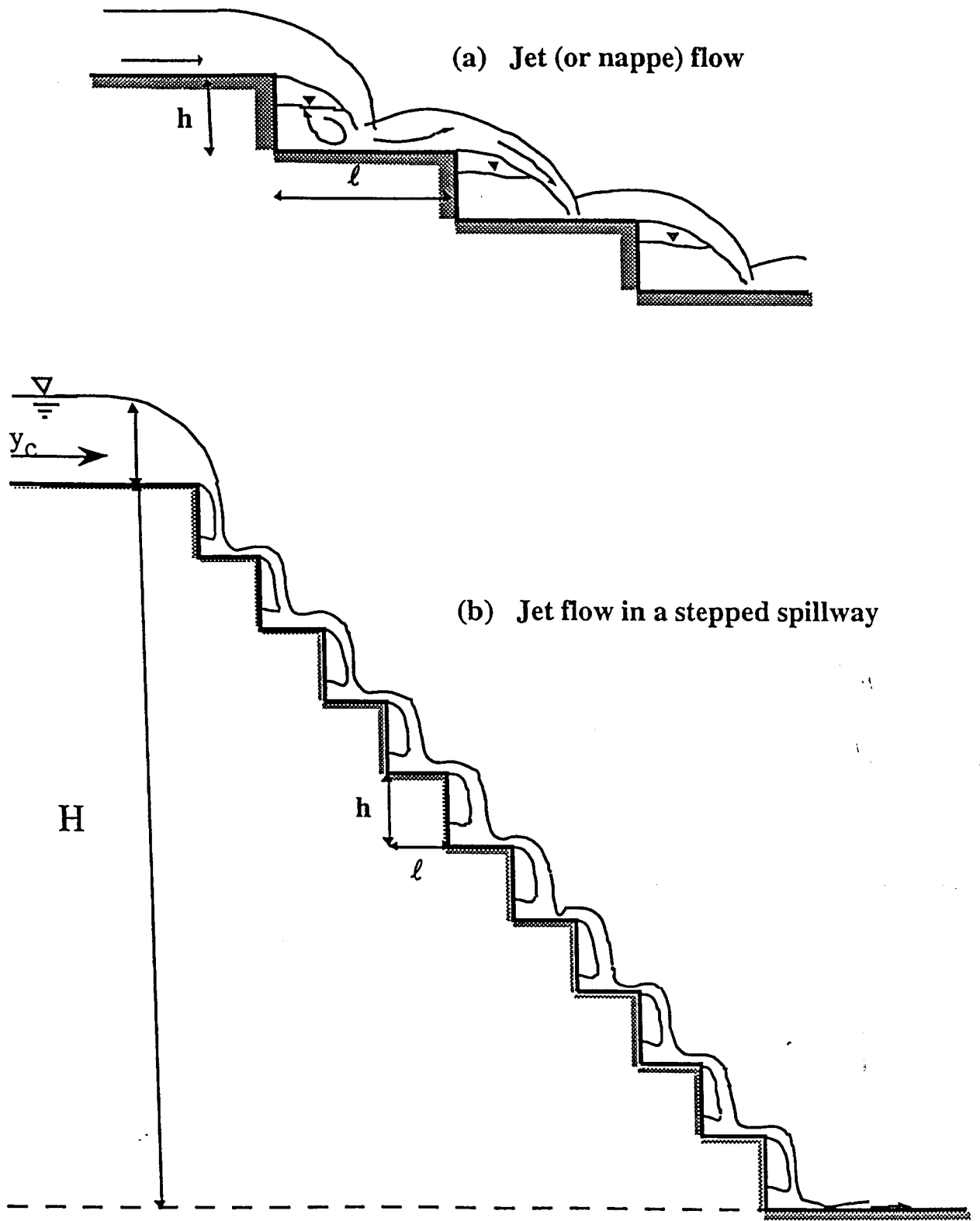


Fig. 1(a-b). Definition sketches of jet flow on stepped spillway

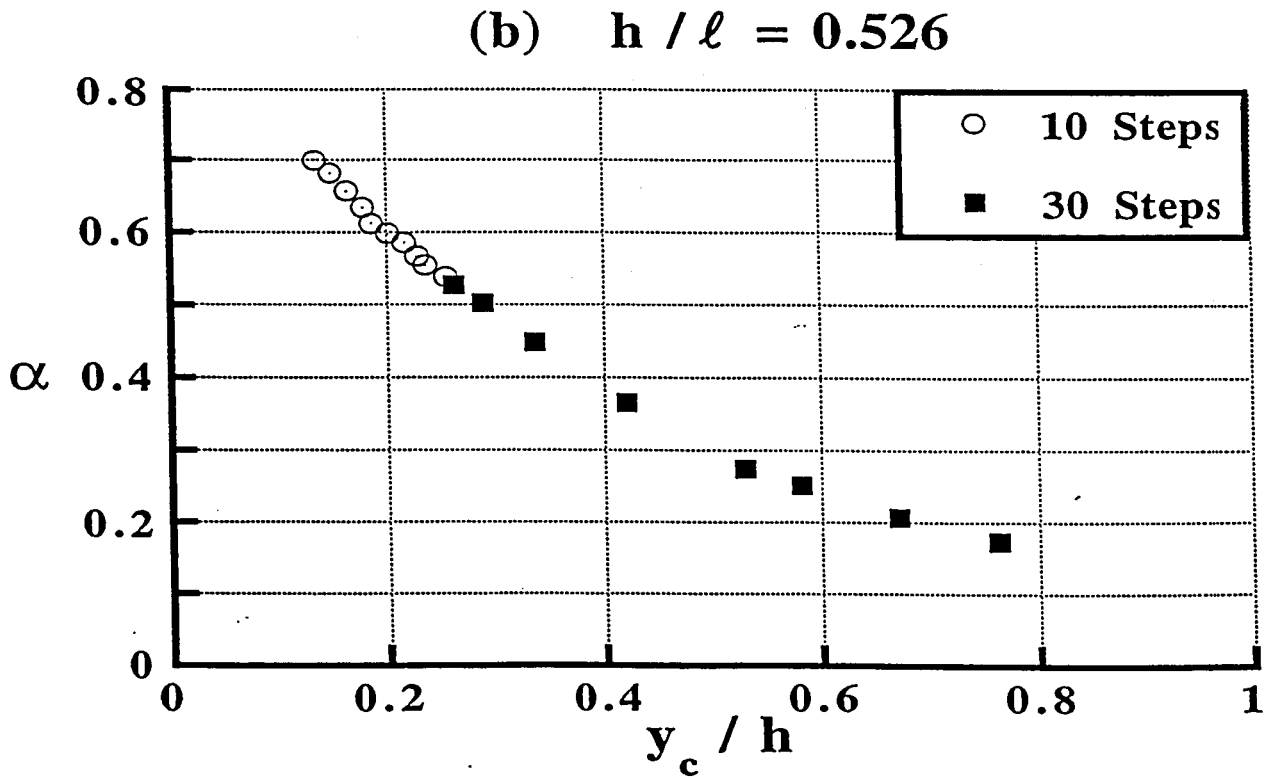
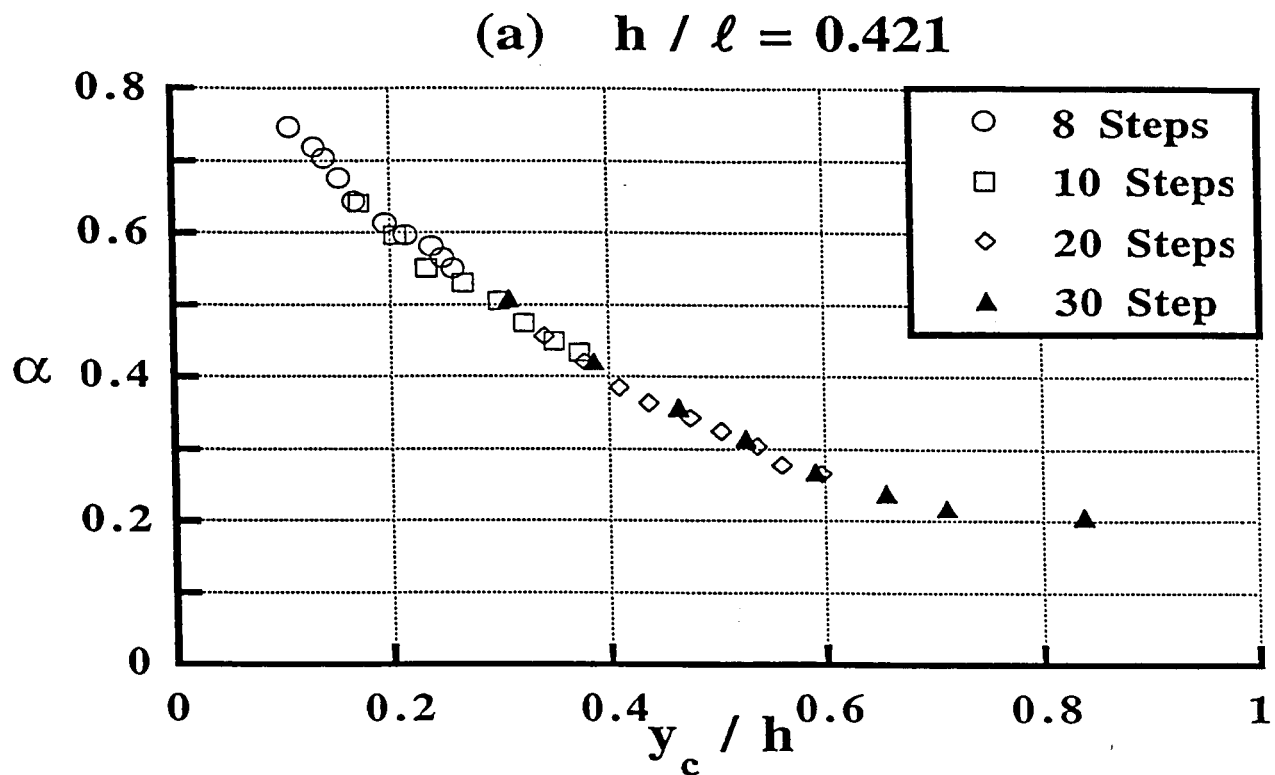


Fig. 2(a-b) Variation of α with y_c / h for $h / \ell = 0.421, 0.526, 0.736,$ and 0.842

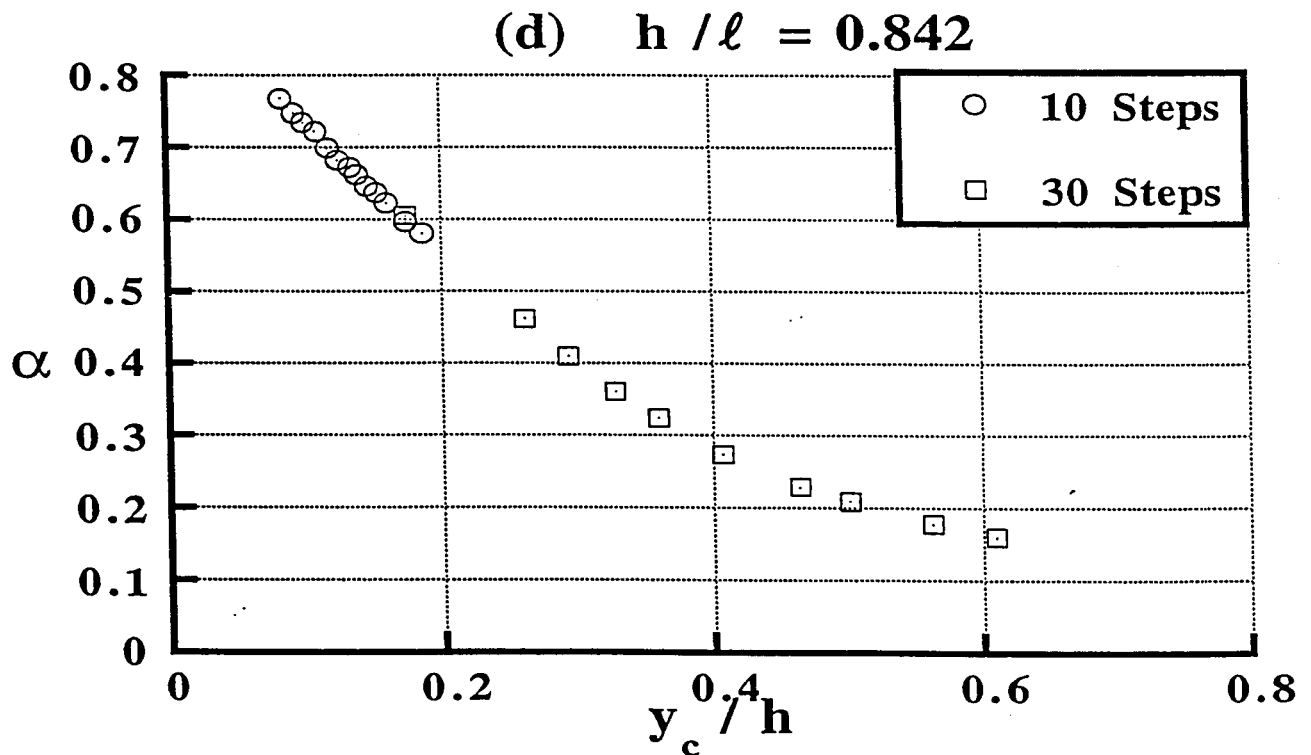
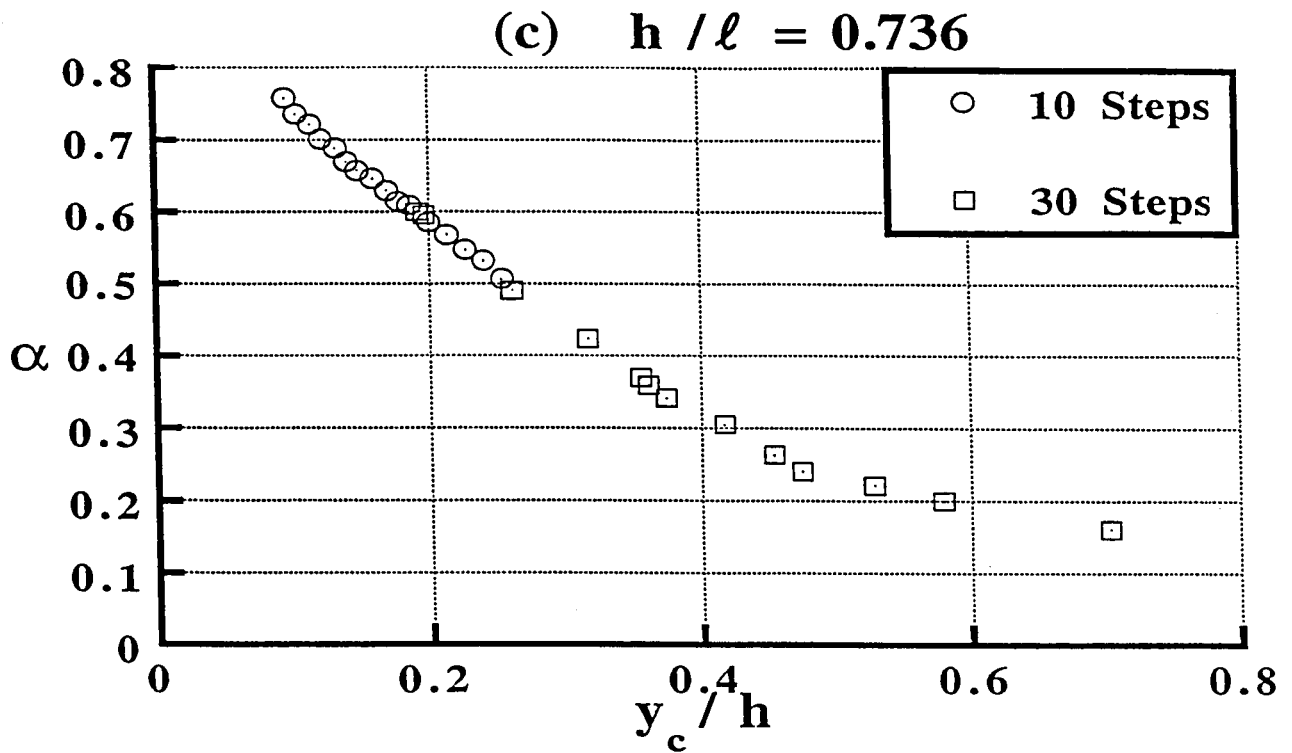


Fig. 2(c-d) Variation of α with y_c / h for $h / \ell = 0.421, 0.526, 0.736,$ and 0.842

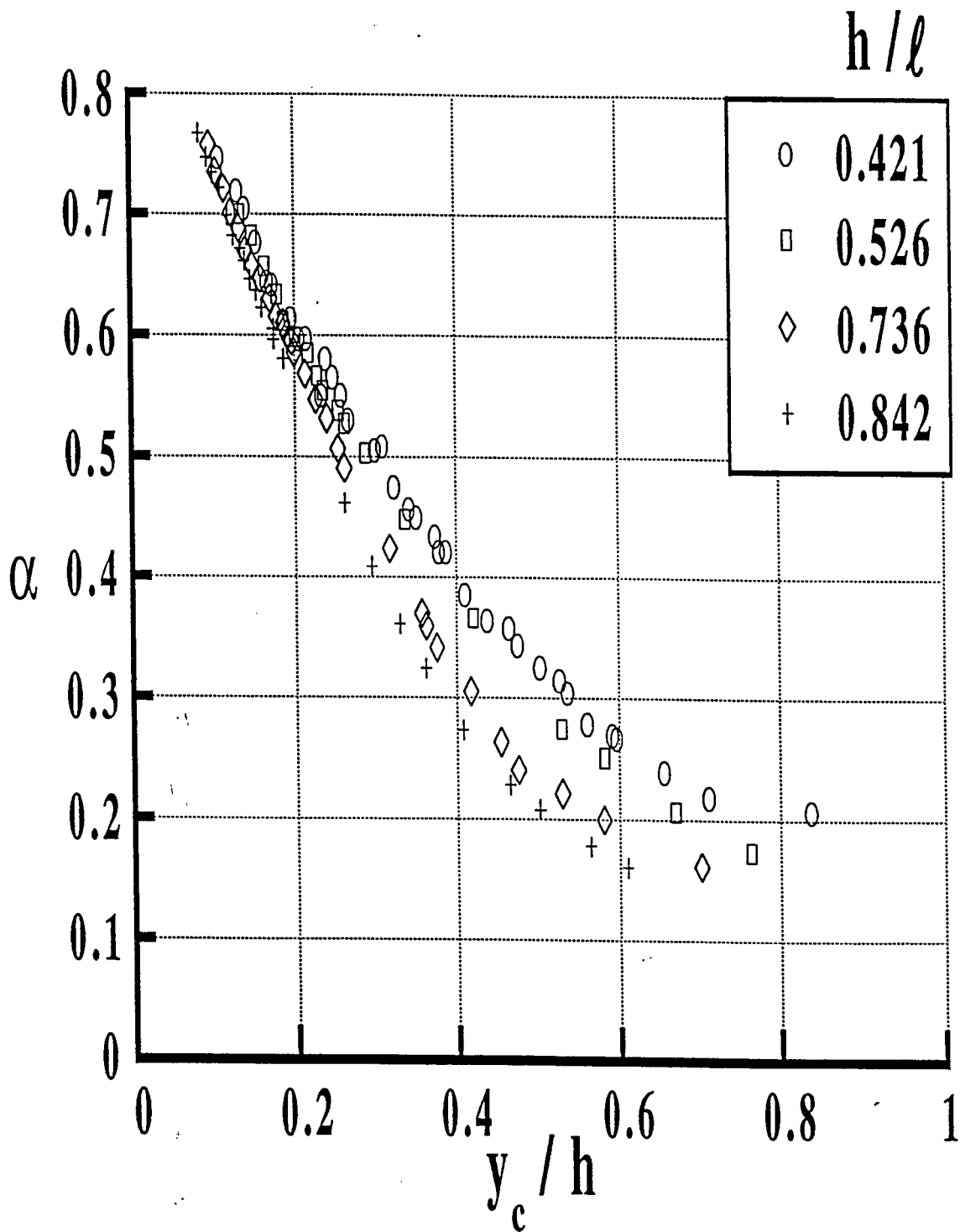


Fig. 3. Consolidated results on the variation of α with y_c/h

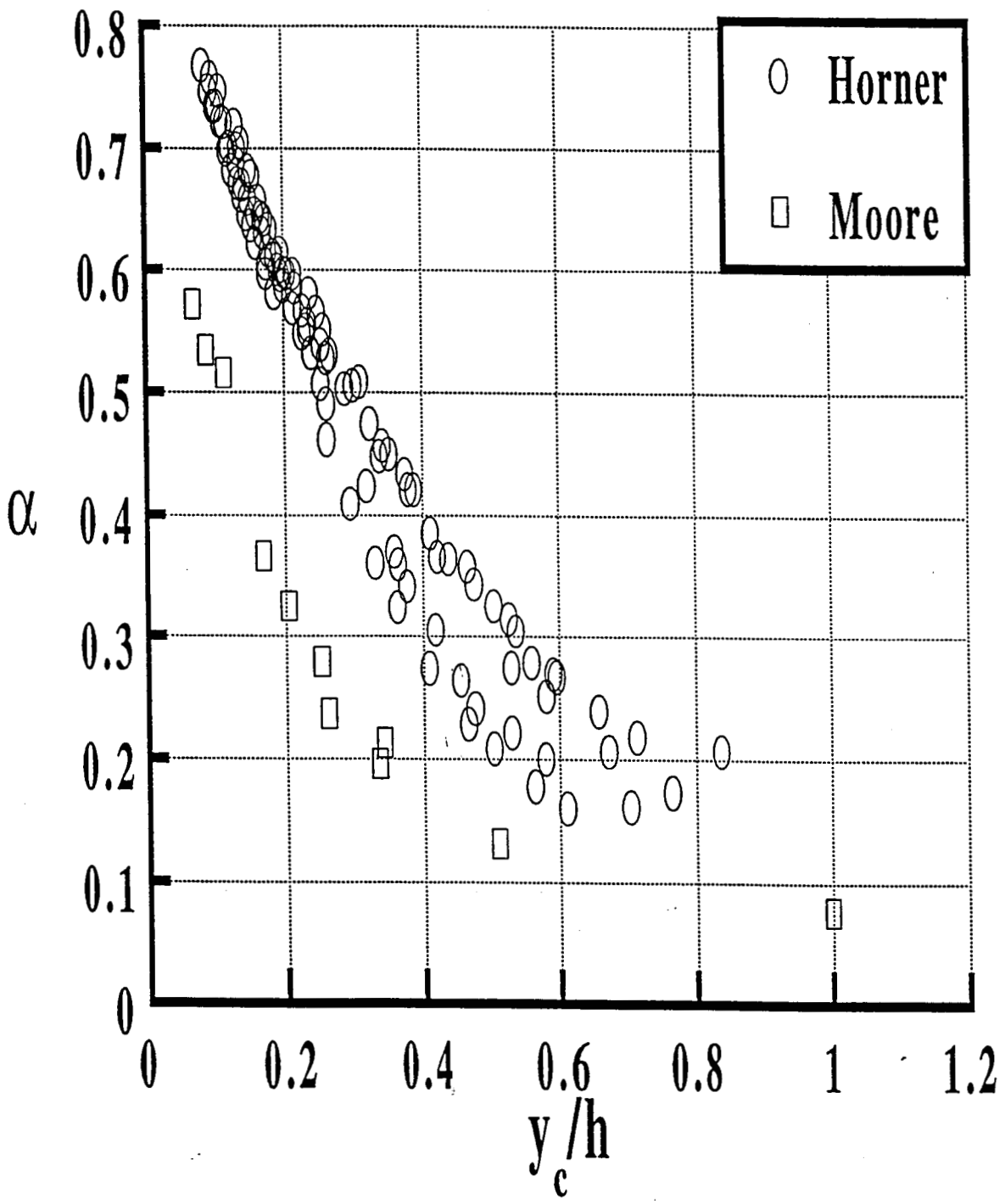


Fig. 4. Variation of α with y_c/h for multiple steps (Horner) and single step (Moore)

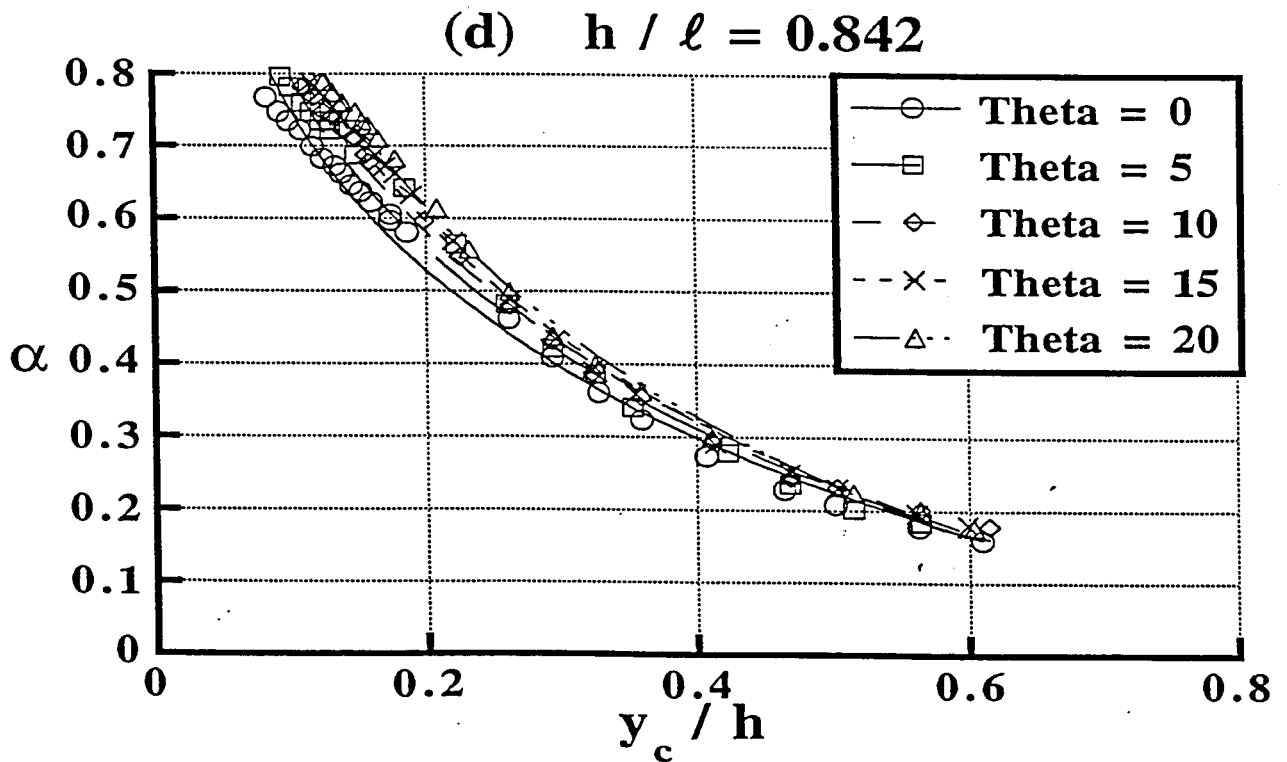
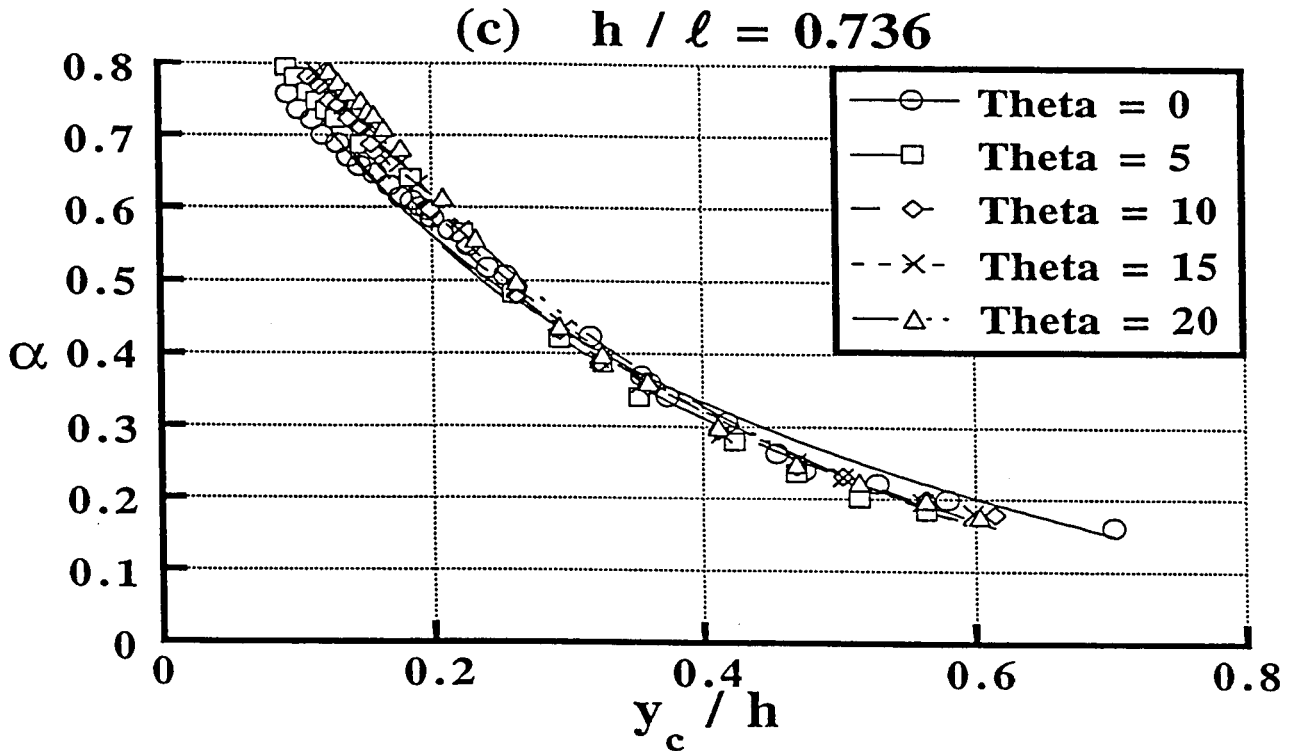


Fig. 5(c-d). Variation of α with y_c / h and several values of h / ℓ for steps with reverse slopes

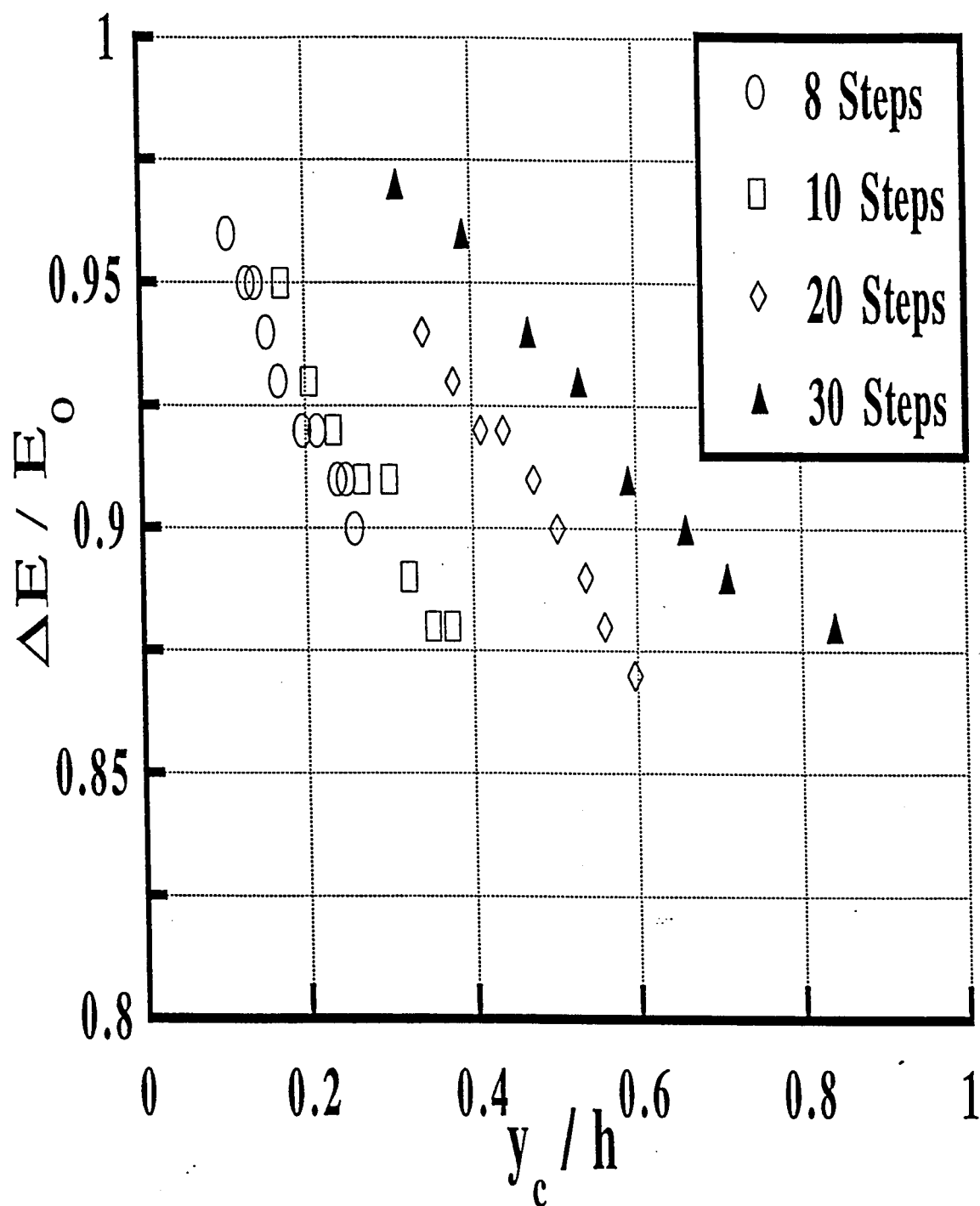


Fig. 6. Variation of relative energy loss over several steps for $h / \ell = 0.421$

~~WARNING~~
THIS MATERIAL MAY BE PROTECTED
BY COPYRIGHT LAW (TITLE 17 U.S.
CODE)

The hydraulic design of stepped spillways

I.T.S. Essery MC MSc MICE MIMunE

M.W. Horner PhD MICE



CONSTRUCTION INDUSTRY RESEARCH AND INFORMATION ASSOCIATION
6 STOREY'S GATE, WESTMINSTER, LONDON, SW1 TELEPHONE 01-839 6881

This research was carried out by Dr. Horner at the University of Birmingham under the general supervision of Mr. Essery, Senior Lecturer and Tutor in the Civil Engineering Department. Dr. Horner now works for the Gwynedd River Authority, Merioneth.

The Association would be pleased to hear from any member firm about its experience in using the information contained in this report, and to receive suggestions for improvements or further research. Members are invited to contact Dr. D.E. Wright, Research Manager in Hydraulic and Public Health Engineering.

Contents

LIST OF ILLUSTRATIONS	5
NOTATION	6
SUMMARY	7
INTRODUCTION	7
Description	7
Previous research	8
Objectives of investigation	8
Hydraulic similitude	8
FLOW BEHAVIOUR	9
Classification	9
Flow type	9
Flow category	11
Flow transition zones	11
TESTS	11
Apparatus	11
Measurement of specific energy and force	14
Information from tests	15
RESULTS	15
Dimensionless presentation of experimental results	15
Scale effect	20
Limit of transition zone	20
Limit of nappe flow	20
Influence of nappe ventilation	20
Skimming flow	23
STILLING BASIN DESIGN	23
General	23
Type 1 basin	25
Type 2 basin	27
Type 3 basin	28
Model study	28
Flood flow capacity	28

Continued overleaf

DESIGN OF PROTOTYPE CASCADES AND STILLING BASINS FOR NAPPE FLOWS	29
General considerations	29
Cascades giving subcritical category flow	30
Cascades giving supercritical category flow	30
Optimum spillage arrangement	31
Wing wall height	31
Approach to cascade	31
Arrangement of steps	32
Aeration and drainage	32
ENERGY OF CASCADE FLOWS	33
CONCLUSIONS	33
Flow behaviour	33
Nappe ventilation	33
Dimensionless presentation of experimental results	33
Scale effect	34
Stilling basin	34
Prototype design	34
REFERENCES	34
APPENDIX 1 APPLICATION OF DESIGN PROCEDURES	34
APPENDIX 2 DERIVATION OF EQUATIONS FOR DESIGN OF STILLING BASINS	37
APPENDIX 3 PLOTS OF FLOW NUMBER AGAINST CASCADE SLOPE, WITH ENERGY NUMBER AS PARAMETER, FOR STEP INCLINATIONS OF 0°, 5°, 10°, 15° AND 20°	39

List of illustrations

Figure 1	<i>Various types of stepped spillway</i>	7
Figure 2	<i>Isolated nappe flow</i>	10
Figure 3	<i>Nappe interference flow</i>	10
Figure 4	<i>Skimming flow</i>	10
Figure 5	<i>Flow categories on inclined steps</i>	12
Figure 6	<i>The 8-step model</i>	14
Figure 7	<i>Flow number plotted against slope of cascade for maximum flow in subcritical category at various step inclinations</i>	16
Figure 8	<i>Flow number plotted against slope of cascade for various values of force number ($\theta = 0^\circ$)</i>	17
Figure 9	<i>Flow number plotted against slope of cascade for various values of force number ($\theta = 5^\circ$)</i>	18
Figure 10	<i>Flow number plotted against slope of cascade for various values of force number ($\theta = 10^\circ$)</i>	18
Figure 11	<i>Flow number plotted against slope of cascade for various values of force number ($\theta = 15^\circ$)</i>	19
Figure 12	<i>Flow number plotted against slope of cascade for various values of force number ($\theta = 20^\circ$)</i>	19
Figure 13	<i>The relationship between flow number and energy number established on four models of different size</i>	21
Figure 14	<i>The relationship between flow number and force number established on four models of different size</i>	21
Figure 15	<i>Maximum transition zone lengths with nappe flow in supercritical category ($\theta = 0^\circ$)</i>	22
Figure 16	<i>Limit of nappe flow at various step inclinations</i>	24
Figure 17	<i>The stilling basins selected for analysis</i>	26
Figure 18	<i>Design curves for type 1 stilling basin</i>	26
Figure 19	<i>Flow number plotted against slope of cascade for various values of energy number ($\theta = 0^\circ$)</i>	39
Figure 20	<i>Flow number plotted against slope of cascade for various values of energy number ($\theta = 5^\circ$)</i>	39
Figure 21	<i>Flow number plotted against slope of cascade for various values of energy number ($\theta = 10^\circ$)</i>	40
Figure 22	<i>Flow number plotted against slope of cascade for various values of energy number ($\theta = 15^\circ$)</i>	40
Figure 23	<i>Flow number plotted against slope of cascade for various values of energy number ($\theta = 20^\circ$)</i>	41

Notation

A	Flow cross-sectional area
b	Flow width
C_D	Weir discharge coefficient
C_J	A constant
c (suffix)	Refers to critical flow
d	Mean flow depth
E_N	Energy number
E_S	Specific energy
F_1	Hydrostatic force (also with other numerical suffixes)
F_B	A frictional force
F_N	Force number
F_P	A horizontal force created by a pressure differential across a nappe
F_S	Specific force
f_o	Function of (also with other suffixes)
g	Acceleration due to gravity
H	Step height
H_W	Wing wall height
L	Step length
L_{B1}	Length of Type 1 basin
L_{B2}	Length of Type 2 basin
L_{B3}	Length of Type 3 basin
L_J	Length of hydraulic jump
L_{JB}	Length of portion of basin in which jump occurs
N_S	Number of steps
Q	Volume rate of flow
q	Flow per unit width
Q_N	Flow number
U	Mean velocity
u	Local velocity
w	Unit weight of water
Z	Height of abrupt rise or drop
α	Energy coefficient
β	Momentum coefficient
θ	Step inclination

Summary

This investigation was concerned with the analysis by model study of the complex flow behaviour down stepped spillways, and with categorising the various types of flow which occur. The tests covered a wide range of step parameters and flow conditions, and included both horizontal steps and those of adverse slope; possible scale effects on models of various sizes were also investigated. By recognising factors which influence the flows, a basis for predicting prototype behaviour was established. The results of the study are presented in a series of dimensionless plots which readily yield the energy and force of flows leaving the spillway.

Normally at the base of the spillway it is necessary to incorporate a stilling basin, and the investigation was extended to include the stilling basin design appropriate to the flow from the spillway.

Design procedures were developed so that the engineer, knowing the overall requirements of spillway flow, may design the most acceptable type of stepped spillway and associated stilling basin.

Introduction

DESCRIPTION

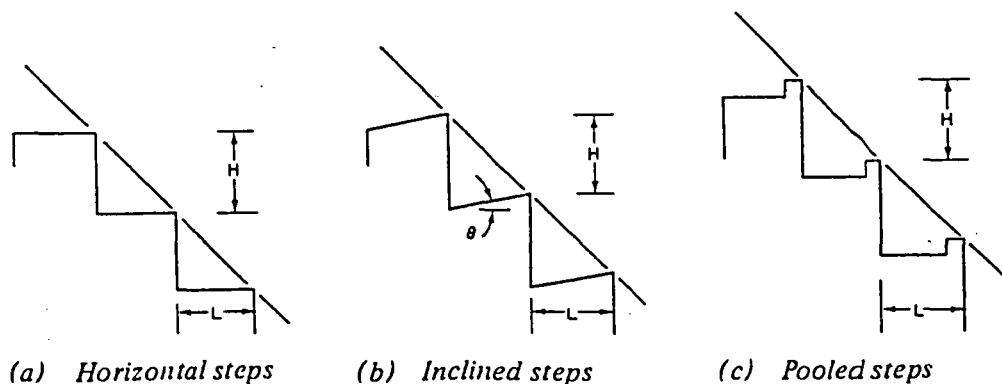
When water passes over a dam spillway, dissipation of the kinetic energy of the flow is essential if dangerous scour in the natural channel below the structure is to be avoided. One method of dissipating the energy of the falling flow is to allow the stream to pass down a stepped spillway.

A stepped spillway consists of an open channel with a series of drops in the invert. Hence, the total fall is divided into a number of smaller falls. At each fall, retarding forces are derived from the reaction of the steps to the descending flow.

In this investigation, an attempt was made to overcome any objections to stepped spillways (which may be based on high prototype construction cost) by considering the use of simple geometry steps (see Figure 1). When designing the spillage arrangements for a dam, the optimum solution can only be found by economic analysis of all the feasible schemes that provide satisfactory energy dissipation. A main objective of the present investigation was, therefore, the provision of basic information to allow the inclusion of cascades in lists of feasible schemes without recourse to model studies.

Figure 1

Various types of stepped spillway



PREVIOUS RESEARCH

Although numerous model studies of projects incorporating spillways have been made, only the research of Poggi^(1, 2) has been devoted to the provision of basic design information applicable to any structure of this type.

Poggi's work involved extensive experimental studies of flow behaviour on a cascade of pooled steps (Figure 1c). However, the objective of his investigations was to provide subcritical approach flow to every drop by creating a hydraulic jump. Thus, complete dissipation of the energy attained by the change in level was achieved on all steps. The consequent design consists of large pools and small drops, inherently a costly structure.

OBJECTIVES OF INVESTIGATION

The basic objectives of this investigation were the solution, by model study, of the complex problem of flow behaviour on a cascade of constant geometry steps, and the provision of fundamental information for the analytical design of such structures as energy dissipating devices. Scale effects were also examined.

HYDRAULIC SIMILITUDE

Dimensional analysis has been used to determine a concise method of presenting experimental data. The specific energy (E_S) and specific force (F_S) were chosen to represent the character of flows entering a horizontal channel at the base of a cascade.

The specific energy is the energy of an open channel flow at a section relative to the bed and is defined by

$$E_S = d + \frac{U^2}{2g} \quad (1)$$

where d and U are depth and mean velocity, respectively, and g is gravitational acceleration. The specific force at a section is defined as the total force per unit weight of water exerted by unit width of flow, where total force is the sum of the momentum flow rate through the section and the hydrostatic force on the section. Specific force is given by

$$F_S = \frac{U^2 d}{g} + \frac{d^2}{2} \quad (2)$$

The specific energy and force are at a minimum at the 'critical' depth. Flow at depths greater than critical is termed 'subcritical', flow at depths less than critical is termed 'supercritical'.

The factors influencing the specific energy and specific force of flows entering a horizontal channel at the base of a cascade, are the number of steps in the cascade (N_S), the overall slope (H/L), the step size (L), the inclination of the tread portion of the step (θ), the discharge per unit width (q) and the gravity effect (g). The symbols used to define step shape and size are shown in Figure 1. Thus

$$E_S = f\left(\frac{H}{L}, L, \theta, N_S, q, g\right) \quad (3)$$

and

$$F_S = \phi\left(\frac{H}{L}, L, \theta, N_S, q, g\right) \quad (4)$$

and by dimensional analysis it can be shown that

$$E_N = f\left(\frac{H}{L}, \theta, N_S, L_N\right) \quad (5)$$

and

$$F_N = \phi\left(\frac{H}{L}, \theta, N_S, L_N\right) \quad (6)$$

where the energy number $E_N = \frac{E_S}{L}$

force number $F_N = \frac{\sqrt{F_S}}{L}$

and flow number $Q_N = \frac{q^{2/3}}{g^{1/3}L} = \frac{d_c}{L}$

where d_c is the critical depth of the flow = $\left(\frac{q^2}{g}\right)^{1/3}$

The flow number is a form of Froude number.

The possible influence of surface tension and viscosity, and the resultant scale effect when predicting prototype performance by application of the Froude criterion alone, is considered later in the text.

Flow behaviour

CLASSIFICATION

The behaviour of water flows on a stepped spillway is both complex and varied. To describe flow conditions concisely it has therefore, been convenient to classify behaviour in the following three ways: flow type, flow category, and flow transition zones. The following general description is based on observations made during the tests.

FLOW TYPE

Visual comparison indicated that two types of flow existed:

Nappe flow which is distinguished by the formation of a nappe at each drop. This type of flow had two aspects:

- (1) isolated nappe flow, in which all the efflux from a step struck the tread portion of the step below.
- (2) nappe interference flow, in which part of the efflux overshot the step below.

Skimming flow which is typified by both the complete submergence of the steps, no nappes being formed as such, and the high air content in the flow.

These characteristic flows appear at progressively increasing discharges and photographs showing these classifications appear in Figures 2, 3, and 4.

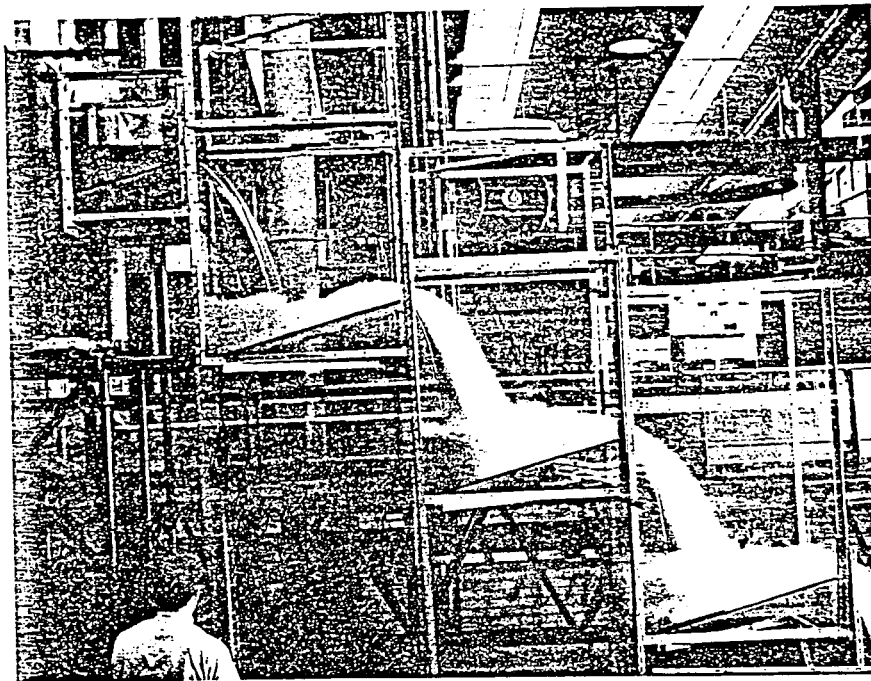


Figure 2

Isolated nappe flow

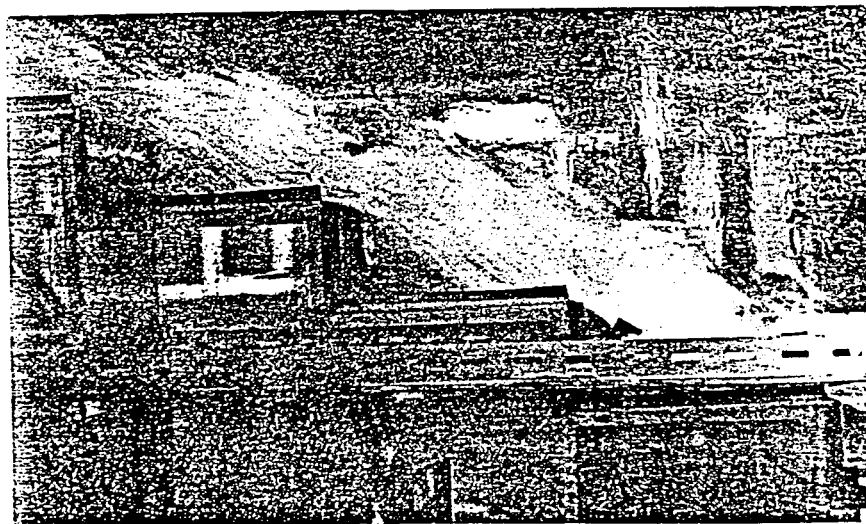


Figure 3

Nappe interference flow

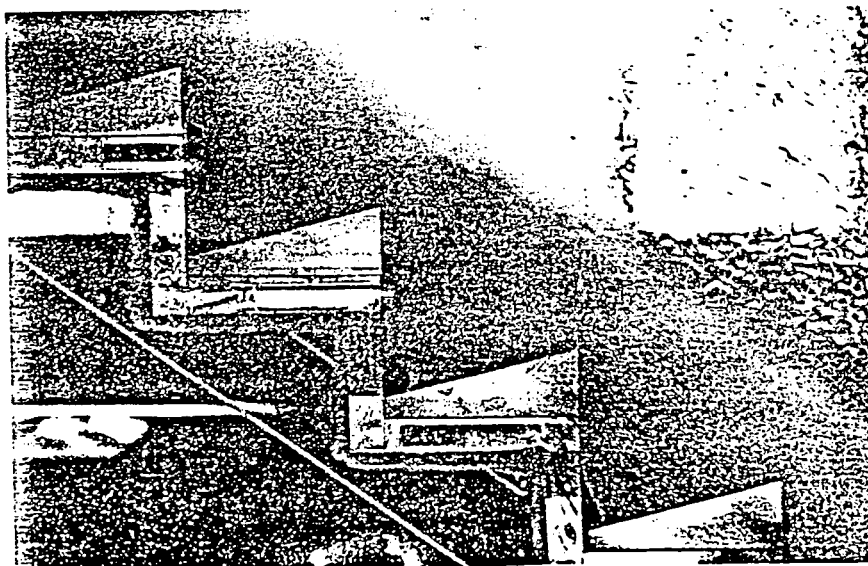


Figure 4

Skimming flow

FLOW CATEGORY

Nappe flow on cascades falls into two main categories: that in which the approach flow to each drop is *subcritical*, and that in which the flow over the entire step is *supercritical*. A *mixed flow* category exists when the two categories occur on one cascade. The flow categories are illustrated in Figure 5 and described below.

Subcritical categories

Flow down stepped cascades is said to be in the subcritical category when at any section (but not at all sections) the depth is greater than the critical depth.

The subcritical category was observed at relatively low discharges and it was distinguished by subcritical pools on all the step surfaces. The flows leaving the steps passed from the subcritical state through critical depth and into the supercritical nappes. As the flow changes from a supercritical to a subcritical state on each step the hydraulic jump is clearly a feature of the phenomenon. This flow category cannot exist on horizontally stepped cascades.

Mixed category

A mixed flow category exists in which supercritical flow occurs in the transition zone and subcritical flow in the uniform zone.

Supercritical category

Flow down stepped cascades is said to be in the supercritical category when at all sections the depth is less than critical.

The following observations of supercritical category flow were made during a preliminary study:

1. After the first drop, the flow is supercritical.
2. Over the initial portion of a cascade the flow accelerates and becomes fragmented in a transition zone.
3. On the lower portion of a cascade flow, conditions are constant and the flow pattern is uniform.
4. The flow is extremely agitated in the uniform zone and nappes are spray-like in appearance.
5. Considerable disturbance of the atmosphere by the descending stream is indicated by a strong draught above the flow leaving the final step of the cascade.

FLOW TRANSITION ZONES

When a flow enters a cascade of constant geometry steps it accelerates in the initial reach of the structure. This section of the cascade is described as the 'transition' zone. On steps lower down the cascade, equilibrium is established and flow geometry is the same at each step although the depth varies across each step. This section is referred to as 'uniform' zone.

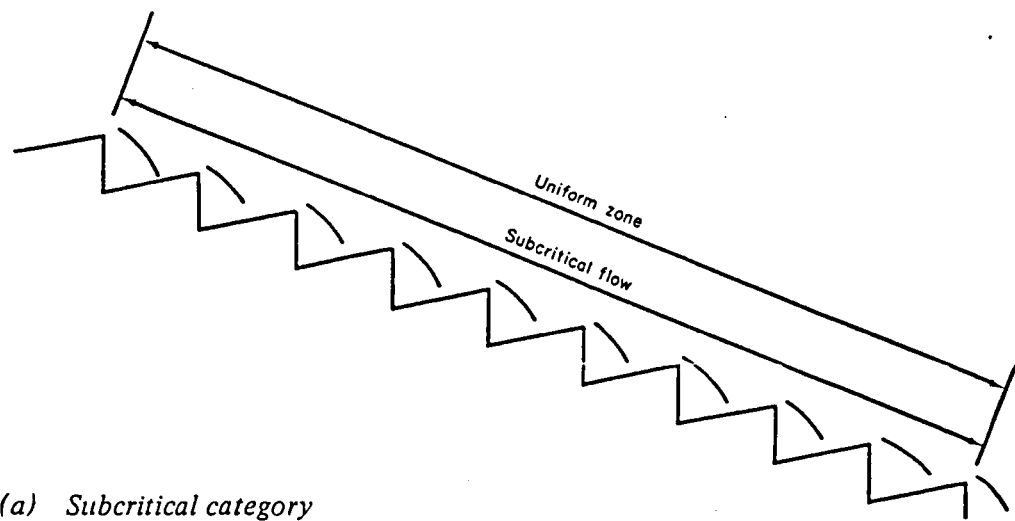
The length of the transition zone is influenced by the physical characteristics of the cascade and by the discharge per unit width. On prototype cascades the length of the transition zone is generally small in comparison with the length of the cascade. In order to provide design information, it has only, therefore, been necessary to make energy and force measurements on flows in the uniform zones.

Tests

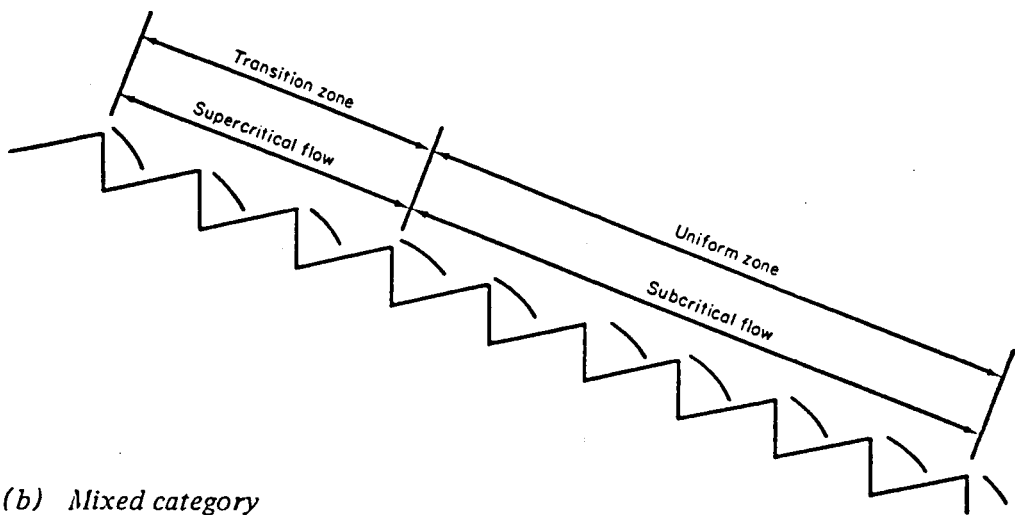
APPARATUS

Details of the various step configurations used in the study and the number of tests made, are given in Table 1.

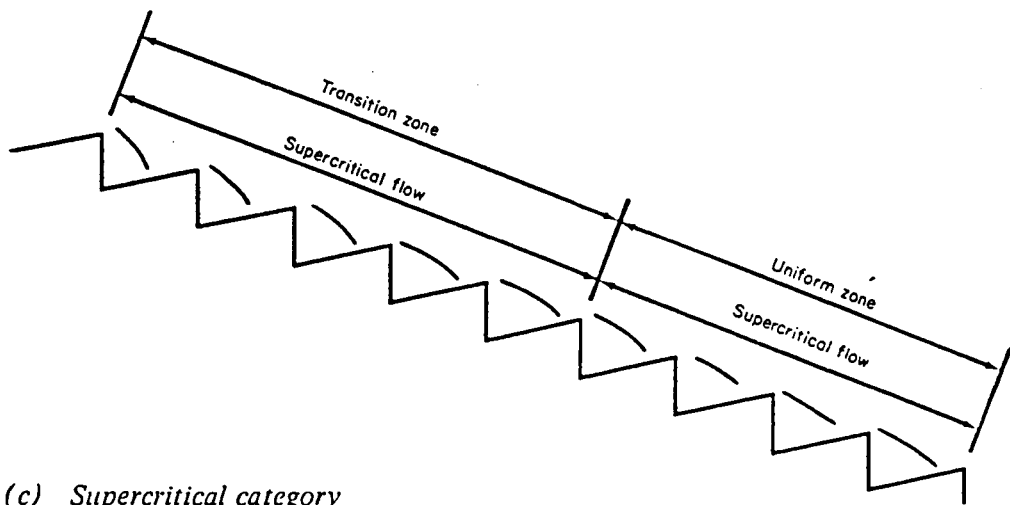
At the heads of all models, stilling reservoirs were located for calming the flows from the laboratory pipework. From these reservoirs, the flows passed to the cascades via short horizontal channels with the same widths as the models they served. With the exception of the 3-step model, all the cascades terminated with horizontal channels incorporating equipment



(a) *Subcritical category*



(b) *Mixed category*



(c) *Supercritical category*

Figure 5

Flow categories on inclined steps

for flow analysis and, in the case of the inclined step models, a section of channel with an adverse slope and length equal to the constant geometry steps preceded the horizontal channel. Figure 6 shows a typical layout.

TABLE 1 Details of tests made on the model cascades

$\frac{H}{L}$	L (mm)	θ (degrees)	Number of steps	Number of tests
0.421	68.1	0	30	12
0.421	68.1	5	30	7
0.421	68.1	10	30	7
0.421	68.1	15	30	7
0.421	68.1	20	30	7
0.421	120.7	0	20	9
0.421	241.3	0	10	8
0.421	241.3	5	10	14
0.421	241.3	10	10	13
0.421	241.3	15	10	11
0.421	241.3	20	10	8
0.421	1067	0	8	10
0.526	68.1	0	30	10
0.526	68.1	5	30	10
0.526	68.1	10	30	10
0.526	68.1	15	30	10
0.526	68.1	20	30	9
0.526	241.3	0	10	13
0.526	241.3	5	10	16
0.526	241.3	10	10	15
0.526	241.3	15	10	15
0.526	241.3	20	10	16
0.631	241.3	0	10	10
0.631	241.3	5	10	8
0.631	241.3	10	10	7
0.631	241.3	15	10	7
0.631	241.3	20	10	6
0.736	68.1	0	30	13
0.736	68.1	5	30	13
0.736	68.1	10	30	15
0.736	68.1	15	30	14
0.736	68.1	20	30	18
0.736	241.3	0	10	18
0.736	241.3	5	10	18
0.736	241.3	10	10	18
0.736	241.3	15	10	18
0.736	241.3	20	10	18
0.842	68.1	0	30	12
0.842	68.1	5	30	13
0.842	68.1	10	30	13
0.842	68.1	15	30	12
0.842	68.1	20	30	13
0.842	241.3	0	10	13
0.842	241.3	5	10	8
0.842	241.3	10	10	8
0.842	241.3	15	10	6
0.842	241.3	20	10	7

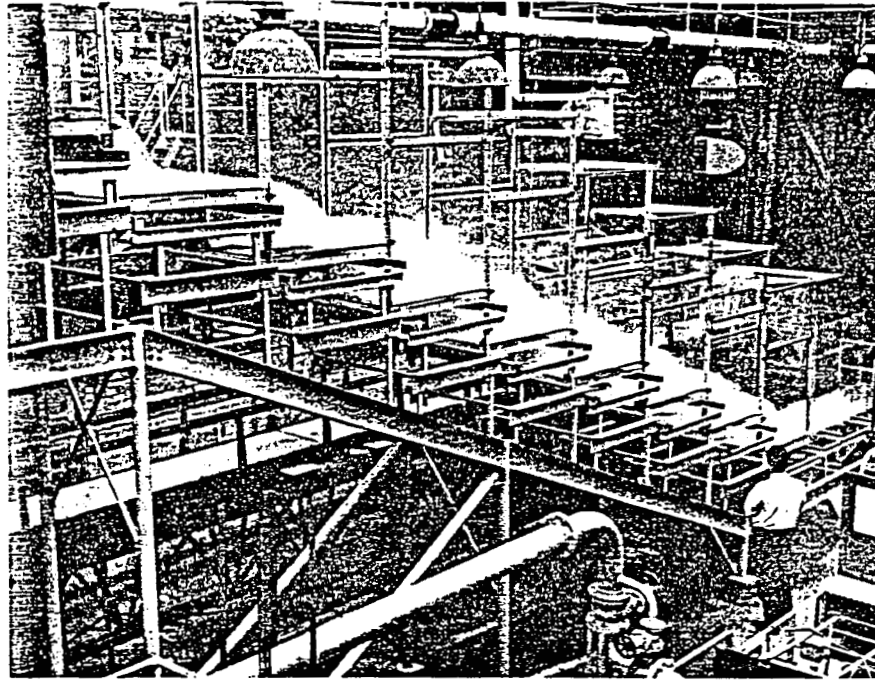


Figure 6

The 8-step model

Pitot tubes were used to determine velocity and, hence, compute values of specific energy and force. For each test flow, 36 measurements were made in the flow at a distance downstream of the last step which was free of the air entrained by the descending streams (This distance varied from 3-step lengths for the largest cascade to 9-step lengths for the smallest). Air did not, therefore, interfere with velocity measurements.

The flows to the 10-step, 20-step and 30-step models were measured by installing orifice plates in the various supply lines feeding water from the laboratory constant head tank. The discharge to the 3-step and 8-step models was measured by Venturimeter.

MEASUREMENT OF SPECIFIC ENERGY AND FORCE

Determination of velocity

The specific energy and the specific force of flows leaving the base of the cascades were computed from measured velocity distributions, by use of the relationships given below. Velocities were found from the pitot traverse results by the subtraction of the static head at a section from the total head at points within that section.

Determination of specific energy and specific force

Considering the cross-sectional area of flow, A , to be composed of a number of streamtubes, each of area ΔA , and moving at velocity U , it may be shown that the specific energy

$$E_s = \Sigma \frac{[(\bar{U}^2)^{3/2} \Delta A]}{2gQ} + \bar{d} \quad (7)$$

where \bar{U}^2 is the mean value of velocity squared. (The term \bar{U}^2 is introduced because this is the form of velocity reading secured by pitot measurement).

Similarly, the specific force per unit width of rectangular channel per unit weight is

$$F_s = \frac{\Sigma(\bar{U}^2 \Delta A)}{gb} + \frac{(\bar{d})^2}{2} \quad (8)$$

INFORMATION FROM TESTS

As previously explained, the approach flow to each drop on an inclined step cascade can be subcritical or supercritical depending on the discharge. The objective of the first series of tests on inclined step cascades was, therefore, the determination of the maximum discharge in the subcritical category on steps of various shape and size.

In the investigation of supercritical flows on horizontal and inclined steps, the specific energy and specific force of flows in the horizontal channels at the bases of a number of cascades have been calculated from Equations (7) and (8).

With all the inclined step models, the agitated and unsteady nature of flows in the mixed category prevented the accurate assessment of the discharge at which the change from the mixed to the supercritical category occurred. No attempt has, therefore, been made to provide this information in dimensionless form.

Results

DIMENSIONLESS PRESENTATION OF EXPERIMENTAL RESULTS

Subcritical category flow The factors influencing the maximum value of discharge per unit width at which subcritical category conditions can exist are overall spillway slope, step size and shape, and gravity. Hence the following functional equation may be written

$$q' = f_o\left(\frac{H}{L}, \theta, L, g\right) \quad (9)$$

where q' is the maximum value of discharge per unit width in the subcritical category. Dimensional analysis of Equation (9) reveals that

$$\frac{q'}{g^{1/2}L^{3/2}} = f_o''\left(\frac{H}{L}, \theta\right)$$

or

$$Q'_N = f_o'\left(\frac{H}{L}, \theta\right) \quad (10)$$

where Q'_N is the maximum value of the flow number in the subcritical category. Thus experimental data may be consolidated into a single set of dimensionless curves. Figure 7 shows the experimental relationship between Q'_N , H/L and θ established by this study.

Supercritical category flow Normally, the results of investigations into supercritical category flows are used to establish dimensionless relationships yielding the depth, the specific energy and the specific force of flows on stepped spillways. However, in this case attempts at plotting the ratio of mean depth to step length against d_c/L for flows on geometrically identical models have yielded poor correlations. The explanation for this is the inaccuracy of depth measurement. For example, with the highly agitated supercritical flows characteristic of this study, errors of up to ± 1.3 mm must be expected in the values of static and total head. In a typical test on a 30-step cascade this would result in depth, total head, specific energy and specific force errors of approximately ± 10 , 1.5 , 4.5 and 3.0% , respectively.

Because the values of the energy and momentum coefficients cannot be assumed to be either constant or close to unity, it is not possible accurately to derive depth from the specific energy or specific force measurements. For the same reason the computation of Froude number from the data yielded by the dimensionless plots is precluded.

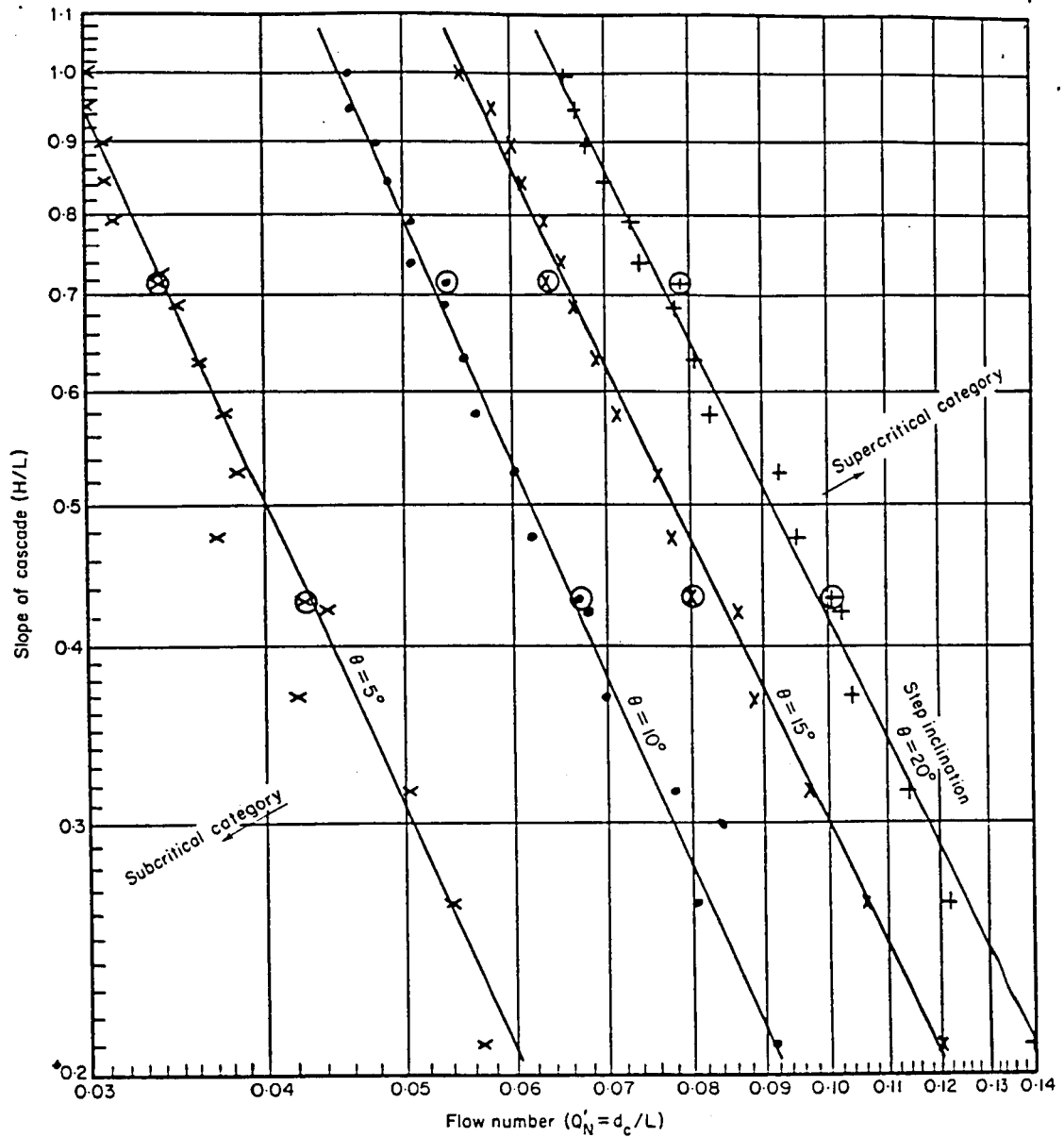


Figure 7

Flow number plotted against slope of cascade for maximum flow in subcritical category at various step inclinations

Legend

x • } Results obtained on models with steps 240 mm long
 x + }

⊗ ⊕ } Results obtained on models with steps 1065 mm long
 ⊗ ⊕ }

The dimensionless functional equations given in Equations (3) and (4) have been used to determine a suitable method of presenting the experimental data pertaining to the supercritical category flows. As measurements were only made on flows forming a uniform zone. N_S is neglected. Hence, Equations (3) and (4) reduce to

$$E_N = f''\left(\frac{H}{L}, \theta, Q_N\right) \quad (11)$$

and

$$F_N = \phi''\left(\frac{H}{L}, \theta, Q_N\right) \quad (12)$$

Plots of flow number, Q_N , against energy (or force) number, E_N (or F_N), with cascade slope, H/L , as the parameter could have been presented, each for a particular value of step inclination, θ . These would have been very congested, however, and for clarity and conciseness the data have been presented in plots of Q_N against H/L , with selected values of E_N (or F_N) as the parameter. If necessary, the user can prepare plots of Q_N against E_N (or F_N) for any particular value of H/L and θ .

The design procedure recommended by the Authors in 'Stilling basin design' uses only the force number, and so the force number results only are given in Figures 8, 9, 10, 11 and 12, at step inclinations of 0° , 5° , 10° , 15° and 20° . For completeness, the energy number data are shown on similar plots in Appendix 3 (Figures 19 to 23).

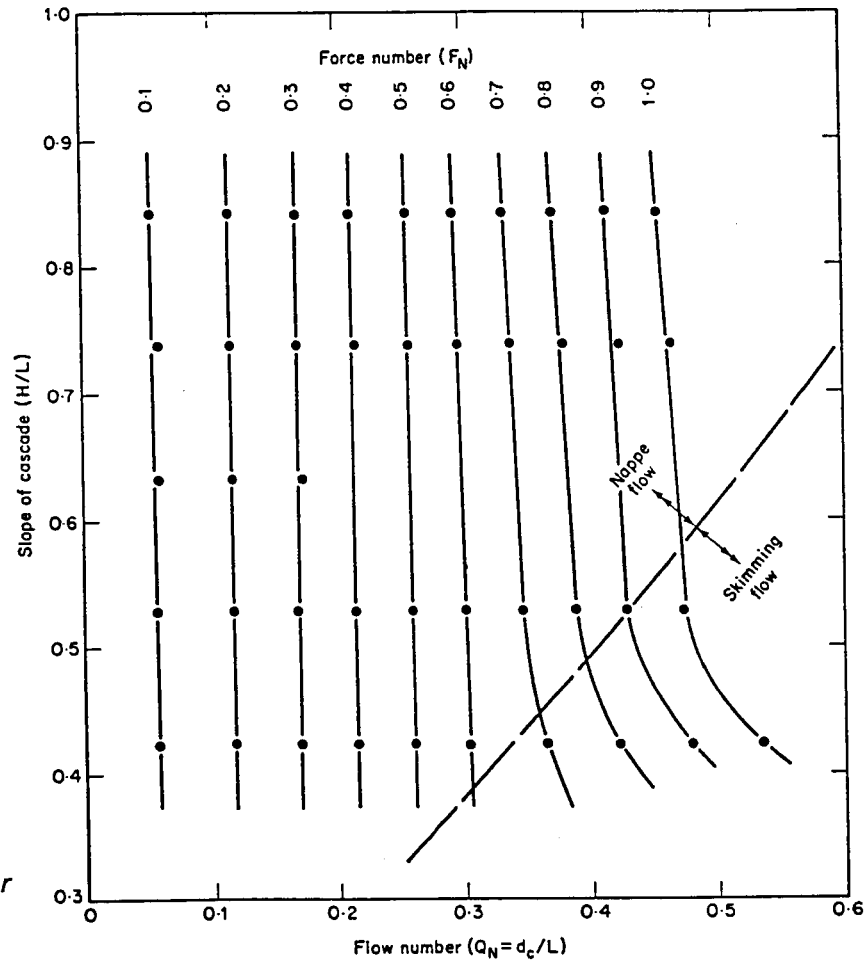


Figure 8

Flow number plotted against slope of cascade for various values of force number ($\theta = 0^\circ$)

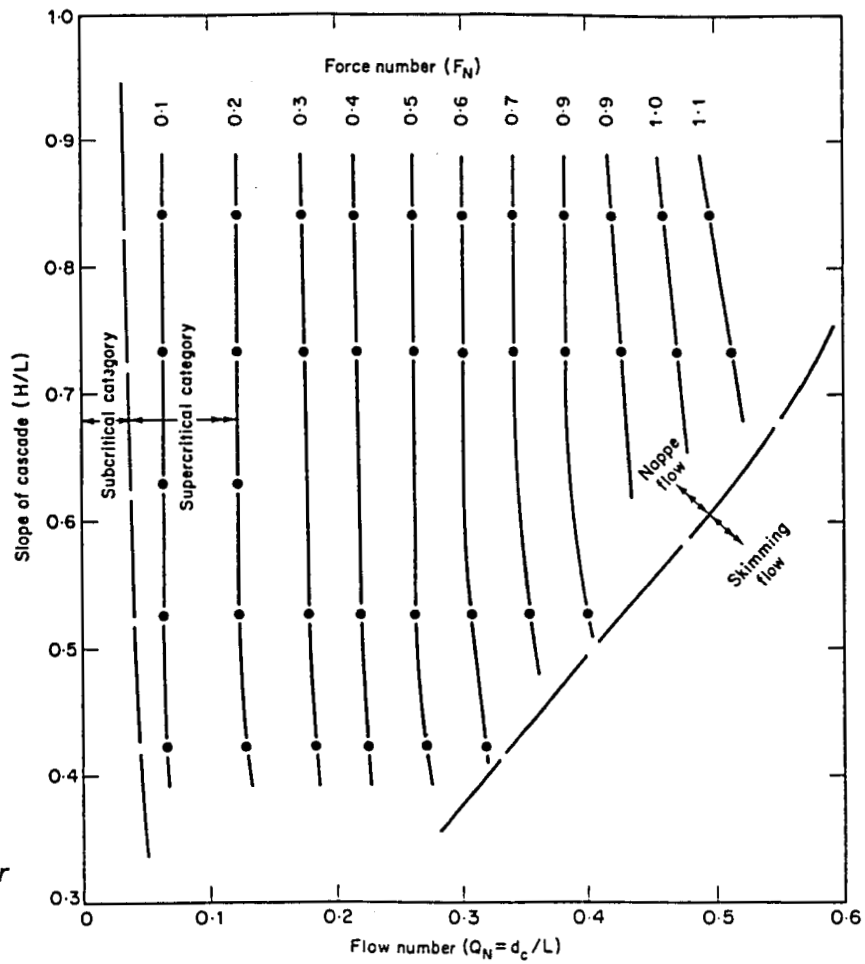


Figure 9

Flow number plotted against slope of cascade for various values of force number ($\theta = 5^\circ$)

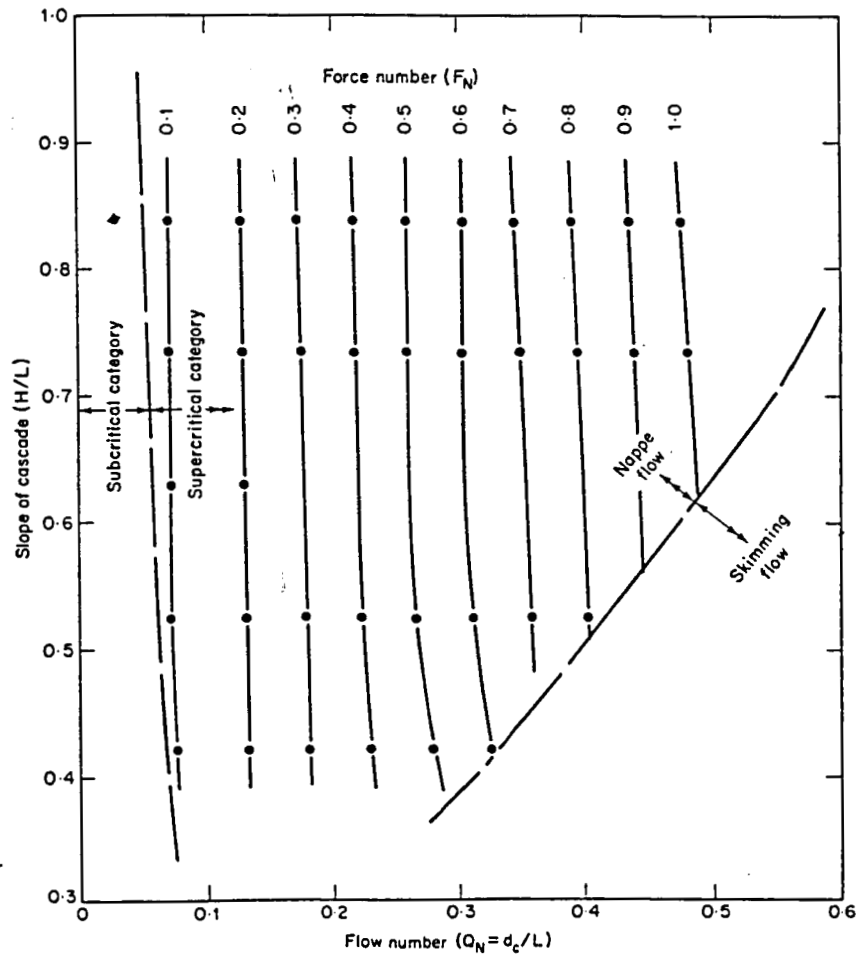


Figure 10

Flow number plotted against slope of cascade for various values of force number ($\theta = 10^\circ$)

Figure 11

Flow number plotted against slope of cascade for various values of force number ($\theta = 15^\circ$)

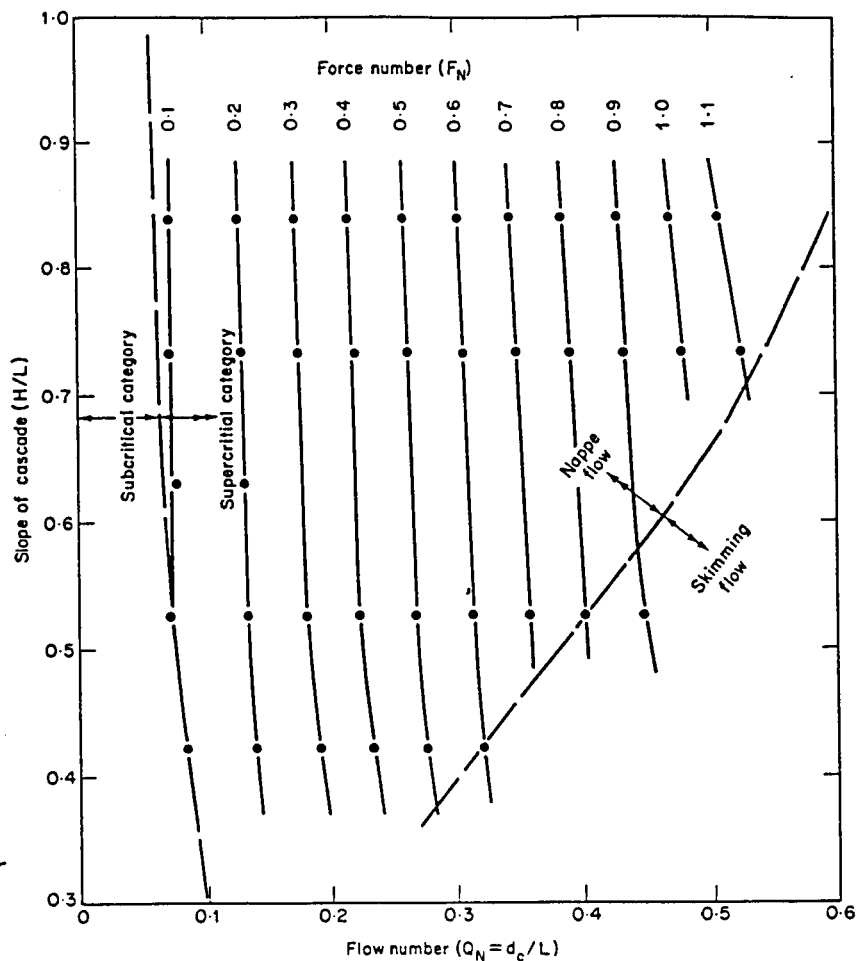
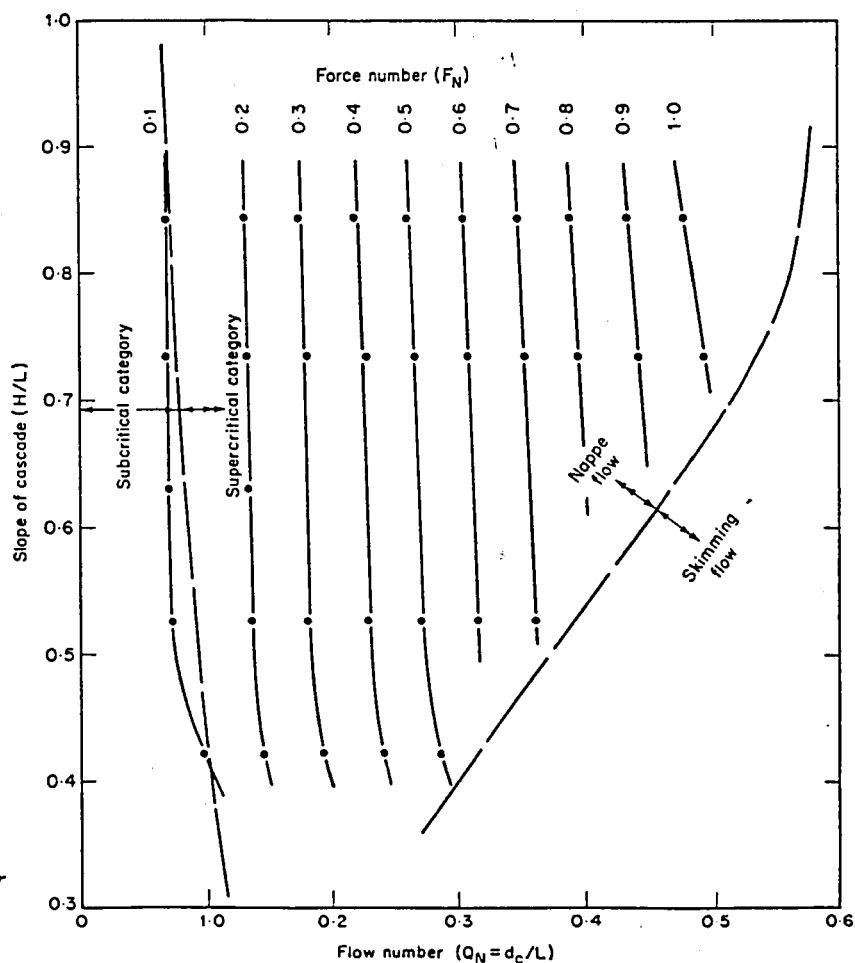


Figure 12

Flow number plotted against slope of cascade for various values of force number ($\theta = 20^\circ$)



SCALE EFFECT

Subcritical category flow

In the case of subcritical category flow the only likely cause of scale effect is excessive surface drag in the model, resulting from low Reynolds number and/or inequality of relative roughness in model and prototype. However, the close agreement exhibited in Figure 7 by data obtained on models with a scalar relationship of 1: 4.42 and different values of relative roughness, since the same material was used in both, indicates that scale has little influence. In view of this lack of scale effect, the dimensionless relationships presented in Figure 7 should provide accurate predictions of the performance of prototype cascades with steps up to 20 times larger than those on the 10-step model (this is a conservative scalar relationship for a spillway model). Hence the relationships may be safely applied to steps with lengths of up to about 5 m.

Supercritical category flow

By neglecting surface tension, viscosity and surface roughness in the derivation of the dimensionless functional Equations (5) and (6), the influences of Weber number, Reynolds number and relative roughness (i.e. ratio of roughness height to hydraulic radius) on cascade flow behaviour, have been assumed to be negligible. If these assumptions are invalid, the effect of scale would be apparent when the results of tests made on models identical in all but size are used to establish dimensionless correlations based on the Froude criterion.

The close agreement exhibited by the dimensionless experimental relationships shown in Figures 13 and 14 and established on four cascades identical in all but size, confirms the validity of applying the Froude criterion alone. However, there is a tendency for the experimental relationships to shift slightly to the right as step size increases. Consequently, use of the curves presented in Figures 8 to 12 and 19 to 23 inclusive to predict the performance of cascades with steps larger than those on any of the models, may be expected to yield values of energy and force slightly greater than those actually occurring on such cascades and so designs based on these data will be slightly conservative.

LIMIT OF TRANSITION ZONE

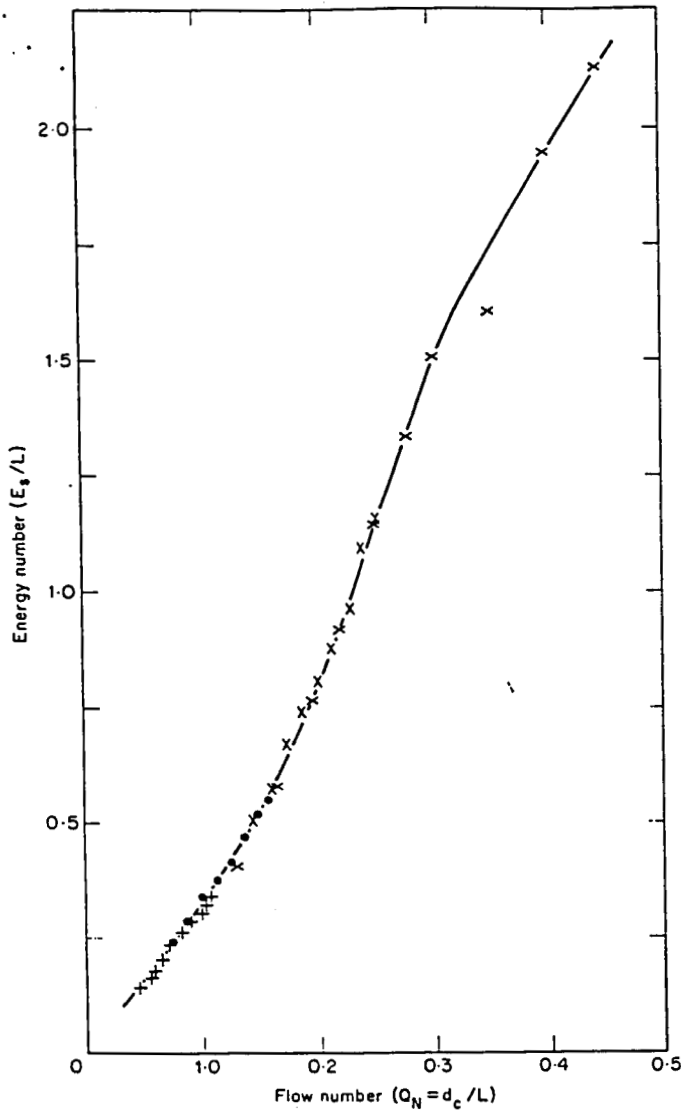
To provide a guide to the minimum length of a cascade for safe application of the energy and force relationships given above, tests were made on four 30-step models with overall slopes covering the range of slope used in the energy and force experiments. The objectives of this investigation were to establish a dimensionless relationship yielding the approximate maximum prototype transition zone lengths that could be created by a nappe flow on an ungated cascade, and to determine the effect of gates on this relationship. To ensure that the transition zone lengths obtained for the various values of overall slope were maxima, horizontal steps were used and the discharge intensity was just less than the minimum for skimming conditions (i.e. nappe flow was in supercritical category). The relation established between the number of steps in the transition zone and H/L is shown in Figure 15. At any discharge, the number of steps on an inclined step cascade over which the transition zone forms is less than the number on a horizontal step cascade with the same overall slope and step size. Tests with sluice gates inserted at the heads of the model cascades revealed that they had negligible effect on maximum transition zone lengths.

LIMIT OF NAPPE FLOW

Figure 16 shows the relationship established on 30-step cascades between H/L and the value of flow number at the boundary between nappe and skimming flow. Because skimming flow could not be created on models with steps larger than those on 30-step cascades, estimates of prototype performance based on the relationships given in Figure 16 can only be regarded as approximate.

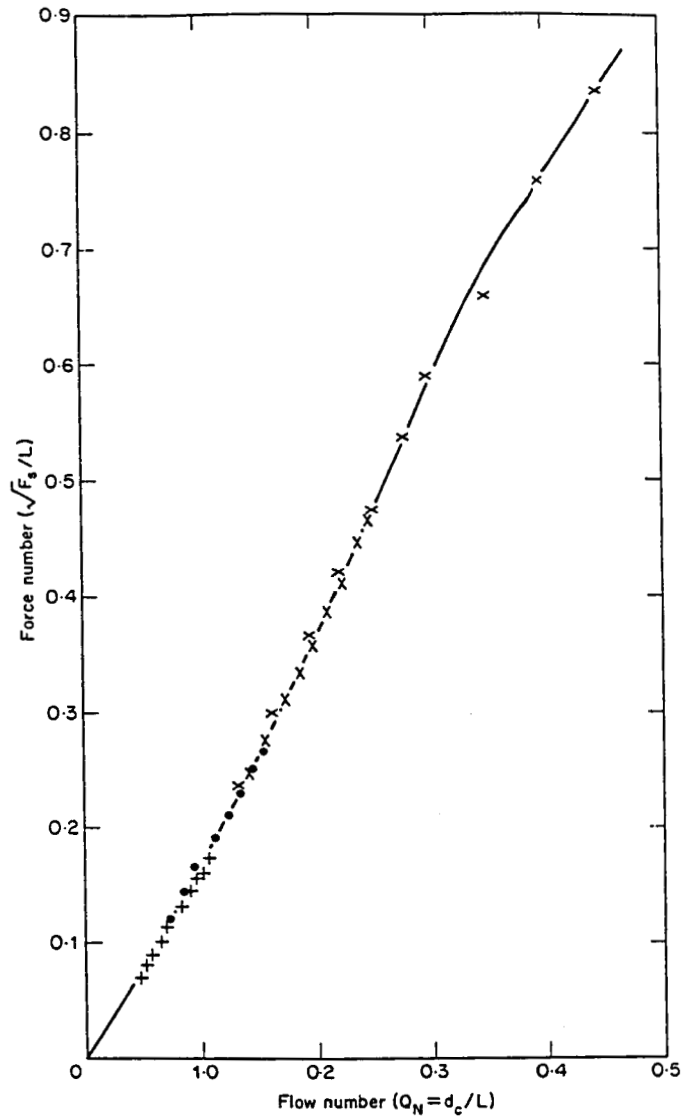
INFLUENCE OF NAPPE VENTILATION

When a flow passes over a weir or a straight drop spillway, a pocket of air is trapped between the downstream side of the structure, the descending stream and the elevated pool. Some of the air in the pocket is entrained in the nappe flow and if this loss is not fully replenished through ventilation the pressure becomes sub-atmospheric and the depth of the elevated pool increases. With complete lack of ventilation the pressure difference across the nappe eventually becomes



- Legend
- + Results obtained on 8-step model
 - Results obtained on 10-step model
 - x Results obtained on 20-step model
 - × Results obtained on 30-step model

Figure 13 The relationship between flow number and energy number established on four models of different size



- Slope of cascade (H/L) = 0.421
Step inclination $\theta = 0^\circ$

Figure 14 The relationship between flow number and force number established on four models of different size

so great that either the flow clings to the downstream face of the structure or a replenishing supply of air breaks through the nappe. In both of these cases, flow behaviour is unsteady.

To assess the influence of nappe aeration on the flow conditions formed on a series of steps, a short visual investigation was made on an inclined step cascade. In this investigation the flow pattern created by a flow with ventilated nappes was compared with the pattern created by the same flow without ventilation. Such comparisons were made over a wide range of discharges in order to determine the influence of aeration on both the subcritical and the supercritical categories of flow behaviour.

In the case of flows in the subcritical category the investigation revealed that the effect of aeration on flow behaviour at each step on a cascade was similar to the influence at a single drop. That is to say, on a cascade with no air vents the pressure beneath the nappes became sub-atmospheric.

Figure 15

Maximum transition zone lengths with nappe flow in supercritical category ($\theta = 0^\circ$)

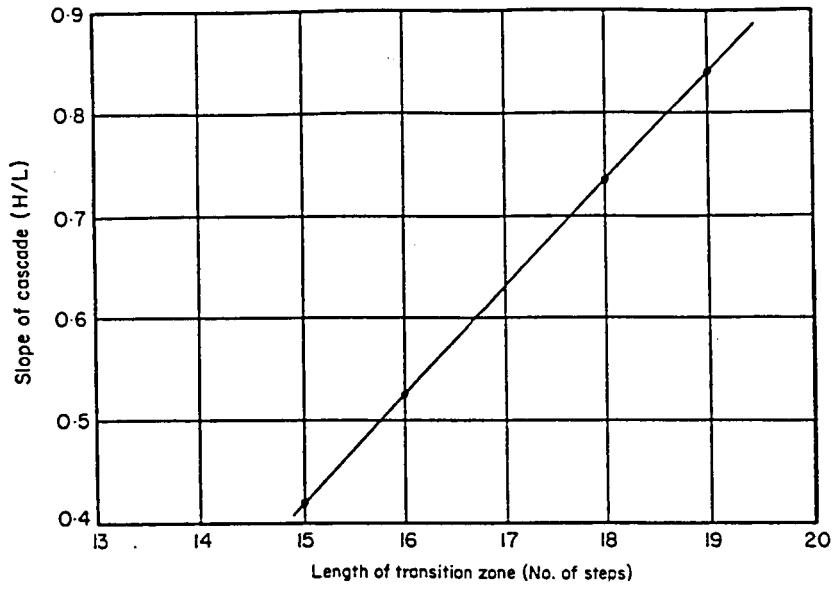
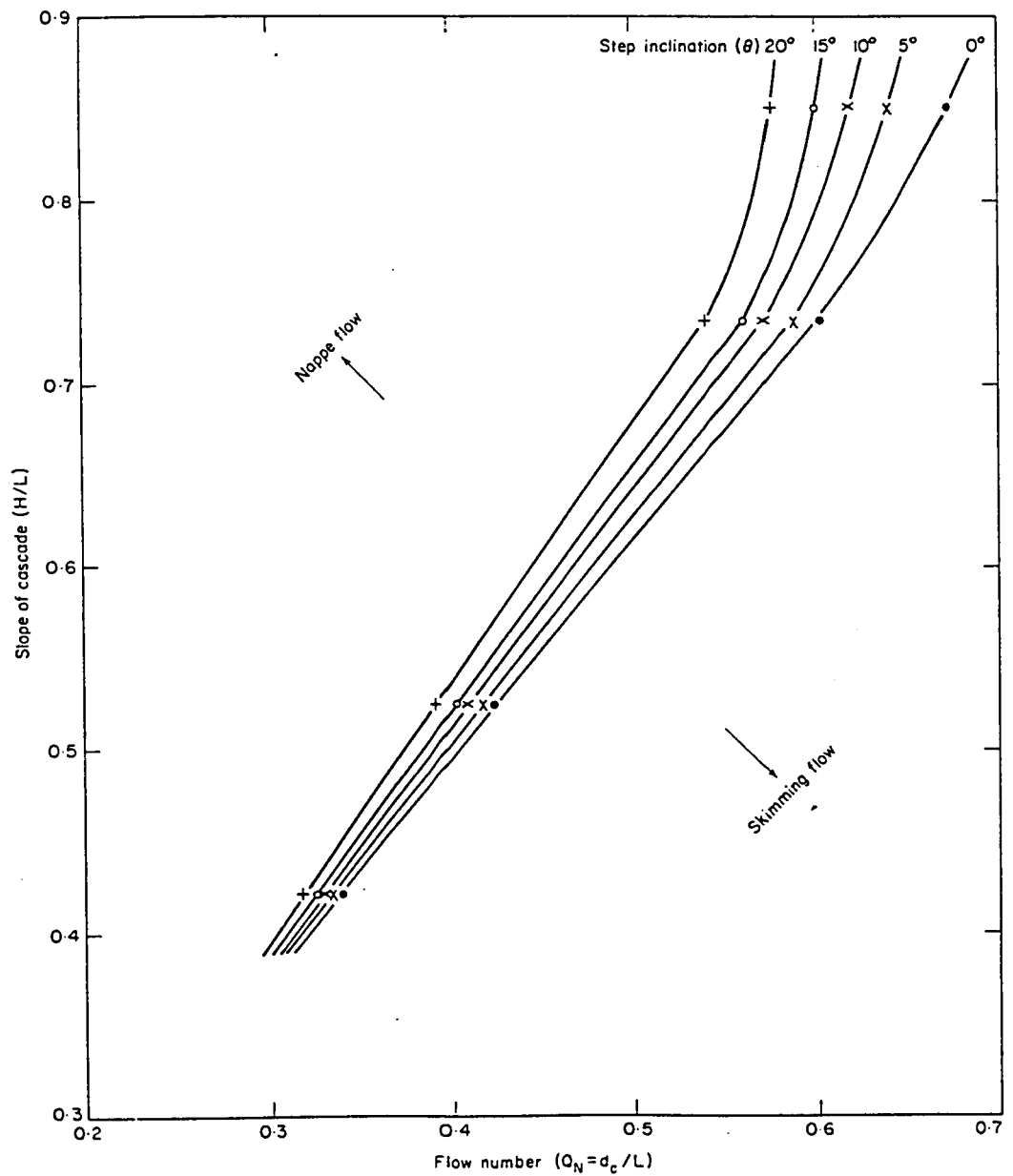


Figure 16

Limit of nappe flow at various step inclinations



With flows in the supercritical category, however, there was no marked difference between the uniform zone flow patterns created on cascades with and without ventilation. Observation of the flow characteristics suggested that the reason for this was the highly fragmented nature of the stream after the first few steps, and the consequent provision of an adequate supply of air through the nappes. The insignificance of nappe ventilation on the uniform zone conditions of this category of flow behaviour has been confirmed by a number of tests. In these tests the energy and force number of a supercritical flow leaving the base of a cascade was determined for steps with and without air vents. Identical values were obtained.

SKIMMING FLOW

Initial tests on a 30-step cascade revealed that air entrainment was a dominant feature of the skimming flow developed on the model. In fact, this type of flow could not be created without air entrainment. The phenomenon of self-aeration is a common characteristic of high velocity spillway flows. It involves the entrainment of air by the flow from the atmosphere above the stream and the diffusion of this air through the flow to create a violently agitated stream with an ill-defined free surface. The following observations were made of skimming flow on a 30-step model:

1. A 'clear water' reach occurred at the head of the cascade. The decreasing depth (and hence increasing velocity) of the flow in this reach indicated that it formed a part of the transitory zone.
2. At a clearly defined section some distance down the cascade, slugs of water were violently ejected from the surface and below this a 'white water' reach in which the flow was a mixture of air and water extended to the base of the model.
3. After a short initial reach in which air concentration was obviously increasing, the conditions in the 'white water' reach appeared to be uniform.

Experiments revealed that boundary layer develops in the 'clear water' reach and aeration commences when boundary layer thickness equals flow depth.

No attempt has been made to provide a basis for quantitatively predicting prototype performance from the results of the model studies of skimming flow for two reasons. Firstly, with air entrained flows no reliable method is at present available. Secondly, the effect of scale, which would undoubtedly result from prediction of prototype performance by application of the Froude criterion alone, could not be estimated. Unfortunately, the larger models used in the study of nappe flow could not be used to assess such scale effects because of the practical difficulties involved in providing the large discharges required to create 'drowned' conditions.

Stilling basin design

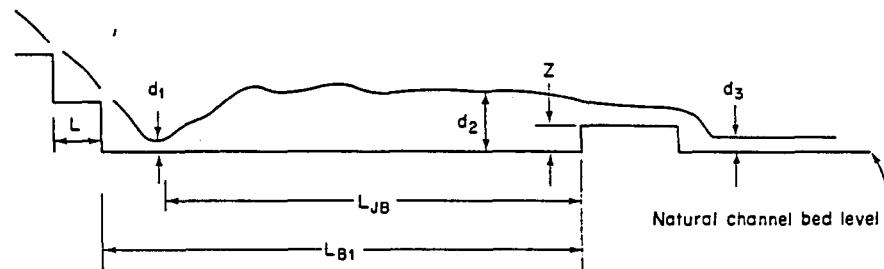
GENERAL

In general, only subcritical flows are acceptable for discharge into the natural watercourses at the base of the spillway. With spillway flows in the supercritical category it is, therefore, necessary to provide a stilling basin. The hydraulic jump type of basin is undoubtedly the most suitable for use in conjunction with a cascade. This is because the large reduction in the specific energy of flows leaving the base of a stepped spillway compared with the specific energy of flows leaving a similar smooth chute results in a relatively small tailwater depths being required for the creation of a jump. Consequently, simple and inexpensive structures suffice.

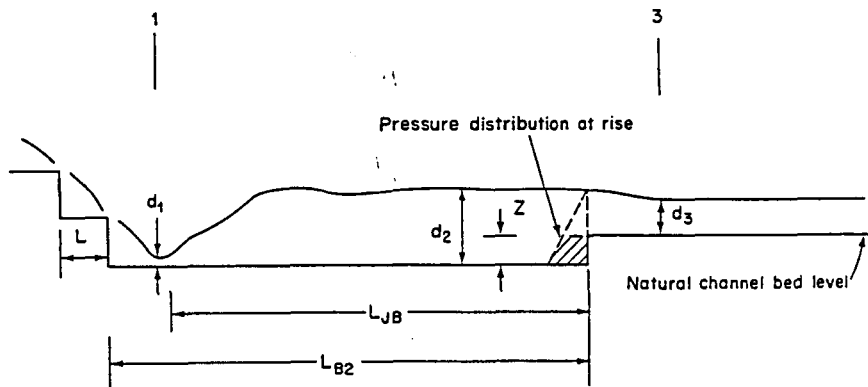
Comparison of the specific energy of a flow leaving the base of a high cascade with the specific energy attained by the same flow on a smooth rectangular chute of equal width, illustrates the effectiveness of the stepped spillway as an energy dissipator. For example, the specific energy of a flow of $42 \text{ m}^3/\text{s}$ leaving a horizontal step cascade 55 m wide with an

overall slope of 1: 2, a total height of 37 m and a step length of 1.1 m would be about 1.7 m. On a smooth chute this flow would attain the same specific energy value at a section only 1.2 m vertically below the crest of the spillway. Entrainment of air at the surface of the supercritical flow on the smooth chute will cause some dissipation of energy, but it would still be considerably greater at the base of the chute than in the case of the stepped spillway.

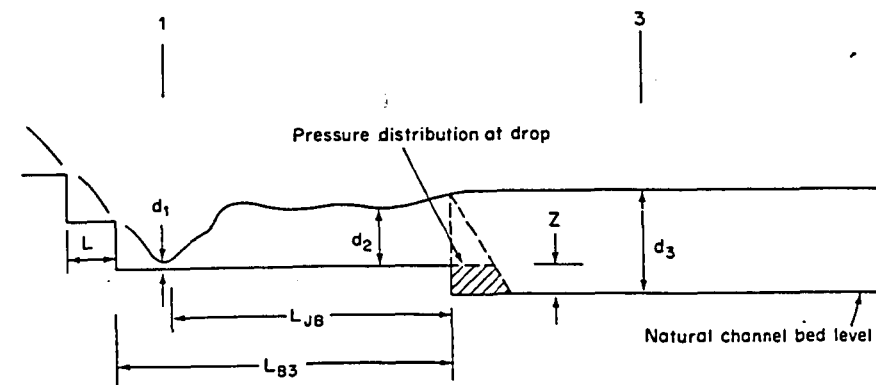
The design of standing wave energy dissipators by the commonly used procedures requires a knowledge of supercritical depth and Froude number. Because it has not been possible to provide correlations which yield these flow parameters accurately, design procedures have been evolved which enable basin sizes to be determined from data obtained from the dimensionless relationships between flow number, slope and force number established by the study of nappe flow. The three types of stilling basin considered are shown in Figure 17. Two of these basins are of the sill variety and are, therefore, for use in situations where the jump rating curve lies above the tailwater rating curve. The third basin is of the abrupt drop type, and, hence, is for use in situations where the tailwater curve is above the jump curve. By providing design procedures for assessing the leading dimensions of standing wave structures for use in locations where tailwater depth is either insufficient or excessive, a basin can be designed for the situations most frequently met in practice.



(a) Basin Type 1



(b) Basin Type 2



(c) Basin Type 3

Figure 17

the stilling basins selected for analysis

TYPE 1 BASIN

By applying the momentum principle and assuming the momentum coefficient β for the subcritical flow is unity, the following relationship between force number, flow number and the ratio of weir height Z to step length L may be obtained

$$\left(\frac{d_c}{L}\right)^3 = \left[\left(\frac{\sqrt{F_S}}{L}\right)^2 - \left\{ \frac{1}{2C_D^{4/3}} \left(\frac{d_c}{L}\right)^2 + \frac{1}{C_D^{2/3}} \left(\frac{d_c}{L}\right) \left(\frac{Z}{L}\right) + \frac{1}{2} \left(\frac{Z}{L}\right)^2 \right\} \right] \left[\frac{1}{C_D^{2/3}} \left(\frac{d_c}{L}\right) + \left(\frac{Z}{L}\right) \right] \quad (13)$$

where F_S is the specific force of the supercritical flow and C_D is the discharge coefficient for the broad crested weir in the equation

$$q = C_D g (d_2 - Z)^{3/2} \quad (14)$$

Equation (13) is derived in Appendix 2. In Figure 18, Z/L has been taken as a parameter and force number plotted against flow number, C_D has been assumed to be a constant with a value of 0.475 (a commonly accepted value in approximate calculations).

With the aid of Figure 18, the weir height required in a Type 1 basin at the base of a cascade of steps of specified geometry may be readily assessed for a stated flow rate. The following procedure is suggested:

1. Calculate d_c for the design flood [$d_c = \sqrt[3]{(Q^2/gb^2)}$]
2. Using the specified value of step length, calculate d_c/L
3. From the appropriate force number-flow number plot (Figures 8 to 12 inclusive) read off $\sqrt{F_S}/L$ for this value of d_c/L
4. Using the design curves shown in Figure 18 read off or interpolate the Z/L value of the curve that passes through the point

$$\frac{d_c}{L}, \frac{\sqrt{F_S}}{L}$$

5. Calculate Z .

Any form of weir may, of course, be used to terminate the Type 1 basin. However, if a broad crested weir block is not used a C_D value of 0.475 is inappropriate and the design curves given in Figure 18 are not applicable. In such cases, use of the following procedure yields weir height more rapidly because new design curves would be necessary for the use of the above procedure:

1. evaluate d_c/L and $\sqrt{F_S}/L$ as described above
2. calculate $\sqrt{F_S}/d_c$
3. using the relationship obtained by simplifying Equation (13)

$$\frac{\sqrt{F_S}}{d_c} = \left[\frac{1}{\frac{1}{C_D^{2/3}} + \frac{Z}{d_c}} + \frac{\left(\frac{1}{C_D^{2/3}} + \frac{Z}{d_c}\right)^2}{2} \right]^{1/2} \quad (15)$$

evaluate $\frac{Z}{d_c}$

4. Calculate Z .

By energy considerations it can be shown that for negligible influence by downstream conditions on the head-discharge relationship, for a broad crested weir d_3 must not exceed $\frac{1}{3}(2d_2 + Z)$. The above equations are, therefore, only applicable to situations where

$$d_3 \leq \frac{1}{3}(2d_2 + Z)$$

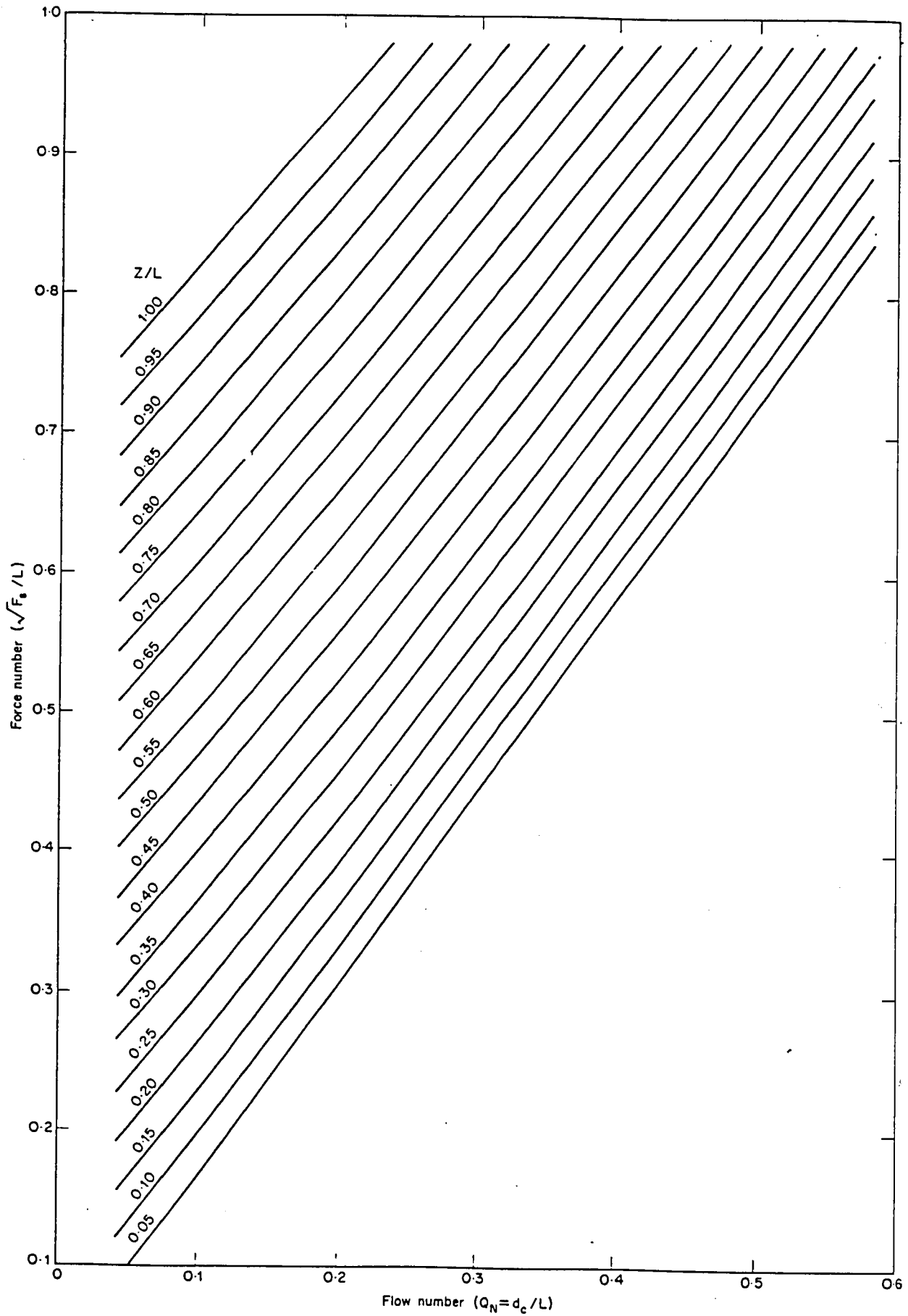


Figure 18 *Design curves for type 1 stilling basin*

Ideally, the length of the stilling basin must be sufficient for complete formation of the jump. This length cannot be determined theoretically but it has been the subject of numerous experimental studies. Unfortunately, because of the effects of scale and the use of different criteria for assessing jump length, the results of these studies show little agreement. However, a feature common to all the relationships established between supercritical Froude number and the ratio of jump length to subcritical depth is the lack of influence of Froude number on the length-depth ratio.

At the risk of slightly overestimating the jump lengths of flows close to the critical state, the ratio L_J/d_2 may therefore be taken as a constant, C_J , the value of which depends on the experimental relationship being used. Hence, to fully accommodate the jump in the stilling basin

$$L_{JB} \geq C_J d_2$$

where L_{JB} is the length of the portion of the basin in which the jump occurs.

If the total length of the basin, L_{B1} , is made to equal the length of the jump then the supercritical stream leaving the penultimate step of the cascade compresses the jump into a length L_J minus the throw of the nappe, and this may result in stilling less satisfactory than that achieved when the full length of the jump is allowed for. Hence, by assuming the nappe throw equals the step length L , the following approximate expression for total basin length is obtained

$$L_{B1} = C_J \cdot d_2 + L$$

As previously indicated, the spread of C_J values reported by the various investigators is considerable.

The value adopted for a particular location should reflect the tolerance of the downstream channel to both waves and high velocity jets within the subcritical flow. If the natural channel cannot tolerate turbulent conditions then a C_J value of 6.1 is appropriate. For channels with rock beds and protected banks, basin lengths computed with a C_J value as low as 3 will prove satisfactory. The use of baffle blocks and other devices that reduce jump length enable values of between 3 and 4 to be used in channels which are susceptible to erosion.

TYPE 2 BASIN

By assuming the pressure diagram for the rise illustrated in Figure 23b, applying the momentum equation between section 1 and 3, and assuming β_3 is unity*, the following equation may be derived:

$$F_S - \left(\frac{d_c^3}{d_3} + \frac{d_3^2}{2} \right) = d_2 Z - \frac{Z^2}{2} \quad (16)$$

Equation (16) is derived in Appendix 2.

The number of variables in Equation (16) prevents a worthwhile simplification of design procedure by the use of a graphical method. The following procedure for evaluating Z is, therefore, recommended:

1. Calculate d_c for the design flood.
2. Using the assumed value of step length, calculate d_c/L .
3. From the force number-flow number curve appropriate to the step shape under consideration (Figures 8 to 12 inclusive, read off the $\sqrt{F_S}/L$ value applicable to the above value of d_c/L .
4. Calculate F_S .

*see Appendix 2.

- Evaluate the subcritical depth d_2 by substituting in the relationship obtained by equating supercritical specific force to subcritical specific force and taking β_2 as unity*.

i.e.
$$F_s = \frac{d_c^2}{d_2} + \frac{d_2^2}{2}$$

- Compute normal depth for the natural channel when carrying the design flood. If the size and shape of the channel at the rise is the same as the size and shape of the natural channel, d_3 may be taken as normal depth. If size and shape change, d_3 must be assessed from normal depth by energy considerations.
- Substitute in Equation (16) and evaluate Z.

The arguments and assumptions made in deriving an equation yielding the length of a Type 1 basin are equally applicable to the Type 2 basin. The following relationship for the Type 2 basin is, therefore, suggested:

$$L_{B2} = C_J d_2 + L.$$

TYPE 3 BASIN

The equation

$$d_3 Z - \frac{Z^2}{2} = \frac{d_c^3}{d_3} + \frac{d_3^2}{2} F_s \quad (17)$$

may be derived by assuming the pressure diagram for the rise shown in Figure 17c, applying the momentum equation between sections 1 and 3 and assuming β_3 is unity.

Equation (17) is derived in Appendix 2.

The dimensionless relationships that can be derived from Equation (17) do not, so far as this study is concerned, form the basis of a worthwhile graphical procedure for evaluating drop height. The following procedure is, therefore, suggested:

- Calculate d_c and determine F_s in the manner described, for the Type 2 basin.
- Evaluate d_3 from the normal depth for the natural channel when carrying the design flood in a manner similar to that described for the Type 2 basin.
- Substitute in Equation (17) and evaluate Z.

The relationships yielding the lengths of the Types 1 and 2 basins may be used for the Type 3 basin. Hence

$$L_{B3} = C_J d_2 + L.$$

where d_2 is obtained from the relationship

$$F_s = \frac{d_c^3}{d_2} + \frac{d_2^2}{2}$$

MODEL STUDY

A number of model basins were used in conjunction with a 30-step cascade to test the validity of the suggested design criteria. With each basin the jump was observed to form at the toe of the nappe developed at the final drop and the jump was fully accommodated within the basin. (C_J values of 6.1 were used to calculate basin length.)

FLOOD FLOW CAPACITY

With natural phenomenon such as floods, there are relationships between magnitude and probability of occurrence which can only be accurately established from long and reliable

records. Hence, when dealing with floods no discharge intensity can be described as a maximum since there is always some probability of it being equalled or exceeded.

It is not economic to design dam spillage arrangements to pass floods which have an almost negligible probability of being equalled or exceeded, even supposing it were possible to assess very low probability flows from the records available. Thus it is prudent to adopt energy dissipation devices which are capable of giving reasonable performance at flows in excess of those for which the structures were designed.

Because the criterion used in developing the basin equations has been adequate stilling and not merely the provision of subcritical conditions, basins designed in accordance with the design procedures recommended in this study will perform as standing wave basins at flows considerably in excess of the discharges used to determine basin dimensions. To illustrate this, the approximate maximum discharges for the formation of subcritical conditions in the model basins have been found. With the Type 1 and 2 basins the criterion used to assess maximum flow has been the formation of a jump prior to the abrupt rise, and with the Type 3 basin the formation of a jump prior to the abrupt drop.

In the case of the Type 1 basin models, the ratios of maximum flow to design flow, which are described as 'factors of safety', were all close to a mean value of about 1.9. For the Types 2 and 3 basins mean factor of safety values of 2.0 and 1.7, respectively, were indicated. The generally higher values of factors of safety for the Types 1 and 2 basins reflect the ability of sills to exert retarding forces considerably in excess of the hydrostatic forces assumed in deriving the design equations. However, in some situations the criterion for defining factor of safety for a Type 3 basin need not be the creation of a jump prior to the drop, and in these cases safety factors would be comparable with those for the Types 1 and 2 basins.

Design of prototype cascades and stilling basins for nappe flows

GENERAL CONSIDERATIONS

Spillage arrangements incorporating stepped spillways may be divided into two types: those in which cascades and stilling basins are used, and those in which adequate stilling is achieved with cascades of inclined steps alone. Design procedures are outlined for both cases and these procedures have been formulated with the objective of providing subcritical flow at natural channel level. In formulating the design procedure set out below, it has been assumed that spillway overall slope, total height, and width are fixed, and that the optimum spillage arrangement incorporating a cascade is to be found for a flood, the intensity of which has been determined by consideration of hydrological factors.

The immediate use of the results of the present investigation limits prototype design to spillways and stilling basins of constant width.

Briefly, the design procedure is:

- (1) Assess the design flood.
- (2) Assess spillway overall slope, total height, and width.
- (3) Overall slope suggests H/L ratio for cascade.
- (4) Determine dimensions of a number of cascades with given H/L ratio to give sub-critical flow.
- (5) Determine the dimensions of a number of cascades [having the H/L value specified in (3) that give supercritical category flow at the design flood].

- (6) For each cascade assess the dimensions of a stilling basin to provide sufficient energy dissipation and fit into the topography.
- (7) Select the optimum arrangement.

The numerical example in Appendix 1 illustrates these procedures.

CASCADES GIVING SUBCRITICAL CATEGORY FLOW

The following procedure may be used to determine the length of steps with inclinations of 5, 10, 15 and 20 degrees which give subcritical category flow at discharges up to and including the design flood:

- (1) Calculate the critical depth of the design flood.
- (2) Using Figure 7, read off the d_c/L (flow number) values appropriate to the specified H/L value and step inclinations of 5, 10, 15 and 20 degrees.
- (3) For each of the four step inclinations divide critical depth by the appropriate flow number value to determine the minimum step length.
- (4) Assess wing wall heights and design the approaches from the reservoir to the heads of the cascades (see 'Wing wall height', page 31, and 'Approach to cascade', page 31).
- (5) Establish suitable arrangements of steps within the specified total height and length of the proposed cascades (see 'Arrangement of steps', page 32).
- (6) Design nappe aeration and step surface drainage facilities (see 'Aeration and drainage', page 32).

Subcritical flow occurs after the final drop providing the nappe formed at this drop strikes a section of channel with an adverse slope equal to that of the preceding steps. The length of this section of channel should be the same as the length of the last step. Beyond the adverse slope, a channel with zero or mild slope ensures that subcritical flow is maintained.

CASCADES GIVING SUPERCRITICAL CATEGORY FLOW

The procedure set out below may be used to design cascades which give supercritical category flow at the design flood. Because of the supercritical state of the streams leaving the bases of these cascades, stilling basin design is also considered.

- (1) Using Figures 8 to 12, inclusive, read off the force numbers at the specified value of H/L for steps with 0, 5, 10, 15 and 20 degrees inclination, respectively.
- (2) Divide the critical depth by the flow number values found in (1) to determine the step lengths of the proposed cascades.
- (3) From the force number values and the step lengths, compute specific force and then, by assuming β is unity, subcritical depth.
- (4) Determine normal depth in the natural channel at the design flood and by assuming constant energy predict the depth of flow in a horizontal rectangular channel with the same width as the cascades.
- (5) By a comparison of the depths computed in (3) and (4), assess the most suitable form of basin for use with each cascade.

- (6) Following procedures of the type given in 'Stilling basin design', design a basin for each cascade.
- (7) From Figure 15, determine the maximum number of steps in the transitory zone at the specified H/L value.
- (8) Calculate the numbers of steps on the proposed cascades and reject any structure which has less than the number found in (7). Rejection is essential because the values of specific energy and force for a flow on a cascade with insufficient steps for the formation of a uniform zone are uncertain.
- (9) Establish suitable arrangements of steps within the specified total height and length of the proposed cascades (see 'Arrangement of steps', page 32).
- (10) Assess wing wall heights and design the approaches from the reservoir to the heads of the cascades (see 'Wing wall height', page 31, and 'Approach to cascade', page 31).
- (11) With incline step cascades design nappe aeration and step surface drainage facilities (see 'Aeration and drainage', page 32).

OPTIMUM SPILLAGE ARRANGEMENT

All the spillage arrangements incorporating cascades and designed in accordance with the foregoing recommended procedures possess similar energy dissipating characteristics when operating at the design flood. In most situations the optimum arrangement consists, therefore, of the structure which costs least. However, in some cases other criteria for determining the optimum arrangement may be desirable. For example, if the probability of the design flood can not be accurately established for a scheme, the ability of the feasible arrangements to provide a subcritical efflux to the natural channel at flow rates in excess of the design flood must be considered when selecting the optimum arrangement.

WING WALL HEIGHT

Wing walls on cascades must not only contain the descending water streams but should also confine the bulk of the spray created above these streams to the cascades. Spray formation is a phenomenon dominated by surface tension and, because the Weber and Froude criteria cannot be satisfied simultaneously, the spray formed above a prototype structure cannot be accurately predicted from observations of a model which possesses the same ratio of inertial to gravity forces as the prototype. However, because it is rarely necessary to confine all spray to a cascade, it is sufficient to be able to estimate the wall heights which contain the heavy spray immediately above the main flow. As the spray heights above cascades were found to be both insensitive to changes in discharge and many times greater than the depth of water flow, wing wall height may be regarded as a function of the state of flow (i.e. subcritical or supercritical) and the step projection alone.

Observation of model conditions indicated that with subcritical category flow, adequate protection from spray was obtained if the normal distance from the line joining the step apexes to the top of the wing wall equalled the step projection measured normal to this line. In the case of supercritical category flow the normal distance between the step apexes and the top of the wing wall needed to be about three times the step projection.

APPROACH TO CASCADE

For the proper application of the results of the model studies presented in this report, the prototype and model should be identical in all but size. Hence, the approach from a reservoir to a prototype cascade should consist of a rectangular open channel, at least one step length long, with the same width as the cascade and with an adverse slope equal to that of the step surfaces.

The uniform zone conditions created with supercritical category flow are not influenced by boundary geometry at the head of the cascade. However, to avoid unduly long transitory zones, approach channel width should equal cascade width.

ARRANGEMENT OF STEPS

By following the procedures set out on pages 30 and 31, the designer obtains the size, shape and minimum number of steps which produce flows with the characteristics given by the dimensionless correlations presented earlier.

However, the specified values of spillway overall slope and total height may not allow cascades to consist of a series of identical steps.

When this difficulty arises with cascades designed to carry subcritical category flows it is recommended that all steps should have identical shape (i.e. the same values of H/L and θ) but the initial or final step should be larger than the other constant geometry steps. Figure 9 indicates that on the larger step the maximum discharge for the formation of a jump is greater than on other steps (i.e. the initial or final step is capable of giving subcritical conditions at flow rates in excess of the design flood). The above solution is recommended because the alternative arrangement using a smaller initial or final step would result in supercritical flow on this step. If the two sizes of steps differ greatly, a number of steps smaller than the single step but larger than the constant size steps may be preferred. These initial or final steps need not be equal in size, providing their shape is identical to that of the other constant geometry steps.

In the case of supercritical category flows, a change in the size or geometry of steps at the head of a cascade only causes the transition zone flow pattern to differ from that created on a cascade of identical steps. Because uniform zone flow characteristics are the same in both cases, the designer is free to select any size or shape of step or steps at the head of a cascade giving supercritical category flows. However, for the data derived from the dimensionless correlations to apply, the cascades must terminate with the constant size steps.

AERATION AND DRAINAGE

Aeration of the nappe created at each step of an inclined step cascade designed for subcritical category flow is essential if unsteady conditions resulting from nappe oscillation are to be avoided. Lack of aeration leads to a general increase in surface disturbance on and below a cascade, and at flow rates in the proximity of the design flood there is a tendency for fluctuating discharge to temporarily sweep jumps off steps. With subcritical category flow, aeration is, therefore, most desirable.

In the case of supercritical category flow, the results of the present study have shown aeration to be unnecessary. However, if inclined steps are used subcritical category flows occur at low discharges and air vents should be provided. With horizontal steps there is no necessity for nappe ventilation.

In general, the most convenient method of providing nappe aeration is by small ducts feeding air from beyond the wing walls to near the top of each drop.

Failure to provide drainage on an inclined step cascade may result in the stagnant pools on step surfaces becoming frozen during cold weather. If spillage should occur with the cascade in this condition the structure would tend to behave as a horizontal step cascade and the energy dissipating efficiency of the spillway would be less than under normal circumstances. Consequently, there would be a possibility of the efflux from the spillage arrangement becoming supercritical.

In view of the above, drainage of all inclined step cascades which are likely to be subjected to freezing temperatures is recommended.

Energy of cascade flows

With cascades carrying subcritical category flow, the energy of the stream leaving each step is approximately the minimum value for the discharge intensity in question. In the case of supercritical category flows, the energy of the stream leaving each step in the uniform zone may be assessed from Appendix 3, Figures 19 to 23, inclusive.

Conclusions

FLOW BEHAVIOUR

1. Three distinct types of flow (isolated nappe, nappe interference and skimming) can be recognised on a stepped spillway, and the energy dissipating and retarding characteristics of a cascade differ with each of these flow types.
2. With all types of flow on cascades of horizontal steps the descending stream is everywhere supercritical after the initial drop. On the upper portion of the cascade the flow passes through a transition zone.
3. Isolated nappe flows form on inclined step cascades at relatively low discharges per unit width. The supercritical nappes formed at each drop pass into subcritical pools on the step surfaces and a uniform flow pattern zone extends over the whole cascade. At discharges above the maximum for subcritical category flow, behaviour on inclined steps is similar to that on horizontal steps.
4. Air entrainment is an important feature of skimming flow on cascades and the mechanism of aeration is the same as that observed with flows in smooth channels by previous investigators.
5. A qualitative understanding of the influence of discharge, overall spillway slope, step size and step shape on the energy and force of flows on a cascade may be obtained by comparison of the steps to roughness projections in an open channel. Hence, energy and force increase with discharge and overall spillway slope, and decrease with step size and the adverse slope of the step surfaces. The transition zone length is similarly affected by these factors.

NAPPE VENTILATION

6. Nappe ventilation should be provided on cascades which carry subcritical category flow so that unsteady conditions are avoided. With supercritical category flow, adequate aeration occurs through the fragmented flow and the provision of nappe ventilation facilities is, therefore, unnecessary. Hence nappe aeration is generally required on inclined step cascades but it is not needed with horizontal steps.

DIMENSIONLESS PRESENTATION OF EXPERIMENTAL RESULTS

7. The plot of slope of cascade against flow number for steps with inclinations of 5, 10, 15 and 20 degrees (Figure 7) readily yields the maximum discharges at which subcritical pools can form on every step of a constant geometry cascade.
8. The dimensionless correlations shown in Figures 8 to 12 and 19 to 23 inclusive enable the specific force and specific energy of supercritical streams leaving cascades of constant geometry steps to be estimated.

SCALE EFFECT

9. With the model sizes used in the study of subcritical category flow, the effects of scale were not apparent. Hence, the assumption that gravity is the dominating influence and viscosity and surface tension have negligible effect is confirmed.
10. In the case of supercritical category flows, slight overestimates of the specific energy and and the specific force of flows leaving the base of a cascade of large steps are obtained when the Froude criterion is applied to measurements made on small steps. Thus designs will be slightly conservative.

STILLING BASIN

11. The design procedures set out earlier, together with the dimensionless force correlations, enable the leading dimensions of three common types of basin to be assessed.

PROTOTYPE DESIGN

12. By following the procedures and recommendations set out earlier, all the hydraulic aspects of spillage arrangements consisting of either cascades alone or cascades and stilling basins, may be designed.

References

1. POGGI, B
Sopra gli scaricatori a scala di stramazzi
L'energia elettrica (Milan) Oct. 1949 26
2. POGGI, B
Lo scaricatore a scala di stramazzi
L'energia elettrica (Milan) Jan. 1956 33

Appendix 1

Application of design procedures

An example of the use of the design procedures outlined in the main body of the Report is given below.

THE PROBLEM

The basic relevant information for the reservoir project for which spillage facilities are required is as follows:

1. A design flood of $42.5 \text{ m}^3/\text{s}$.
2. An overall spillway slope of 1 : 2 (i.e. $H/L = 0.50$)
3. A spillway width of 54.8 m
4. A total spillway height of 36.6 m
5. A flow depth at the design flood of 0.457 m imposed by the natural watercourse on a horizontal, rectangular channel located at the base of the proposed cascade. The channel is equal in width to the cascade.

To illustrate the application of the suggested design procedure, two feasible spillage arrangements are designed. The first of these consists of a cascade of steps with inclinations of 20 degrees which is designed to carry subcritical category flow. Secondly, the dimensions of both a series of steps with 15 degrees inclination carrying supercritical category flow and a Type 1 basin are assessed.

CASCADE GIVING SUBCRITICAL CATEGORY FLOW

The procedure set out on page 30 is used to determine step geometry.

1. Calculate critical depth:

$$d_c = \sqrt[3]{\frac{Q^2}{gb^2}} = \sqrt[3]{\frac{42.5^2}{9.81 \cdot 8^2}} = 0.394 \text{ m}$$

2. Determine d_c/L from Figure 8:

$$\frac{d_c}{L} \text{ value appropriate to } \frac{H}{L} = 0.5 \text{ and } \theta = 20^\circ \text{ is } 0.092$$

3. Calculate step length:

$$L = \frac{d_c}{d_c/L} = \frac{0.394}{0.092} = 4.287 \text{ m}$$

say 4.29 m

4. Assess wing wall height and design approach channel:

Using the criterion of wing wall height equals step projection, walls 3.35 m high are required. The approach channel must be 54.8 m wide and have a 20-degree adverse slope.

5. Arrange steps:

An initial step 8.23 m long and 4.11 m high followed by 15 steps 4.33 m in length and 2.16 m high is a suitable arrangement (see page 32).

6. Aeration and drainage facilities:

Because the cost of nappe aeration and step surface drainage facilities is negligible in comparison with the total costs of the proposed structures, these features need not be considered in the initial stages of design.

CASCADES GIVING SUPERCRITICAL CATEGORY FLOW AND TYPE 1 BASIN

The method used to compute cascade dimensions is basically that given in pages 30 and 31.

1. Calculate the flow number d_c/L for specified value of force number, The step geometry of a cascade giving a force number value of 0.6 is found (in practice the optimum arrangement would be found by trying a range of values). From Figure 11 the appropriate d_c/L value is 0.317.
2. Calculate step length:

$$d_c = 0.394 \text{ m}$$

and

$$L = \frac{d_c}{d_c/L} = \frac{0.394}{0.317} = 1.24 \text{ m}$$

3. Compute specific force and subcritical depth.

$$\frac{\sqrt{F_s}}{L} = 0.6$$

but

$$L = 1.24 \text{ m}$$

∴

$$F_s = 0.556 \text{ m}^2$$

Now
$$F_s = \frac{d_c^3}{d_2} + \frac{d_2^2}{2}$$

$$\therefore 0.556 = \frac{0.394^3}{d_2} + \frac{d_2^2}{2}$$

$$\therefore d_2 = 1.01 \text{ m}$$

4. Determine d_3 :

d_3 is specified as 0.457 m

5. Select suitable form of stilling basin:

For a Type 1 basin

$$d_3 \leq \frac{1}{3}(d_2 + Z)$$

i.e. $d_3 \leq 0.515 \text{ m}$

This form of basin is, therefore, appropriate.

6. Design basin:

The first of the procedures set out on page 25 is followed.

$$d_c = 0.394 \text{ m}$$

$$d_c/L = 0.317$$

$$F_N = 0.6$$

From Figure 18, $Z/L = 0.29$

$$\therefore Z = 0.29 \times 1.24 = 0.359 \text{ m (say 0.36 m)}$$

$$L_{B1} = (6.1 \times 1.01) + 1.24 = 7.40 \text{ m}$$

7. Determine the minimum number of steps:

From Figure 15 the minimum number of steps on the proposed cascade is 16.

8. Calculate the number of steps on the proposed cascade.

9. There will be 58 identical steps 1.24 m long and 0.625 m high with an initial step 0.67 m in length.

10. Assess wing wall height and design approach channel.

Using the criterion of three times the step projection, a wing wall height of 2.59 m is required.

The approach from the reservoir to the head of the cascade should preferably have a width equal to that of the cascade. (see pages 31 and 32).

11. For the reasons previously given, aeration and drainage facilities need not be considered at this stage.

Appendix 2 Derivation of equations for design of stilling basins

TYPE 1 BASIN EQUATION

For a hydraulic jump to form on the horizontal bed of a rectangular channel specific forces of the supercritical and subcritical flows must be equal. That is

$$\frac{\beta_1 Q^2}{g b d_1} + \frac{d_1^2 b}{2} = \frac{\beta_2 Q^2}{g b d_2} + \frac{d_2^2 b}{2}$$

dividing by b and substituting q for Q/b

$$\frac{\beta_1 q^2}{g d_1} + \frac{d_1^2}{2} = \frac{\beta_2 q^2}{g d_2} + \frac{d_2^2}{2}$$

But
$$F_S = \frac{\beta_1 q^2}{g d_1} + \frac{d_1^2}{2}$$

and
$$d_c^3 = \frac{q^2}{g}$$

Therefore assuming β_2 is unity
$$F_S = \frac{d_c^3}{d_2} + \frac{d_2^2}{2}$$

Now from energy considerations the discharge across unit width of a broad crested weir can be shown to be given by

$$q = C_D \sqrt{g} (d_2 - Z)^{3/2}$$

where C_D is the coefficient of discharge. Dividing by \sqrt{g} and substituting $d_c^{3/2}$ for $\frac{q}{\sqrt{g}}$

$$d_c^{3/2} = C_D (d_2 - Z)^{3/2}$$

Hence
$$d_2 = \frac{1}{C_D^{2/3}} d_c + Z$$

Combining equations
$$F_S = \frac{d_c^3}{\left(\frac{1}{C_D^{2/3}} d_c + Z\right)} + \frac{\left(\frac{1}{C_D^{2/3}} d_c + Z\right)^2}{2}$$

Therefore
$$d_c^3 = \left[\frac{\left(\frac{1}{C_D^{2/3}} d_c + Z\right)^2}{F_S} \right] \left[\frac{1}{C_D^{2/3}} d_c + Z \right]$$

Dividing by L^3 and rearranging

$$\left(\frac{d_c}{L}\right)^3 = \left[\left(\frac{\sqrt{F_S}}{L}\right)^2 - \left\{ \frac{1}{2 C_D^{4/3}} \left(\frac{d_c}{L}\right)^2 + \frac{1}{C_D^{2/3}} \left(\frac{d_c}{L}\right) \left(\frac{Z}{L}\right) + \frac{1}{2} \left(\frac{Z}{L}\right)^2 \right\} \right] \left[\frac{1}{C_D^{2/3}} \left(\frac{d_c}{L}\right) + \left(\frac{Z}{L}\right) \right]$$

Figure 20

Flow number plotted against slope of cascade for various values of energy number ($\theta = 5^\circ$)

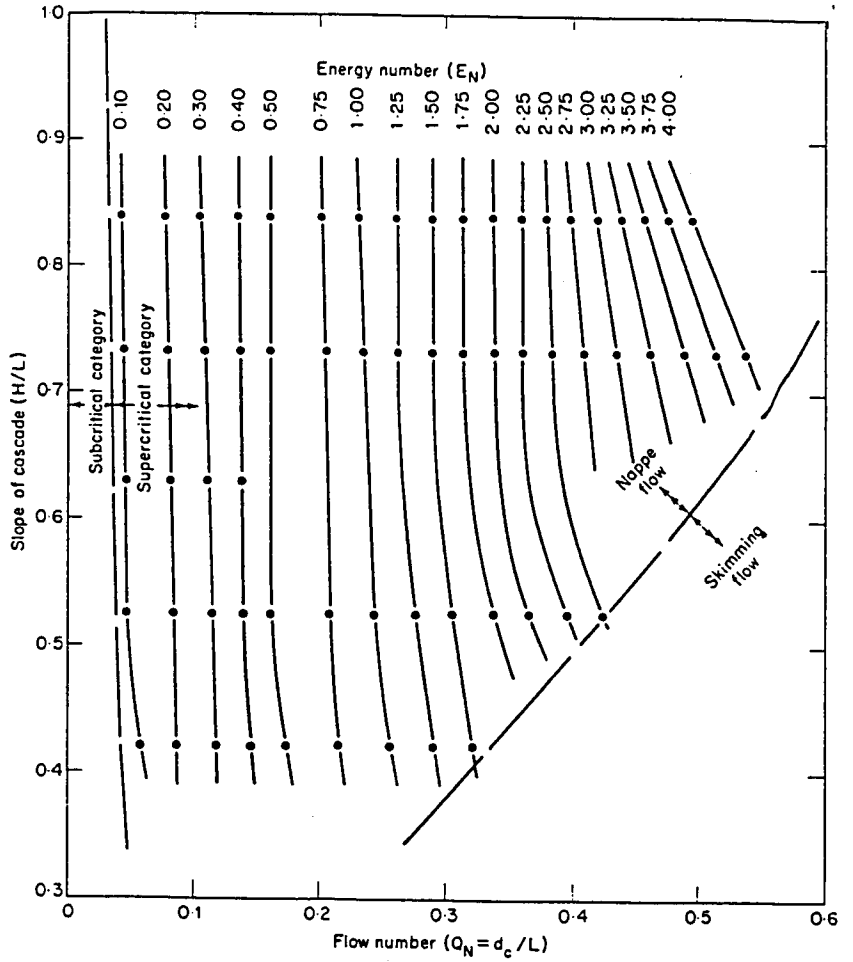
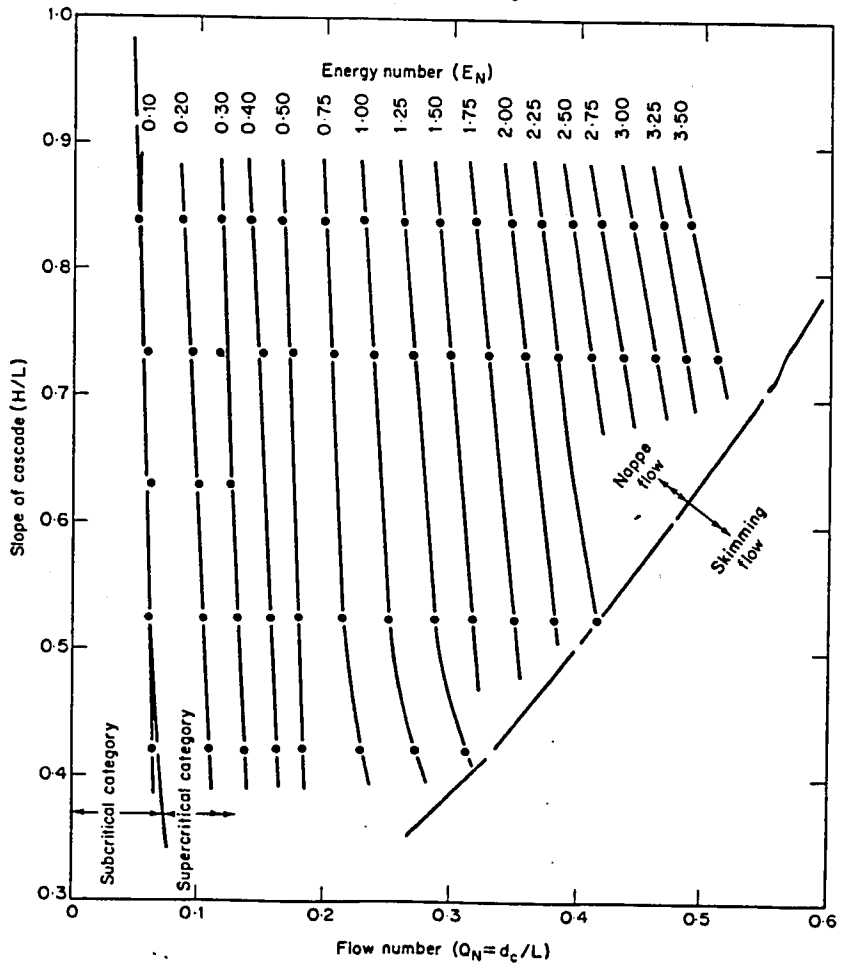


Figure 21

Flow number plotted against slope of cascade for various values of energy number ($\theta = 10^\circ$)



TYPE 2 BASIN EQUATION

Consider the illustration of the Type 2 basin shown in Figure 17. Applying the momentum equation between sections 1 and 3 and assuming the illustrated pressure diagram for the rise,

$$\left(\frac{\beta_1 Q^2}{gbd_1} + \frac{d_1^2 b}{2}\right) - \left(\frac{\beta_3 Q^2}{gbd_3} + \frac{d_3^2 b}{2}\right) = \frac{d_2^2 b}{2} - \frac{(d_2 - Z)^2 b}{2}$$

that is, the force on the rise is equal to the difference between the specific force of the supercritical flow and the specific force of the subcritical flow just downstream of the rise. Dividing by b and substituting q for Q/b

$$\left(\frac{\beta_1 q^2}{gd_1} + \frac{d_1^2}{2}\right) - \left(\frac{\beta_3 q^2}{gd_3} + \frac{d_3^2}{2}\right) = \frac{d_2^2}{2} - \frac{(d_2 - Z)^2}{2}$$

But

$$F_s = \frac{\beta_1 q^2}{gd_1} + \frac{d_1^2}{2}$$

and

$$d_c^3 = \frac{q^2}{g}$$

Therefore, assuming β_3 is unity

$$F_s - \left(\frac{d_c^3}{d_3} + \frac{d_3^2}{2}\right) = \frac{d_2^2}{2} - \frac{(d_2 - Z)^2}{2}$$

and simplifying

$$F_s - \left(\frac{d_c^3}{d_3} + \frac{d_3^2}{2}\right) = d_2 Z - \frac{Z^2}{2}$$

TYPE 3 BASIN EQUATION

Consider the illustration of the Type 3 basin shown in Figure 17. Applying the momentum equation between sections 1 and 3 and assuming the illustrated pressure diagram for the drop,

$$\left(\frac{\beta_3 Q^2}{gbd_3} + \frac{d_3^2 b}{2}\right) - \left(\frac{\beta_1 Q^2}{gbd_1} + \frac{d_1^2 b}{2}\right) = \frac{d_3^2 b}{2} - \frac{(d_3 - Z)^2 b}{2}$$

that is, the force on the drop is equal to the difference between the specific force of the subcritical flow just downstream of the drop and the specific force of the supercritical flow. Dividing by b and substituting q for Q/b

$$\left(\frac{\beta_3 q^2}{gd_3} + \frac{d_3^2}{2}\right) - \left(\frac{\beta_1 q^2}{gd_1} + \frac{d_1^2}{2}\right) = \frac{d_3^2}{2} - \frac{(d_3 - Z)^2}{2}$$

But

$$F_s = \frac{\beta_1 q^2}{gd_1} + \frac{d_1^2}{2}$$

and

$$d_c^3 = \frac{q^2}{g}$$

Therefore, assuming β_3 is unity

$$\left(\frac{d_c^3}{d_3} + \frac{d_3^2}{2}\right) - F_s = \frac{d_3^2}{2} - \frac{(d_3 - Z)^2}{2}$$

Simplifying

$$d_3 Z - \frac{Z^2}{2} = \frac{d_c^3}{d_3} + \frac{d_3^2}{2} - F_s$$

Appendix 3 Plots of flow number against cascade slope, with energy number as parameter, for step inclinations of 0° , 5° , 10° , 15° and 20°

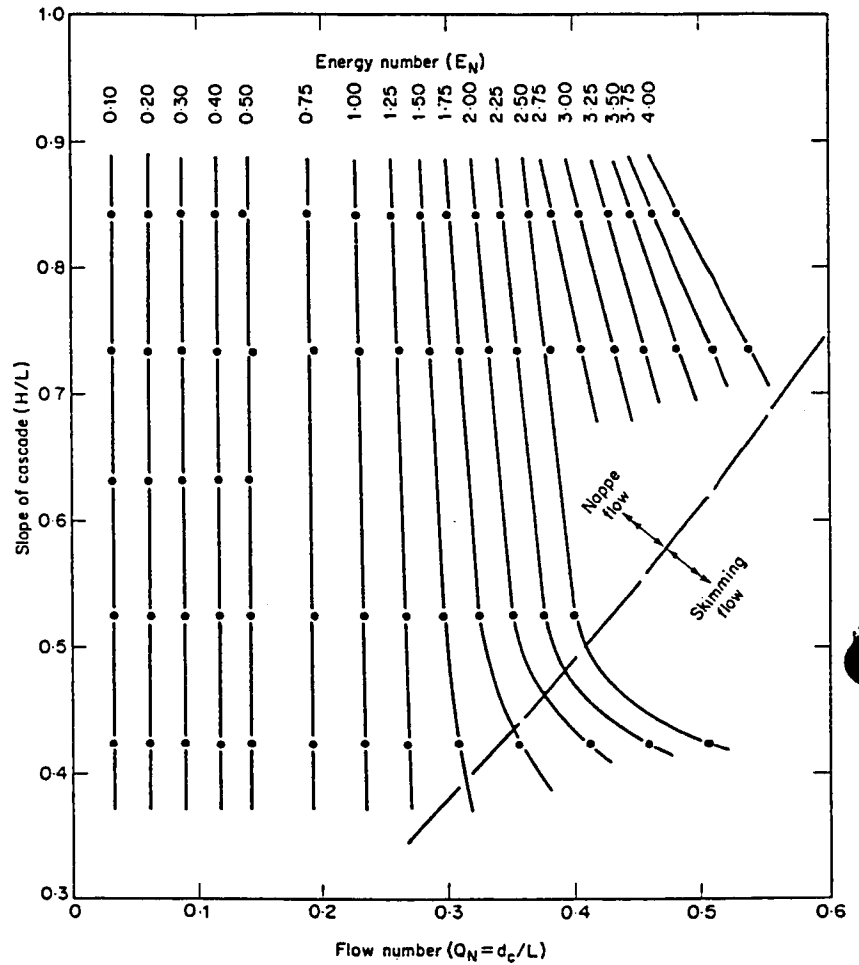


Figure 19

Flow number plotted against slope of cascade for various values of energy number ($\theta = 0^\circ$)

Figure 22

Flow number plotted against slope of cascade for various values of energy number ($\theta = 15^\circ$)

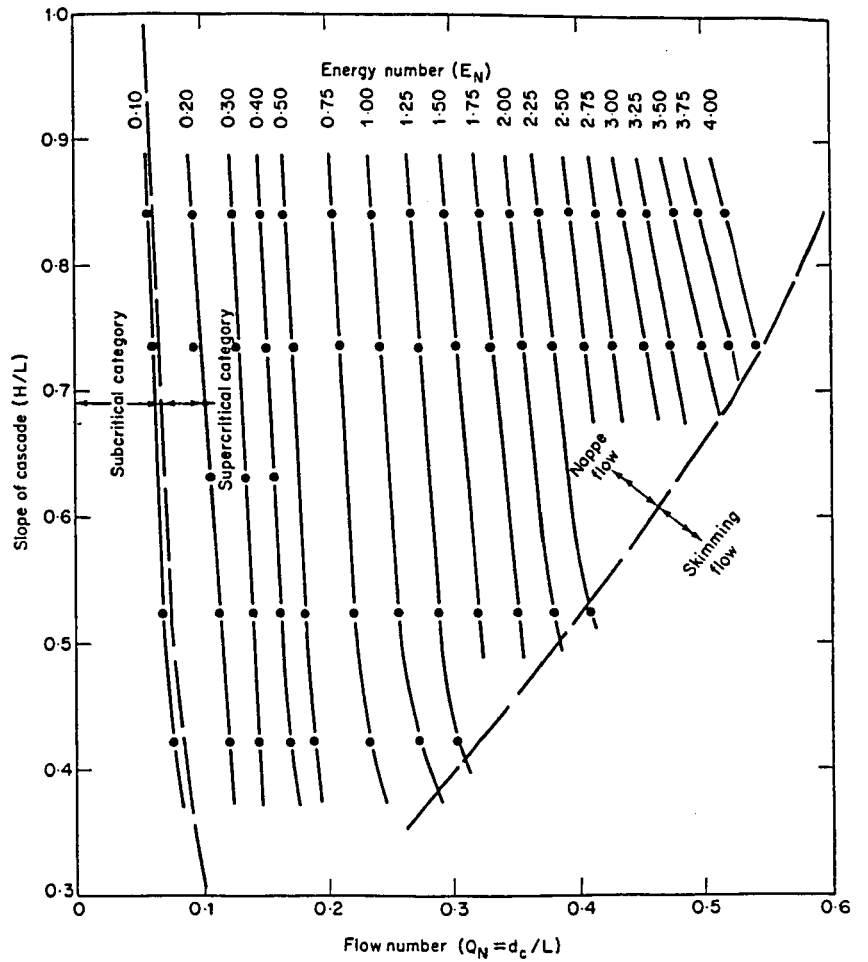


Figure 23

Flow number plotted against slope of cascade for various values of energy number ($\theta = 20^\circ$)

